AD-A105 520 AIR FORCE INST OF TECH WRIGHT-PATTERSON AFB OH F/G 8/12
MECHANISM OF ICE CRYSTAL GROWTH HABIT AND SHAPE INSTABILITY DEV--ETC(U)
AUG 81 G D SWOBODA.
UNCLASSIFIED AFIT-CI-81-327 NL

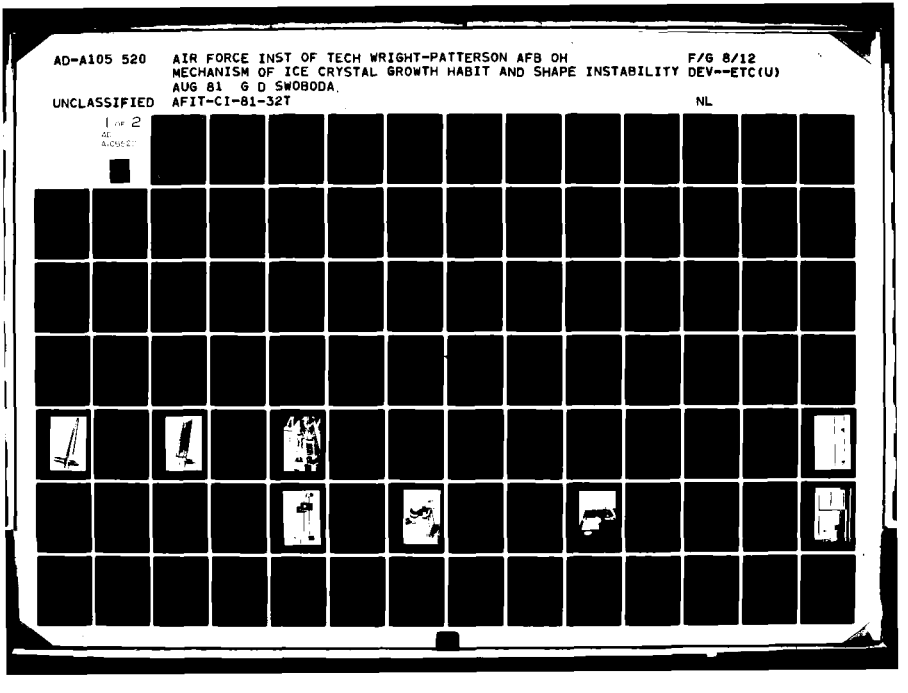

UNCLASS

SECURITY CLASSIFICATION OF THIS PAGE (When Data Entered)

LEVEL II

REPORT DOCUMENTATION PAGE

READ INSTRUCTIONS BEFORE COMPLETING FORM

1. REPORT NUMBER: 81-32T	2. GOVT ACCESSION NO.: AD-A105 520
3. RECIPIENT'S CATALOG NUMBER:	
4. TITLE (and Subtitle): Mechanism of Ice Crystal Growth Habit and Shape Instability Development Below Water Saturation	5. TYPE OF REPORT & PERIOD COVERED: THESIS/DISSERTATION
	6. PERFORMING ORG. REPORT NUMBER:
7. AUTHOR(s): Gerald Douglas Swoboda	8. CONTRACT OR GRANT NUMBER(s):
9. PERFORMING ORGANIZATION NAME AND ADDRESS: AFIT STUDENT AT: Univ of Utah	10. PROGRAM ELEMENT, PROJECT, TASK AREA & WORK UNIT NUMBERS:
11. CONTROLLING OFFICE NAME AND ADDRESS: AFIT/NR, WPAFB OH 45433	12. REPORT DATE: August 1981
	13. NUMBER OF PAGES: 125
14. MONITORING AGENCY NAME & ADDRESS (if different from Controlling Office):	15. SECURITY CLASS. (of this report): UNCLASS
	15a. DECLASSIFICATION DOWNGRADING SCHEDULE:

16. DISTRIBUTION STATEMENT (of this Report)

APPROVED FOR PUBLIC RELEASE; DISTRIBUTION UNLIMITED

DTIC ELECTE OCT 0 9 1981 E

17. DISTRIBUTION STATEMENT (of the abstract entered in Block 20, if different from Report)

29 SEP 1981

FREDRIC C. LYNCH, Major, USAF
Director of Public Affairs
Air Force Institute of Technology (ATC)
Wright-Patterson AFB, OH 45433

18. SUPPLEMENTARY NOTES

APPROVED FOR PUBLIC RELEASE: IAW AFR 190-17

19. KEY WORDS (Continue on reverse side if necessary and identify by block number)

20. ABSTRACT (Continue on reverse side if necessary and identify by block number)

ATTACHED

DD FORM 1 JAN 73 1473 EDITION OF 1 NOV 65 IS OBSOLETE

UNCLASS

SECURITY CLASSIFICATION OF THIS PAGE (When Data Entered)

AD A105520

DTIC FILE COPY

81-30T

MECHANISM OF ICE CRYSTAL GROWTH HABIT AND SHAPE INSTABILITY DEVELOPMENTS BELOW WATER SATURATION

by

Gerald Douglas Swoboda

A thesis submitted to the faculty of
The University of Utah
in partial fulfillment of the requirements for the degree of

Master of Science

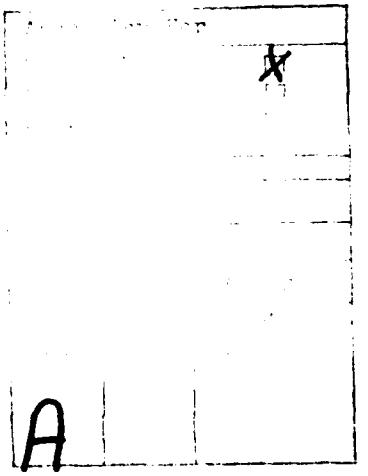

Department of Meteorology
The University of Utah

August 1981

THE UNIVERSITY OF UTAH GRADUATE SCHOOL

SUPERVISORY COMMITTEE APPROVAL

of a thesis submitted by

Gerald Douglas Swoboda

This thesis has been read by each member of the following supervisory committee and by majority vote has been found to be satisfactory.

June 11, 1981 — Norihiko Fukuta
Chairman: Norihiko Fukuta

11 JUNE 1981 — Kenneth Sassen
Kenneth Sassen

June 11, 1981 — Elford G. Astling
Elford G. Astling

THE UNIVERSITY OF UTAH GRADUATE SCHOOL

FINAL READING APPROVAL

To the Graduate Council of The University of Utah:

I have read the thesis of Gerald Douglas Swoboda in its final form and have found that (1) its format, citations, and bibliographic style are consistent and acceptable; (2) its illustrative materials including figures, tables, and charts are in place; and (3) the final manuscript is satisfactory to the Supervisory Committee and is ready for submission to the Graduate School.

June 11, 1981 Norihiko Fukuta
Date

Norihiko Fukuta
Member, Supervisory Committee

Approved for the Major Department

L. H. Lattman
Chairman, Dean

Approved for the Graduate Council

James L. Clayton

ABSTRACT

Ice phase process in supercooled clouds play dominant roles in development of updrafts and downdrafts as well as various forms of precipitation. In a supercooled cloud, an ice phase process begins normally with vapor diffusional growth of ice crystals. Consequently, the vapor diffusional growth of ice crystals is of importance in cloud physics.

Starting from the concept of the wedge-shaped ice thermal diffusion chamber of Schaller and Fukuta, where ice crystals can be grown under a range of ice supersaturations at a constant temperature in quiescent, temperature-stratified air, and by considering design and operational limitations, a new wedge-shaped ice thermal diffusion chamber was designed and constructed for this study of ice crystal growth habit and shape instability. This chamber and supporting apparatus define an experimental system capable of adequately controlling the temperature and supersaturation fields around the growing crystal. In addition to the wedge-shaped chamber, apparatus defining this experimental system are the pre-chamber, ice crystal slide mechanism, lateral microscope slide mechanism, sample transfer device, and outer environmental chamber. The original wedge-shaped chamber has been modified to minimize errors in aspect ratio, transient supersaturaitons, relaxation time, and non-linearity of temperature. An ordinary pre-conditioned meat baster is used for transferring homogeneously nucleated ice crystals from one environment to another. The pre-chamber is a simplified

parallel plate ice thermal diffusion chamber and allows generated seed ice crystals to be transferred and impregnated on a fine fiber. The rapid transfer of small seed ice crystals on the fiber, from the pre-chamber to the wedge-shaped chamber, and the rotation of these crystals in the chamber were accomplished by the ice crystal slide mechanism. The lateral microscope-slide mechanism allowed observation of ice crystals in all parts of the working area of the wedge-shaped chamber. The controlled environment of a deep freezer was utilized to accommodate all pieces of apparatus.

With this improved experimental system, the following are new findings in the area of ice crystal growth habit and shape instability. Under all ice supersaturation (S_i-1), i.e., 1, 5, 7 and 10%, as the temperature warms from low values, a gradual increas in 2a and c values occurred followed by a more rapid increase as water saturated conditions were approached. For some (S_i-1), a sharp decrease in 2a and c was noted just below water saturation. These trends can be explained if we assume three growth mechanisms, i.e., a two-dimensional nucleation mechanism at cold temperatures, an adhesive mechanism at warmer temperatures, and the liquid-like-layer mechanism at conditions just below water saturation. Ice crystal habit varied as a function of time at -8°C under (S_i-1) between 5 and 7%. Plotted as a function of temperature and ice supersaturation, 2a and c data showed definite zones of growth maxima. Ice crystal habit (2a/c) showed a complex relationship with temperature and ice supersaturation, especially in the region just below water saturation where the liquid-like layer mechanism appears to exist. Wulff's crystals were found to exist at cold temperatures under

(S_i-1) at 1%. Double plates were found at temperatures warmer than -10°C under (S_i-1) between 0 and 5%. Surface characteristics of ice crystals varied as a function of temperature and (S_i-1) with smooth surfaces at cold temperatures and low (S_i-1) and ragged surfaces existing at warmer temperatures and low (S_i-1). In addition, transformtion of hexagonal plates into sector plates and the appearance of prism face cavities happened at cold temperatures between 30 to 35 minutes and at warmer temperatures, as conditions approach water saturation, within the observation time of 10 minutes.

TABLE OF CONTENTS

ABSTRACT iv

LIST OF FIGURES viii

ACKNOWLEDGEMENTS xii

CHAPTER

1. INTRODUCTION 1

2. HISTORY OF ICE CRYSTAL AND SHAPE INSTABILITY STUDIES . . . 3

3. EXPERIMENTAL TECHNIQUES USED IN THE PAST 9

3.1 General Considerations for Ice Crystal Growth Habit and Shape Instability Studies 9
3.2 Methods of Ice Crystal Generation 10
3.2.1 Homogeneous Ice Nucleation 10
3.2.2 Heterogeneous Ice Nucleation 11
3.2.3 Laboratory Techniques Previously Used for Ice Crystal Generation 12
3.3 Methods for Ice Crystal Growth Studies 13
3.3.1 Convection Chamber 14
3.3.2 Mixing Cloud Chambers 15
3.3.3 Diffusion Chambers 17
3.3.4 Thermal Diffusion Chambers 18
3.3.4.1 Parallel plate chamber 20
3.3.4.2 Horizontal gradient parallel plate chamber 20
3.3.4.3 Wedge-shaped chamber 22

4. EXPERIMENTAL APPARATUS 23

4.1 Method of Ice Crystal Generation and Ice Crystal Growth Used in This Study 23
4.1.1 Ice Crystal Generation by Adiabatic Expansion of Air 23
4.1.2 Wedge-Shaped Ice Thermal Diffusion Chamber . . 24
4.2 Apparatus Used in This Study 32
4.2.1 Design Considerations 32
4.2.1.1 Heat transfers 32
4.2.1.2 Aspect ratio 34
4.2.2 Final Design and Construction 35
4.2.2.1 Wedge-shaped chamber 36
4.2.2.2 Pre-chamber 39

TABLE OF CONTENTS (continued)

4.2.2.3 Ice crystal slide mechanism 47
4.2.2.4 Lateral microscope slide mechanism . 55
4.2.2.5 Sample transfer device 57
4.2.2.6 Outer environmental chamber 62
4.2.3 Supporting Equipment 65

5. EXPERIMENTAL PROCEDURE 69

5.1 Nylon Fiber Preparation 69
5.2 Chamber Air Pre-Conditioning 69
5.3 Preparation of the Ice Surfaces 71
5.4 Ice Crystal Generation and Transfer 72
5.5 Ice Crystal Insertion into the Wedge-Shaped Chamber . 73
5.6 Photographic Measurement of Ice Crystals 73

6. EXPERIMENTAL RESULTS AND DISCUSSION 75

6.1 Growth Behavior of the Basal Plane of Ice 76
6.2 Growth Behavior of the Prism Plane of Ice 80
6.3 Ration of the Diameter of the Basal Plane and Height of the Prism Plane or 2a/c 88
6.4 Ice Crystal Growth Habit as a Function of Temperature and Ice Supersaturation 96
6.5 Ice Crystal Growth Characteristics 104

7. CONCLUSIONS AND RECOMMENDATIONS 108

7.1 Instrument Development 108
7.2 Ice Crystal Growth Habit and Shape Instability Studies 109
7.3 Recommendations for Future Research 111

APPENDICES 113

A. SOLUTION FOR $\nabla p = 0$ 114

B. NON-LINEARITY OF TEMPERATURE 116

C. DERIVATION OF THE RADIATIVE HEAT TRANSFER EQUATION 119

REFERENCES 122

LIST OF FIGURES

Figure		Page
1.	Fukuta's supercooled fog chamber	16
2.	Horizontal gradient parallel plate ice thermal diffusion chamber	21
3.	Develoment of ice and water supersaturations in a parallel plate ice thermal diffusion chamber	25
4.	Design of the new wedge-shaped ice thermal diffusion chamber used in this study	27
5.	Vapor density profile in the wedge-shaped ice thermal diffusion chamber	29
6.	Profile of supersaturation with respect to ice in the wedge-shaped ice thermal diffusion chamber	31
7.	Photograph of the wedge-shaped ice thermal diffusion chamber	40
8.	Photograph of the wedge-shaped ice thermal diffuson chamber with top plate removed	42
9.	Photograph of the wedge-shaped ice thermal diffusion chamber and primary supporting equipment in their operational configuration	44
10.	Pre-chamber	48
11.	Ice crystal slide mechanism	50
12.	Photograph of the ice crystal slide mechanism	53
13.	Lateral microscope slide mechanism	56
14.	Photograph of the lateral microscope slide mechanism	58
15.	Photograph of the lateral microscope slide mechanism with the Wild M5A stereomicroscope attached	60
16.	Photograph of the outer environmental chamber with insulated lid attached	63
17.	Photograph of the TERAK min-computer	67

LIST OF FIGURES (Continued)

18. Ice crystal diameter 2a plotted as a function of temperature at different times of growth under ice supersaturation (S_i-1) at 1% 77

19. Ice crystal diameter 2a plotted as a function of temperature at different times of growth under ice supersaturation (S_i-1) at 5% 78

20. Variation of ice crystal habit plotted as a function of time at a temperature of -8°C and different ice supersaturation (S_i-1) 79

21. Ice crystal diameter 2a plotted as a function of temperature at different times of growth under ice supersaturation (S_i-1) at 7% 81

22. Ice crystal diameter 2a plotted as a function of temperature at different times of growth under ice supersaturation (S_i-1) at 10% 82

23. Ice crystal height c plotted as a function of temperature at different times of growth under ice supersaturation (S_i-1) at 1% 83

24. Ice crystal height c plotted as a function of temperature at different times of growth under ice supersaturation (S_i-1) at 5% 85

25. Ice crystal height c plotted as a function of temperature at different times of growth under ice supersaturation (S_i-1) at 7% 86

26. Ice crystal height c plotted as a function of temperature at different times of growth under ice supersaturation (S_i-1) at 10% 87

27. Ratio of ice crystal diameter and height 2a/c plotted as a function of temperature after 50 minutes of growth under ice supersaturation (S_i-1) at 1% 91

28. Ratio of ice crystal diameter and height 2a/c plotted as a function of temperature after 50 minutes of growth under ice supersaturation (S_i-1) at 5% 92

29. Ratio of ice crystal diameter and height 2a/c plotted as a function of temperature after 50 minutes of growth under ice supersaturation (S_i-1) at 7% 94

LIST OF FIGURES (Continued)

30. Ratio of ice crystal diameter and height 2a/c plotted as a function of temperature after 50 minutes of growth under ice supersaturation (S_i-1) at 10% 95

31. Variation of ice crystal diameter 2a plotted as a function of temperature and ice supersaturation after 50 minutes of growth 97

32. Variation of ice crystal height c plotted as a function of temperature and ice supersaturation after 50 minutes of growth 99

33. Variation of the ratio of ice crystal diameter and height 2a/c plotteed as a function of temperature and ice supersaturation after 50 minutes of growth 102

B1. The center-line temperature deviation T plotted under different narrow end temperatures of ice in the wedge-shaped ice thermal diffusion chamber 117

ACKNOWLEDGEMENTS

I wish to express my sincere thanks to Dr. Norihiko Fukuta for his continual support and, especially, for his technical and theoretical expertise, which he willingly shared in support of this study.

I would like to thank Robert E. Heck for his assistance in the design and construction of various pieces of experimental apparatus.

And a special thanks to my parents, Gerald W. and Ruth M. Swoboda, for dedicating 21 years of their lives for me.

And to Debbie, who provided moral and psychological support during this endeavor, I wish to express my thanks and love.

This material is based upon work supported by the Division of Atmospheric Sciences, National Science Foundation under Grant ATM 8004108.

Chapter 1

INTRODUCTION

The existence of an abundant amount of water, in all its phases, i.e., gas, liquid and solid, distinguishes planet earth from all others in our solar system. Life itself relies on water to survive. Man, being composed almost entirely of water, also requires water to subsist and the production of food he consumes is dependent upon water. For this basic reason, the obtainment of water has been the cardinal objective of the human race. Throughout history, the availability and location of oceans, lakes, and rivers as well as the occurrence of precipitation have dictated the activities of civilizations. Plentiful amounts of water have caused civilizations to thrive while the absence of water has led to the demise of entire populations. Precipitation processes, in a complex ecological cycle, transport water from earth's surface to the atmosphere and back. It occurs in various forms including rain, snow, and hail. These transport processes can be a boon to mankind or likewise can violently destroy it as in the case of flooding caused by heavy rain, tornadoes, water spouts, hurricanes, and associated electrical phenomena. For the most part, man has been at the mercy of nature and its dictates but in modern times he has advanced to intellectual and technological levels whereby the modification, if not the control, of precipitation development is both feasible and practical. An understanding of the physical properties of precipitation

mechanisms becomes important if the prediction and control or modification are to be achieved.

The ice phase cloud processes have come to be understood as important in formation of all precipitations with the exception of some tropical showers. A great deal of research in the cloud physics field has been conducted on ice phase processes and a great deal more is required before the mechanisms involved are fully understood. The field of study can be divided into many distinct areas, each equally important in gaining insight into the complex relationship between the ice phase processes and the resultant processes including precipitation.

The variations that snowflakes or ice crystals exhibit in the atmosphere have long mystified both scientist and non-scientist alike. It is this variation of ice crystal habit and shape instability and the mechanisms involved that are focused on in this study.

This study has been carried out with two main goals in mind: first, to design, build and operate an environmental chamber capable of observing ice crystal growth processes under controlled conditions as accurately as possible; second, to monitor growing ice crystals with the intent of gathering new information on ice crystal habit and shape instability.

A review of previous ice crystal habit and shape instability studies is given in Chapter 2. Chapter 3 presents a discussion on experimental techniques used in previous studies. Apparatus including design considerations, final design, and construction used in this study are described in Chapter 4. Chapter 5 consists of experimental procedures while experimental results and discussion are reported in Chapter 6. Conclusions and recommendations are presented in Chapter 7.

Chapter 2

HISTORY OF ICE CRYSTAL HABIT AND SHAPE INSTABILITY STUDIES

The numerous variations that snow crystals exhibit in the atmosphere have motivated a great deal of observation and research in the field of cloud physics. Considerable progress has been made towards the understanding of ice crystal growth habit and shape instability; however, much work is still required in order to attain a clearer understanding of the physical processes involved. Many different approaches have been taken to tackle this difficult problem, but there has yet to advance one satisfactory solution. Previous investigations can be broken down into studies of habit, of growth rates, and of step parameters.

The change in the basic or primary ice crystal habit growing from vapor was found to be a function of temperature (aufm Kampe, et al., 1951; Nakaya, 1954). As the temperature is lowered from 0°C, while holding the vapor pressure at water saturation, the basic ice crystal shape varies in the following sequence: plate, column, plate, column. For conditions between ice and water saturations, temperature alone was found to be insufficient to define the basic ice crystal growth. Hallett and Mason (1958) showed that habit is dependent only upon the immediate environment at a given time and not upon the form or habit the crystal may have achieved previously. Gold and Power (1954) observed the ice crystal habit of natural snow during snowfall

periods and related this information to meteorological data at the time of the snowfall. A dependence of natural crystal habit on temperature was in reasonable agreement with laboratory results. Later studies (Hallett and Mason, 1958; Kobayashi, 1961; Ryan et al., 1976) and field experiments (Hallett, 1965; Kukuchi and Uyeda, 1979; Ono, 1969 and 1970) provided data more accurate than those of the earlier experiments. Detailed habit regimes have been shown from laboratory studies by Lamb and Hobbs (1971) and for natural atmospheric ice crystals by Magono and Lee (1966).

In addition to changes of ice crystal habit with temperature, Hallett and Mason (1958) found the existence of three temperature zones where crystal growth took place more rapidly than elsewhere: 0 to -2°C, -4 to -6°C, -14 to -16°C. The rate of mass increase, of an ice crystal growing at water saturation, varies with temperature. Maxima occur at about -5 and -15°C and a minimum at about -8°C (Hallett, 1965; Fukuta, 1969).

Although temperature is generally accepted as being a primary controlling factor of ice crystal growth habit, supersaturation controls secondary ice crystal habits such as the transition from plates to dendrites and from prisms to needles or sheaths (Mason, 1957; Hallett and Mason, 1958; Kobayashi, 1961). Development of spatial structures of ice crystals, dendrites in particular, is the result of shape instability of crystal growth (Mullins and Sekirka, 1963) where a sudden growth takes place at the tips of the crystals when triggered by nucleation, with limited surface migration of water molecules. Dendritic growth normally does not take place when the ice crystal is still small. The instability of the shape is, therefore, a function of the crystal

size as well as the supersaturation.

The temperature dependence of the mass growth rate of ice crystals at water saturation had been intepreted in terms of the variations with temperature, of the difference in equilibrium vapor pressure over ice and that over water, together with changes in the electrostatic capacity of a crystal with temperature as the ice crystal habit varied. Although these two factors play important roles in determining the mass growth rate, account must be taken of the surface kinetics as reflected in the deposition coefficient at different temperatures (Lamb and Hobbs, 1971).

The deposition coefficient, interpreted as the fraction of impinging vapor molecules which are successful at actually being incorporated into the ice lattice (Lamb and Scott, 1974) has been suggested as a contributing factor to ice crystal habit variations. These variations of the deposition coefficient with temperature seem to be related to the peaks in the rate at which an ice crystal accumulates mass (Hallett, 1965; Fukuta, 1969). Lamb and Hobbs (1971) compared the linear growth rates of the two major crystallographic planes, i.e., prism and basal planes, as a function of temperature. They found that when the linear growth rate of the basal plane is greater than that of the prism plane, platelike crystals grow, and when the reverse holds, columnar crystals grow. The conclusion drawn was that the alternation of basic ice crystal habit with temperature is a consequence of the fact that linear growth rates of the basal and prism planes of ice fluctuate with temperature and that the linear growth rate of both planes at any temperature is proportional to the velocity of steps at that temperature. Similarities of experimentally determined trends

in ice crystal growth habit, deposition coefficients, temperature, and velocities of step propagation have been demonstrated (Hallett, 1961; Kobayashi, 1967; Mason et al., 1963); however, prevous attempts to explain the measured temperature dependence of the step velocity on ice crystals have not been wholly successful (Hobbs and Scott, 1965). In a simplified way, the trends with temperature of all growth variables (linear growth rates, step velocity, and migration distance) may be thought of as a superposition of a strong average trend upward with increasing temperature together with nearly discontinuous change between each maximum and associated minimum.

More current thought considers ice crystal growth habit as a consequence of the difference in behavior of surface water molecules such as migration, nucleation, landing and leaving on the basal and prism planes (Rogers and Vali, 1978; Pruppacher and Klett, 1978). Vapor transport, determined by the diffusion field near the growing crystal, must be in concert with the thermal transport field. The deposition coefficient must therefore be the consequence of the surface processes of water molecules (Fukuta, 1978). Variation of the deposition coefficient on the basal and prism planes is expected when the habit develops, and in fact does, as shown by the variation of deposition coefficients with respect to temperature on the basal plane (Armstrong and Fukuta, 1977). Changing deposition and thermal accommodation coefficients, on the basal and prism planes, have caused a reorientation of thinking with regards to ice crystal growth kinetics. Previously accepted Maxwellian surface conditions have been proven not to exist and have been replaced with the new non-Maxwellian kinetics (Fukuta, 1978), which include the effects of the deposition and thermal

accommodation coefficients. Features of the non-Maxwellian theory of crystal growth include slower growth rates, cooler crystal surfaces compared to that of a Maxwellian crystal, and indirect routes of vapor and heat transport.

Throughout the history of study of ice crystal habit development many mechanisms for this behavior have been postulated. Of these mechanisms, one has persistently resurfaced; i.e., the liquid-like layer. The possible existence of a liquid-like layer on the surface of ice was first mentioned by Faraday (1859). Faraday's liquid-like layer was not considered to be normal water, for it was assumed to be in *equilibrium on one side with ice and on the other side with the vapor.* This theory offered an early explanation, although no proof, for the many unusual surface properties of ice. Weyl (1951) considered the existence of the liquid-like layer from an energetic standpoint. Polarization of ice surface ions plus a recession of positive ions there would reduce the electric field at the surface. He considered this transition layer to have the characteristics of liquid and estimated the thickness at few hundred molecules. Fletcher (1962, 1963, and 1968) tried to develop a quantitative theory of the surface structure of ice. His approach was partly thermodynamic coupled with statistical mechanics. The objective of his approach was tc show that the free energy of ice can be reduced if a liquid-like layer forms on the surface. Fletcher calculated definite equilibrium thicknesses of the liquid-like layer at about 10 angstroms, increasing as temperatures get warmer. The growth of snow crystals from the vapor phase was interpreted by Lacmann and Stranski (1972) with the aid of a quasi-liquid layer. More recently, growth of ice with a Vapor to Quasi-Liquid-Layer to Solid mechanism

was presented by Kuroda and Lacmann (1980). This theory is based on the premise that there are three growth mechanisms: (1) vapor to quasi-liquid-layer to solid mechanism, (2) adhesive mechanism, (3) two-dimensional-nucleation mechanism. Although this approach appears generally correct, the assumption was used that in determining the change in surface free energy, the liquid-like layer is extended from the surface to the core of the ice crystal. Possibly a more correct approach would be to extend the liquid-like layer only to a depth where the surface exerts a strong enough force on ice to cause a phase change from solid to liquid. This depth would not be the entire surface to core thickness of the ice crystal, therefore free energy calculations would be less than predicted by Kuroda and Lacmann.

As can be seen from the above discussion, many theories have been postulated as to the reasons of changing ice crystal growth habit. No single theory or combination of theories has satisfactorily described the mechanisms involved in ice crystal growth. Much ground work has been laid so far, but many more theoretical as well as experimental studies must be accomplished before ice crystal phenomena will be adequately explained.

Chapter 3

EXPERIMENTAL TECHNIQUES USED IN THE PAST

3.1 General Considerations for Ice Crystal Growth Habit and Shape Instability Studies

The primary concern for ice crystal growth habit and shape instability studies is the accurate control of supersaturation. In this regard, even the best measurements previously performed using diffusion chambers are now somewhat suspect for the main reason that the measurements had been carried out before the aspect ratio problem of thermal diffusion chambers was brought up (Tomlinson and Fukuta, 1979). Re-evaluation of previous habit studies, including the determination of threshold conditions under which dendritic growth just starts, is needed under properly controlled temperature and supersaturation, the latter in particular, starting from small quiescent ice crystals.

Exploration of the mechanism for habit development, particularly under the influence of the possible effect of the liquid-like layer on ice, appears necessary. The study requires identification of a specific phenomenon which directly and sensitively relates to the behavior of the layer. Desirably, the study should be carried out without influence of substrates (Frank, 1975). The problem may also have implications in other fields were ice crystals are involved such as glaciology.

The basic experimental system should include the ice crystals, the surrounding environment, and the observation device, in addition to the subsequent analysis. Each of these must be well-defined and properly secured.

3.2 Methods of Ice Crystal Generation

Ice crystal growth studies, regardless of what specific behavior of the ice crystal is being observed, normally require ice crystal generation, or more simply, initial ice nucleus activation or ice nucleation. Techniques used for the generation of ice crystals and their subsequent use by previous investigators are as varied as the different environments in which the crystals are grown.

Ice nucleation in the atmosphere can generally be divided into two groups, i.e. homogeneous and heterogeneous.

3.2.1 Homogeneous Ice Nucleation

Homogeneous ice nucleation occurs when the phase change in the solid state takes place entirely without the aid of a foreign particle or surface. Temperatures at or below -40°C (Schaefer, 1948) are required for homogeneous ice nucleation. Two possible subdivisions of homogeneous ice nucleation exist, i.e., homogeneous freezing which occurs after either homogeneous or heterogeneous condensation, and homogeneous deposition. Homogeneous freezing preceded by homogeneous condensation is the commonly accepted mechanism for homogeneous ice formation. Experimental evidence, as well as theoretical estimation, has shown that homogeneous deposition is unlikely in the atmosphere. For homogeneous deposition nucleation to occur, the rate has to be

greater than that for condensation, or in other words, the free energy of critical embryo formation for the deposition nucleation has to be less than that for condensation nucleation. Experiments by Maybank and Mason (1959) have shown just the opposite.

The fact that ice crystals appear in the atmosphere at temperatures warmer than -40°C indicate that although homogeneous ice nucleation does exist, it is not the primary mechanism of ice crystal nucleation.

3.2.2 Heterogeneous Ice Nucleation

Heterogeneous ice nucleation can be defined as the mechanism for the vapor and/or liquid phase change to the solid state with the aid of a foreign particle or surface. It is heterogeneous ice nucleation that is thought to be the primary mechanism of ice formation in the atmosphere.

Foreign particles and other natural surfaces found in the atmosphere have been labeled as Ice Nuclei (IN) by cloud physicists. IN exist in small numbers in the atmosphere; however, the number varies greatly due to geographical location, time of day and year, and general meteorolgoical conditions. By comparison, the number of ice nuclei are up to three orders of magnitude less than that of cloud condensation nuclei in the atmosphere. Since the formation of ice crystals have been found to be important in precipitation processes, the effect of injecting additional IN into supercooled clouds, to enhance precipitation or weather modification, has been studied in laboratory as well as in field experiments.

Three subdivisions of heterogeneous ice nucleation exist

(Schaller and Fukuta, 1979). The first is heterogeneous deposition nucleation and involves the direct phase transition from the vapor to the solid on a foreign particle or surface, i.e., IN. This type of nucleation is favored under large supercooling and small supersaturation with respect to ice. Heterogeneous condensation-freezing nucleation, which is considered as an important contributor to cloud processes, involves all three phases. Vapor condenses onto an IN first. Then the droplet is frozen to form the solid phase (ice crystal). Contact-freezing is the final subdivision of heterogeneous nucleation and requires a collision between a supercooled droplet and an ice nucleus particle. Upon contact, the supercooled droplet is frozen. Contact-freezing can occur at warmer temperatures than either deposition or condensation-freezing nucleation does.

3.2.3 Laboratory Techniques Previously Used for Ice Crystal Generation

The present study does not utilize effective IN or heterogeneous ice nucleation. It does, however, require ice crystals that are free of effects of IN. For this reason, the basic laboratory techniques of ice crystal generation were reviewed with the intent of utilizing the most suitable method for our study.

One area of ice crystal studies is concerned exclusively with effective IN and ice nucleation. The injection of natural as well as artificial IN into expansion cloud chambers, mixing cloud chambers, diffusion chambers and thermal diffusion chambers, with the intent of observing ice nucleation is the goal of these studies. Likewise, the observation of individual ice crystals in similar chambers, their habit, growth and behavior is another field of study. Both areas of study have

one basic process in common, that is the initial ice nucleus activation or ice crystal generation. Many methods of ice crystal generation have been employed and following are a few that we considered for our study.

aufm Kampe et al. (1951) seeded supercooled fog with dry ice, silver iodide, and cobalt iodide for investigations of the influence of temperature on the shape of ice crystals growing at water saturation. Similarly, Mason (1953) seeded supercooled clouds in a room-sized cloud chamber with dry ice or silver iodide for his study of the growth of ice crystals. Natural snow crystals were caught and placed in an insulated box cooled by dry ice during the experiments of Gold and Powers (1954). Seeding of a supercooled fog by a chilled brass rod was the technique used by Fukuta (1969) in his study of the growth of small ice crystals. Distilled water droplets rapidly frozen in a cold box containing dry ice and then transferred to a thermal diffusion chamber was the method used by Rottner and Vali (1974) in their study of ice crystal growth habit. Finally, Ryan et al. (1974 and 1976) used a rapid adiabatic expansion of air called the "popping bubble technique" in their studies of the densities and growth rates of ice crystals. It is this last method of ice crystal generation that we chose for our study and it will be explained in more detail later.

3.3 Methods for Ice Crystal Growth Studies

The study of ice crystal growth in their natural environment is difficult because even if they are captured, the environmental conditions, the influence of aircraft and other equipment used in the capture, the timing and human error make an accurate determination of the ice crystal growth history difficult. For this reason, researchers

have attempted to reproduce the natural environment of ice crystal growth in the laboratory as accurately as possible. A series of different chambers have been developed for their laboratory studies. Although there are many different designs of chambers used in ice crystal studies, each having certain advantages and disadvantages, we shall discuss four main groups and give examples of each, that appear unique and relevant to this study. They are convection chambers, mxing cloud chambers, diffusion chambers, and thermal diffusion chambers

3.3.1 Convection Chamber

Nakaya (1954) carried out a series of experiments to determine the effects of different environmental conditions on ice crystal habit using a convection cloud chamber. The ice crystals were grown on a rabbit hair stretched on a frame and suspended in a convective air stream containing warm vapor which came out of an electrically heated reservoir. The level of supersaturation was controlled by varying the temperature of the vapor source. The temperature of the air immediately surrounding the crystals was a function of the temperature of the vapor source and that of the thermostat which surrounded the entire apparatus. Ice crystals were grown under different combinations of temperature and supersaturation. Nakaya's chamber relied upon convection, which must have caused fluctuations in both the temperature and supersaturation. In addition, unless fog formation had been completely prevented water supersaturation was not achieved and if it had, the temperature measurement was unlikely to be accurate. Even with these problems, Nakaya reported data showing the relationships of temperature and suersaturation on ice crystal growth habit.

3.3.2 Mixing Cloud Chambers

aufm Kampe et al. (1951) and Mason (1953) studied the growth of ice crystals in mixing cloud chambers. Room-sized cold chambers, of known and controllable temperatures, were injected with steam producing a supercooled cloud. Ice crystals were grown under a condition near water saturation after seeding the cloud with dry ice or silver iodide. Ice crystals were replicated by the Formvar method (Schaefer, 1948b) and subsequently studied under the microscope. Although reasonable temperature and supersaturation control could be maintained, the effects of growth competition among formed ice crystals were unknown. In addition, crystals could be grown at only one level of saturation, i.e., water saturation.

An experimental study on the growth of small ice crystals was conducted by Fukuta (1969). The cloud chamber (Fig. 1) was built with double walled plexiglass, cooled with a 70% aqueous glycerine solution to a predetermined temperature, circulating between the walls. A black cloth was placed on a wood frame 6 mm inside the wall to prevent frost. A cooled copper chamber was placed on top of the plexiglass cloud chamber to serve as a fog source and precooler. Waterwarmed electrically, supplied moisture at the top of the copper chamber and the fog was formed on condensation nuclei existing in the room. Two thermocouples were used to record the temperature. The cloud chamber was illuminated through a slit by a light beam chopped at a known time interval. Under the predetermined time intervals of illumination, photographs were taken of the falling ice crystals, providing fall velocity measurements. For ice crystal growth and habit measurement, the plexiglass chamber was placed in a freezer an after an equilibrium

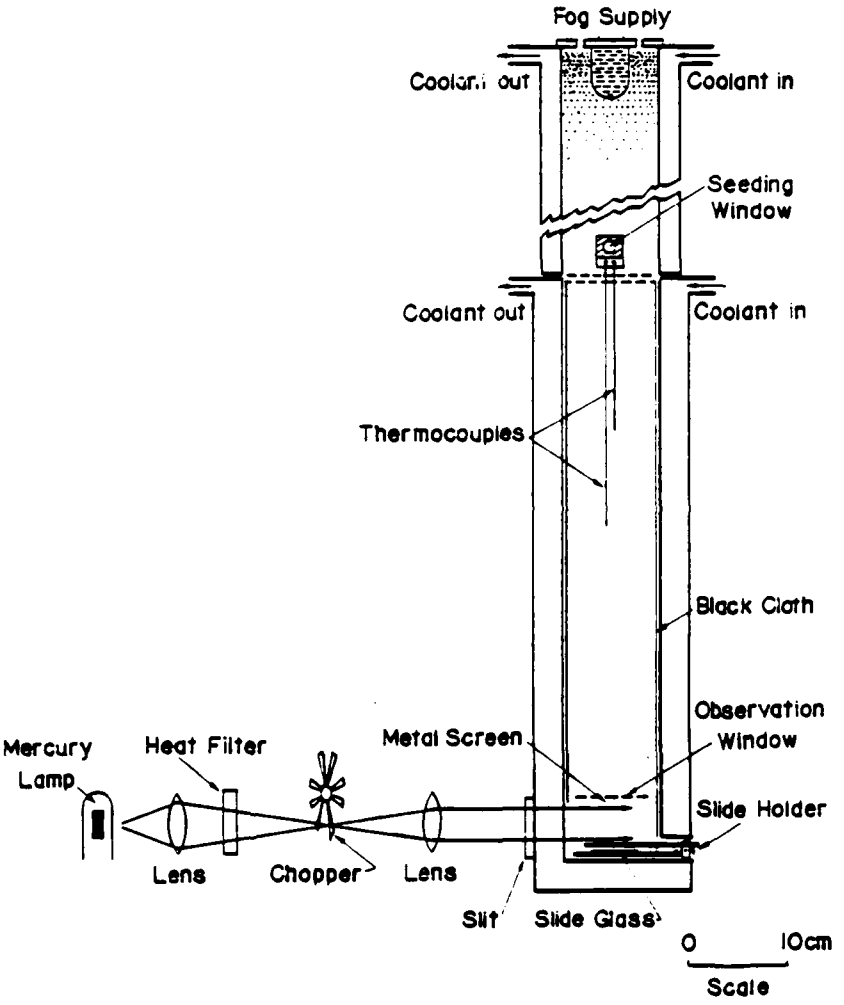

Figure 1. Fukuta's supercooled fog chamber (Fukuta, 1969: Experimental studies on the growth of small ice crystals. J. Atmos. Sci. 26, p522.).

was established, the supercooled fog was seeded. Ice crystals grew, fell out, and were caught on glass slides covered with silicone oil and subsequently photographed under a microscope. The photomicrographs were directly used to determine ice crystal habit and dimensions, but for accurate mass determinations the ice crystals were rapidly melted and diameters of the resulting droplets were measured. Fukuta's chamber was unique in that he could analyze simultaneously many different facets of ice crystals; however, the crystals could only be kept aloft for approximately one minute and, as such, fall velocities, growth, and habit development of ice crystals were limited with respect to this time.

3.3.3 Diffusion Chambers

A diffusion chamber utilizes diffusional transportation of water vapor saturated at the environmental temperature onto a sample crystal held on a cold stage where the temperature is lower. The pressure of water vapor arriving at the ice crystal surface is the same as that in the environment, so that the supersaturation on the ice crystal surface can easily be estimated and controlled.

Shaw and Mason (1955) studied the growth of ice crystals with the aid of a diffusion chamber. In their chamber, crystals were held on a metal surface with independently controlled temperature and supersaturation. The metal surface was located in the center of a cylindrical metal chamber. The walls of the cylinder were hollow and could be cooled to a desired temperature by circulating chilled petrol through the enclosed space. Ice covered the inner walls and base of the chamber such that the air in the experimental chamber, which was stirred

by a small fan, was saturated with respect to ice at a predefined temperature. A thermocouple embedded in the surface of the ice layer at the bottom of the chamber recorded the temperature. The metal plate, on which the ice crystals grew, was supported on a copper rod, which was insulated from the chamber and dipped into liquid air. The plate was cooled, by varying the electric current through a heating coil, to a desired temperature which was lower than that of the surrounding air. The temperature of the crystals was recorded by a thermocouple placed immediately below the metal surface, and the saturation ratio of the air in the immediate vicinity of the crystal was obtained as the ratio of the equilibrium vapor pressure of the air in the experimental space ice-saturated at the wall temperature and that ice-saturated at the plate temperature respectively. Ice crystals were viewed through a microscope, photographed at 1 minute intervals, and the growth rates were determined from measurements made on the negatives by a micrometer eyepiece. Ice crystals were studied at temperatures from -5 to -40°C under conditions of saturation relative to liquid water.

3.3.4 Thermal Diffusion Chambers

Thermal diffusion chambers, which are actually a special type of cloud chamber, have been widely used in both cloud condensation nuclei (CCN) and ice crystal studies. The first thermal diffusion chamber was developed for use in nuclear physics by Langsdorf (1934) but was not used for atmospheric studies until 1952 (Schaefer, 1952). Advantages of these chambers are that they are convectively stable and capable of reproducing reasonably accurate temperature and supersaturation fields. The principle of a thermal diffusion chamber is the diffusion of heat

and water vapor downward through the horizontally stratified air layers of different temperatures creating different degrees of supersaturation.

To understand the mechanisms of ice crystal growth, a controlled environment was required where temperature and supersaturation could be accurately maintained. The thermal diffusion chamber satisfied this requirement. In a thermal diffusion chamber, a temperature difference is maintained usually between two horizontal and parallel metal plates with the top being warmer than the bottom. The top plate, either wet porous or ice coated, acts as a vapor source while the bottom plate, similarly coated, acts as a vapor sink. On both plates, the saturation ratio with respect to the condensed phase is unity, since there is no vapor density excess. Constant gradients of temperature and water vapor pressure exist in the stable air of the thermal diffusion chamber. Since the saturation vapor pressure for water or ice varies non-linearly with temperature, a supersaturation appears at points between the plates. The supersaturation or excess vapor density is maximum approximately at the mid-point between the two plates, i.e., the center of the chamber. Maximum supersaturation values in the chamber may be raised or lowered by increasing or decreasing the temperature difference between the plates for a given centerline temperature. Unlike a diffusion chamber, ice crystals are generally grown suspended between the two plates in a thermal diffusion chamber.

Problems inherent to thermal diffusion chambers include aspect ratio or the ratio of width to height (Twomey, 1963; Fitzgerald, 1970; Elliot, 1970; Saxena et al., 1970; Tomlinson and Fukuta, 1979), the small vertical height usually required in the chamber, and possible

initial transient supersaturations when a sample is introduced.

Thermal diffusion chambers can be either static or dynamic and although many types have been developed, three distinctive chambers showed promise for this study. They are the parallel plate chamber, the horizontal gradient chamber, and the wedge-shaped chamber.

3.3.4.1 Parallel plate chamber. Hallett and Mason (1958) utilized a thermal diffusion chamber for the study of ice crystal growth. Ice crystals were grown on a thin nylon or glass fiber suspended vertically between two ice plates and different supersaturations were achieved by the position of crystals growing on the fiber and by lengthening or shortening the distance between the ice plates. With this chamber, Hallett and Mason were able to grow ice crystals at temperatures between 0 and -5°C with supersaturations ranging from a few to 300%. Results of ice crystal growth habit were similar but more extensive than those produced by Nakaya (1954). Errors in temperature and vapor pressure fields in this study could have been large due to the generally small aspect ratio.

3.3.4.2 Horizontal gradient parallel plate chamber. A new and unique horizontal gradient, continuous flow, ice thermal diffusion chamber was built by Tomlinson (1980) for the study of condensation-freezing and deposition nucleations. The chamber (Fig. 2) constructed of copper plates and Plexiglass, cooled by thermoelectric modules, had a working height of 6 mm between the top and bottom plates, which were coated with ice. Excess heat generated by the thermoelectric modules was carried away by antifreeze from a circulating bath. Heat pipes soldered to the top and bottom plates aided in maintaining uniform

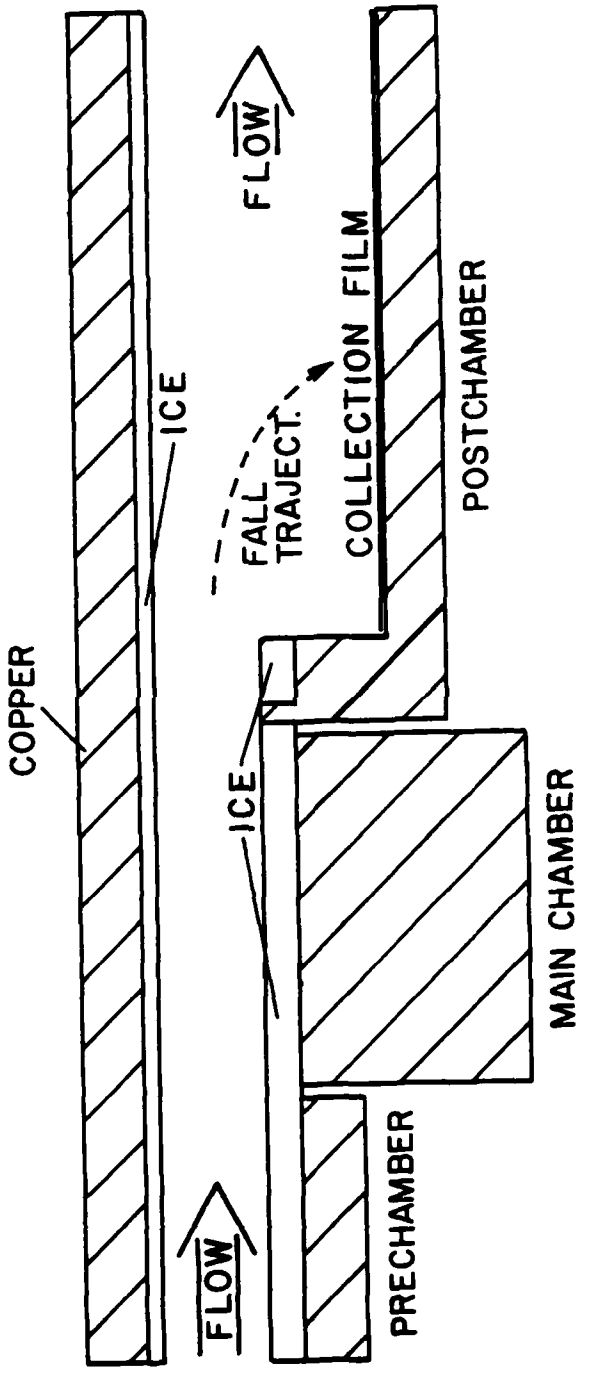

Figure 2. Horizontal gradient parallel plate ice thermal diffusion chamber (Tomlinson, 1980).

steady-state temperature conditions.

Constant temperatures and supersaturation were achieved in the vertical center of the chamber by sandwishing the sample air with filtered air. Sample thickness was adjusted by controlling its flow rate. The prechamber was used to recondition the sample air so as to be devoid of supersaturations when the sample air entered the main chamber. A 15 cm length of the prechamber allowed steady-state conditions to be quickly achieved. The top plate of the main chamber was held isothermal while a temperature gradient was maintained across the bottom plate. The result was a range of supersaturation across the horizontal median plane of the chamber with near isothermal conditions. Nucleated ice crystals were collected, after falling into the post chamber, on copy film and recorded by use of a camera for subsequent analysis.

3.3.4.3 Wedge-shaped chamber. A new geometry was introduced to thermal diffusion chambers when Schaller and Fukuta (1979) developed the wedge-shaped ice thermal diffusion chamber. With a triangular design, as opposed to previously used rectangular chambers, they could produce a range of supersaturations at a constant temperature, along a median plane within the chamber under stable air stratification. This, therefore, eliminated the disadvantage of a single set of temperature and supersaturation in the conventional rectangular thermal diffusion chambers. Ice nucleation studies were conducted utilizing this chamber. Since the wedge-shaped ice thermal diffusion chamber is the apparatus we chose for our experiments, a detailed discussion will be given later.

Chapter 4

EXPERIMENTAL APPARATUS

4.1 Method of Ice Crystal Generation and Ice Crystal Growth Used in this Study

A review of previous ice crystal experiments was made in an attempt to find a method of ice crystal generation and growth that could be tailored to our study. Ice crystals grown by rapid adiabatic expansion of air was our choice for clean ice crystal generation as was the wedge-shape ice thermal diffusion chamber our choice for ice crystal growth studies.

4.1.1 Ice Crystal Generation by Adiabatic Expansion of Air

Rapid adiabatic expansion was the method of ice crystal generation used in this study. A standard chest freezer cooled to -27°C was used as the environmental chamber. The moisture source was provided by blowing our breath into the chamber until a supercooled fog formed. Ice crystals were formed by the "popping bubble" technique, by which a small polyethylene bubble, commonly found in protective packaging material, was placed in the supercooled fog and compressed. When compressed, the bubble popped and following the principle of rapid adiabatic expansion, multitudes of ice crystals were formed. Addition of moisture into the chamber insured the crystals would grow to a sufficient size to be transferred to our working apparatus, which will be explained later. This process of ice crystal generation was well suited to our needs

since it was first simple to achieve, second, the number of ice crystals generated was easily reproducible and third, there was no effect of contamination to the ice crystal.

4.1.2 Wedge-Shaped Ice Thermal Diffusion Chamber

Our choice of primary apparatus for studying ice crystal growth habit and shape instability was the wedge-shaped ice thermal diffusion chamber developed by Schaller and Fukuta (1979). With this chamber, they studied ice nucleation on aerosol particles under freely suspended conditions and the design of the chamber allowed observation of ice nuclei, for a given sample, over a range of supersaturations under the selected temperature. This chamber eliminated the time-consuming process of observing ice nucleation under one given set of temperature and supersaturation as found in parallel plate diffusion chambers and eliminated the problem of changing sample characteristics which was apt to happen during the multitude of experiments required in a parallel plate chamber. The wedge-shaped design of this ice thermal diffusion chamber offered a feature which we desired for our study, i.e., a steady-state supersaturation field varying as a function of horizontal position under a constant temperature.

The mechanism by which supersaturations with respect to ice and water develop in a normal parallel plate thermal diffusion chamber operated at subfreezing temperatures is shown in Figure 3. The top plate A is kept warmer than the bottom plate C, and both plates are covered by ice such that the water vapor pressure is saturated with respect to ice at both the top and bottom plates. T_B is the temperature in the middle of the chamber with the developed temperature and vapor fields

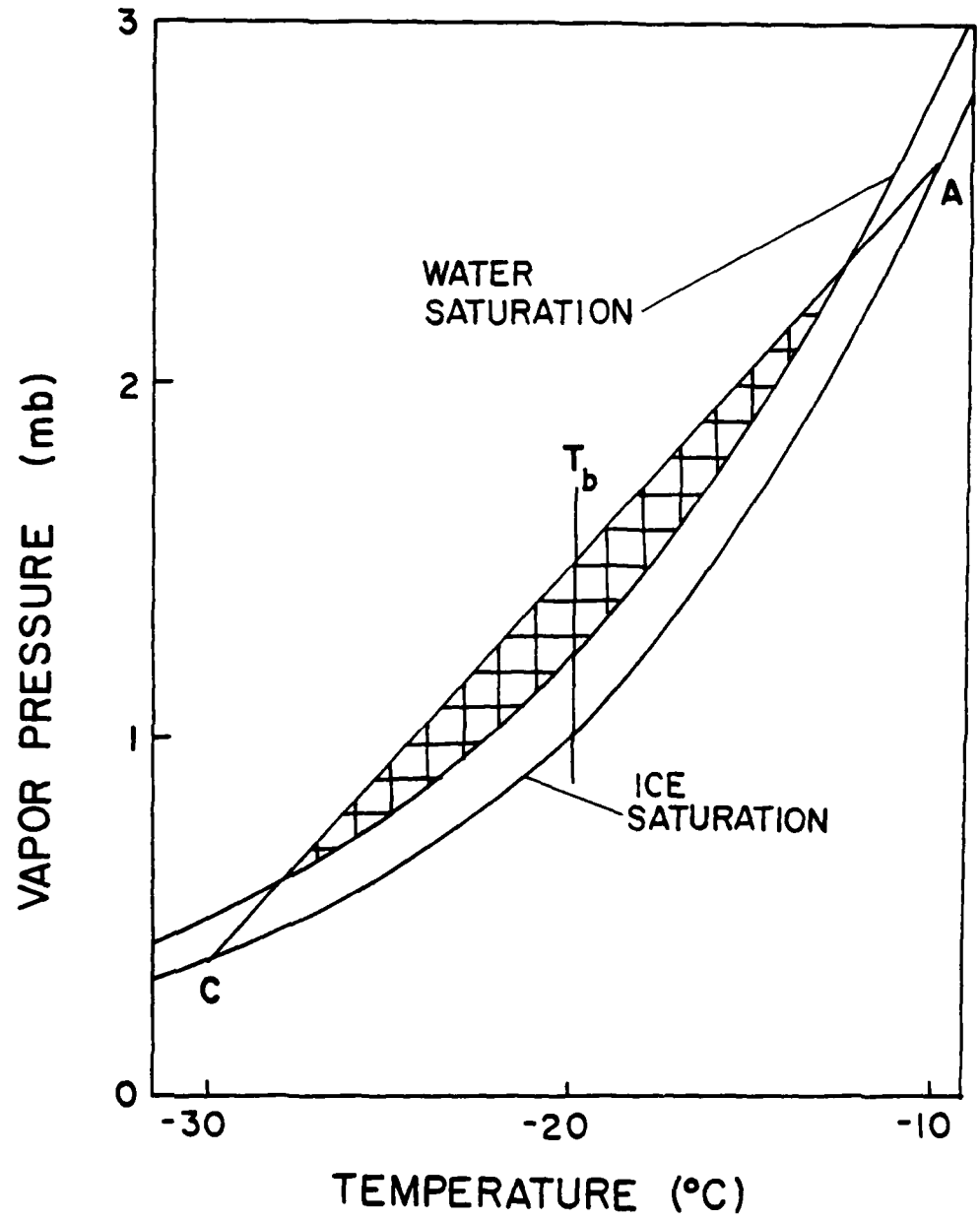

Figure 3. Development of ice and water supersaturations in a parallel plate ice thermal diffusion chamber. (Schaller and Fukuta, 1979: Ice nucleation by aerosol particles. Experimental studies using a wedge-shaped ice thermal diffusion chamber. J. Atmos. Sci., 36, p1789.).

falling on a straight line connecting A and C. Saturation vapor pressure curves for ice and water are concave upward, with the curve for water saturation slightly above that for ice saturation. In a parallel plate ice thermal diffusion chamber, as seen in Figure 3, the top and bottom plates A and C are saturated with respect to ice while interior points in the chamber are either supersaturated with respect to ice or water depending on the temperature difference maintained between the plates. Maximum supersaturation occurs approximately at the midpoint of the chamber height.

A diagram of our wedge-shaped ice thermal diffusion chamber, an improved version of the previous chamber used by Schaller and Fukuta (1979), is shown in Figure 4. It is in some respects similar to the parallel plate chamber but has certain advantages. One advantage is that the wedge-shaped geometry allows us to achieve almost stable stratification of the air at different temperatures. Temperature stratification discrepancies will be discussed later. In the chamber, a temperature gradient occurs both along the wedge-shaped plates, with the top and bottom points of the wide end having the warmest and coldest temperatues respectively, and vertically through the chamber air space. The developed temperature and vapor pressure fields produce a horizontally varying maximum supersaturation at a constant temperature, another advantage of the present chamber.

Operation of the wedge-shaped ice thermal diffusion chamber is based on the following principle. When the temperature and vapor pressure fields in the chamber are under steady-state conditions, the following relations are satisfied with sufficient accuracy:

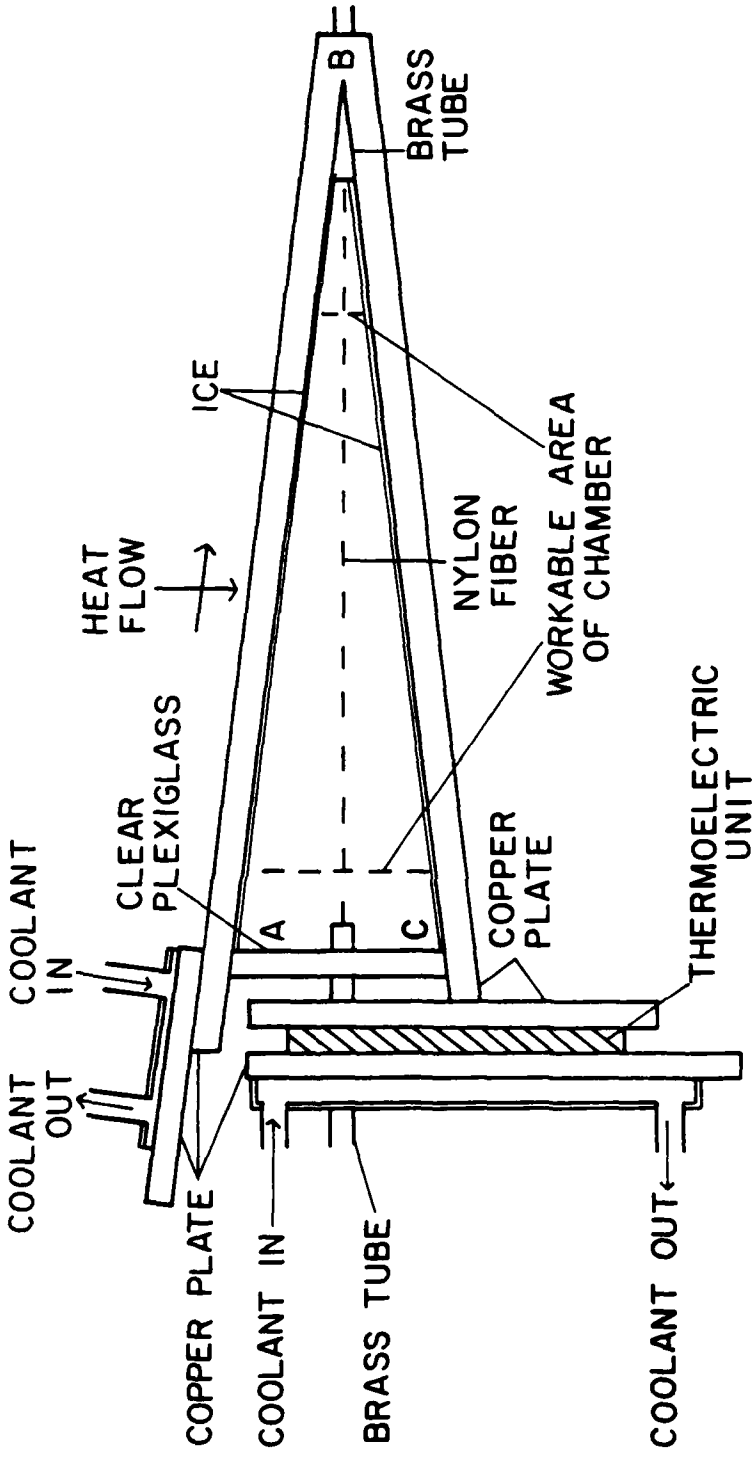

Figure 4. Design of the new wedge-shaped ice thermal diffusion chamber used in this study.

$$\nabla^2 T = 0 \ , \tag{1}$$

and

$$\nabla^2 p = 0 \ , \tag{2}$$

where T is the temperature, p the vapor pressure and ∇^2 the Laplacian operator. Approximating the saturation water vapor pressure over ice on the top and bottom plates along the direction of heat flow by a quadratic function of temperature, i.e., expanded Clausius-Clapeyron equation truncated after the third term, and describe the temperature in the x-y plane, where x is the horizontal direction parallel to the plane of the paper in Figure 4 and y the vertical direction, the solution of (1) is a plane and the solution of (2) is a hyperbolic paraboloid similar to the vapor density profile (Schaller and Fukuta, 1979) shown in Figure 5. A detailed description of the solution is given in Appendix A. The supersaturation with respect to ice is given by

$$(S_i - 1) = \frac{p}{p_s} - 1 \ , \tag{3}$$

where p_s is the saturated vapor pressure over ice and is a function of temperature only. The supersaturation on the horizontal, center plane of the chamber can thus be determined by the temperature and vapor pressure profiles. Katz and Mirabel (1974) showed that an assumption of linear vapor pressure and temperature profiles for a parallel-plate thermal diffusion chamber resulted in errors of supersaturation on the order of 10%. Schaller and Fukuta (1979) confirmed that in the wedge-shaped thermal diffusion chamber, although the quadratic vapor field results in a higher supersaturation value, the linear appoximation

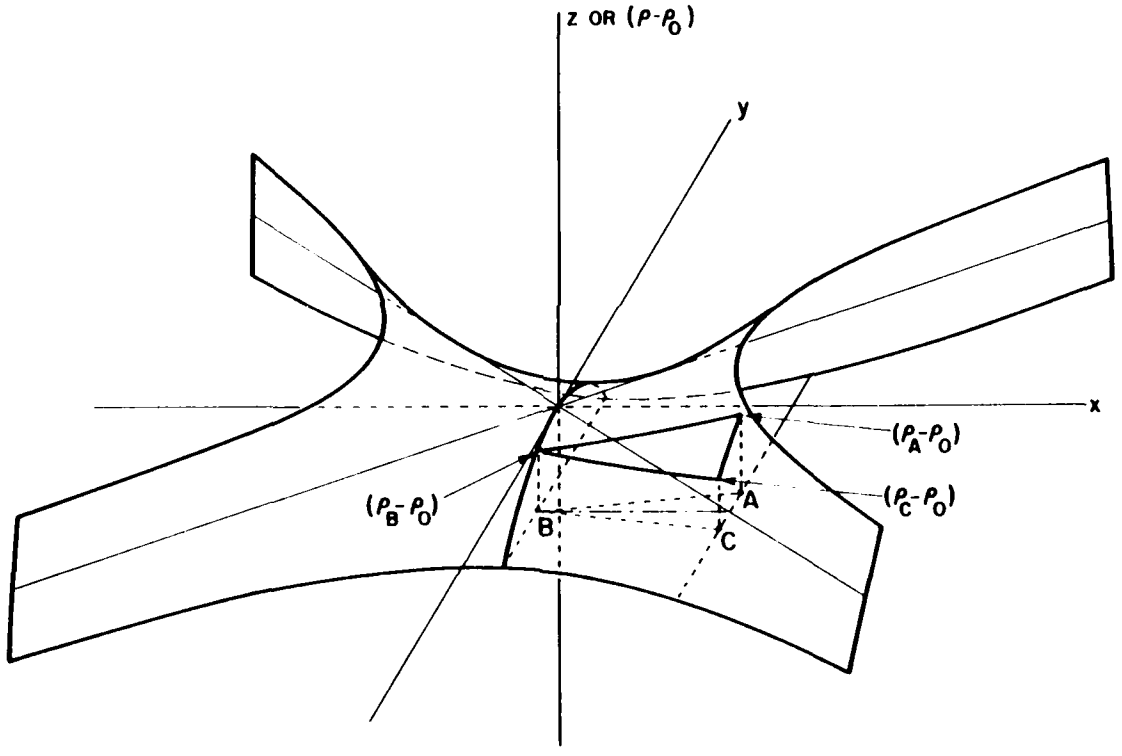

Figure 5. Vapor density profile in the wedge-shaped ice thermal diffusion chamber (Schaller and Fukuta, 1979: Ice nucleation by aerosol particles. Experimental studies using a wedge-shaped ice thermal diffusion chamber. J. Atmos. Sci., 36, p1800.).

for vapor density (or vapor pressure) for supersaturation computations is sufficient in most cases. The expected relative error of 10% in supersaturation values was of the same magnitude as other relative errors in the chamber and thus ignored. Using linear vapor pressure and temperature profiles, temperatures and supersaturations were calculated by means of the following relationships:

$$T_m = \frac{(T_t + T_b)}{2} , \tag{4}$$

where T_m is the centerline temperature, T_t and T_b are the top and bottom plate temperatures respectively, and

$$(S_{im}-1) = \frac{(p_{ti} + p_{bi})}{2p_{mi}(T_m)} - 1 , \tag{5}$$

and

$$(S_{wm}-1) = \frac{(p_{ti} + p_{bi})}{2p_{mw}(t_m)} -1 , \tag{6}$$

where $(S_{iw}-1)$ and $(S_{wm}-1)$ are the centerline supersaturations with respect to ice and water respectively, p_{ti} and p_{bi} are the saturation vapor pressures with respect to ice at the top and bottom plate temperatures, and p_{mi} and p_{mw} are the saturation vapor pressures of ice and water at the mean temperature in the center of the chamber. An example of supersaturation profile (Schaller and Fukuta, 1979) with respect to ice is shown in Figure 6. A zone of water supersaturation can exist at the wide end as well as a zone of supersaturation with respect to ice in the rest of chamber. Combinations of the top and bottom plate

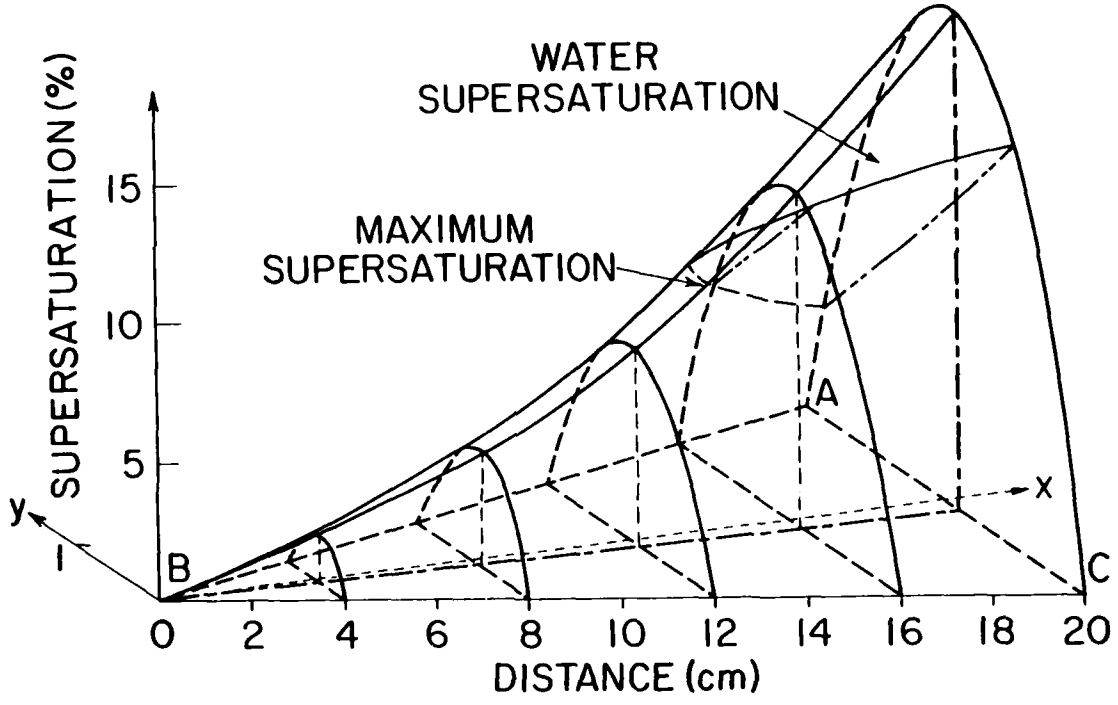

Figure 6. Profile of supersaturation with respect to ice in the wedge-shaped ice thermal diffusion chamber. A, B, and C are the highest, the apex and the lowest points of the chamber. (Schaller and Fukuta, 1979: Ice nucleation by aerosol particles. Experimental studies using the wedge-shaped ice thermal diffusion chamber. J. Atmos. Sci., 36, p1791.).

temperatures will adjust these zones of supersaturation.

Upon experimentation, it was found that the temperature profiles along the top and bottom plates were normally not linear. In fact, the only true linear temperature profiles existed when the center-line temperature of the wedge-shaped chamber was approximately the same as that of the outer environmental chamber. A discussion and description of this non-linearity of temperature is given in detail in Appendix B.

4.2 Apparatus Used in This Study

4.2.1 Design Considerations

Once we decided on using the principle of the wedge-shaped ice thermal diffusion chamber (Schaller and Fukuta, 1979), certain design problems arose which required solutions before construction could begin. Two major problems were encountered and solved to an acceptable degree of error, i.e., heat transfers and aspect ratio.

4.2.1.1 Heat transfers. One objective of using the wedge-shaped ice thermal diffusion chamber was to reproduce accurate temperature and vapor pressure profiles throughout the interior of the chamber. For this reason, the extents of heat transfer were calculated for various chamber configurations to determine which design would give the most accurate temperature and vapor pressure profiles within the chamber, i.e., temperature and vapor pressure profiles with the least inherent errors. Four mechanisms of heat transfer are involved in the wedge-shaped chamber.

The first is the sensible heat flux through the chamber air space defined by the relationship

$$q_s = \frac{dq}{dt} = - AK_a \frac{dT}{dz} , \tag{7}$$

where A is the surface area of the heat passage in the chamber, K_a is the thermal conductivity of air, T is the temperature, and z is the vertical coordinate.

The second is the latent heat flux carried by the vapor diffusional process through the chamber air space, expressed by

$$q_l = L_d \frac{dm}{dz} = - AL_d D \frac{d\rho}{dz} , \tag{8}$$

where L_d is the latent heat of deposition, D is the diffusion coefficient of water vapor in air and ρ is the vapor density.

Radiative heat transfer is the third process considered. It is characterized by the equation (see Appendix C, for detailed derivation)

$$q_r = \frac{\sigma\varepsilon A}{1-R^2} \left[(T_i^4 + RT_i^4) - (T_j^4 + RT_i^4) \right] , \tag{9}$$

where σ is the Stephan-Boltzman constant, R is the reflectivity of ice, ε is the emmissivity of ice, and T_i and T_j are the average temperatures in degrees Kelvin of the top and bottom plates.

The last is the heat conductio through the copper plates given by

$$q_k = \frac{dq}{dt} = - A_c K_c \frac{dT}{dy} , \tag{10}$$

where K_c is the thermal conductivity of copper, A_c the cross sectional area of copper plates perpendicular to the direction of heat flow, and y the length of the copper plates.

The intent of calculating these four heat fluxes was to determine which, if any, could be neglected so that our temperature and vapor pressure determinations at interior points of the chamber would become easier. The length, width and thickness of the copper plates of the wedge along with the average vertical distance between the plates were varied and the values of q_s, q_l, q_r, and q_k were compared to the sum of the heat fluxes q or

$$q = q_s + q_l + q_r + q_k \ . \tag{11}$$

Scale analysis of heat transfers showed the contribution of q_s was 4.5%, q_l was 0.1%, q_r was 5.8%, and q_k was 89.5%. Therefor, by eliminating the sensible heat flux, the diffusional latent heat flux, and the radiative heat flux from our computations, we incurred approximately a 10% error which is of the same order of magnitude with other relative errors determined for the wedge-shaped chamber.

4.2.1.2 Aspect ratio. An understanding of the aspect ratio, defined as the ratio of the diameter to height of a chamber, is a must to obtain accurate ice crystal habit and growth data. Typically, thermal diffusion chambers are constructed using highly heat-conductive metal for the top and bottom plates while the side walls are constructed of either a lesser heat conducting or a thermally insulating material.

For the case of infinite top and bottom plates, the vapor pressure and temperature fields are well-defined. For finite plates, however, regardless of composition of the side walls, an influence on the temperature and vapor fields is exerted by the side walls (Twomey, 1963). Early theoretical discussions, as well as experimental applications,

of thermal diffusion chambers assumed two infinite parallel plates.

The question was raised (Fitzgerald, 1970; Elliott, 1971) as to what aspect ratio is large enough to permit the assumption of diffusion between infinite parallel plates. A minimum acceptable ratio, to support this assumption, must be determined in terms of the dimensions of a thermal diffusion chamber and the experimental technique required to attain accurate data.

Problems of inaccurate data acquisition may be encountered by too great a vertical depth (Byers, 1965). Hallett and Mason (1958) were forced to vary the distance between parallel plates in order to vary the temperatures of the plates, which induced aspect ratio problems. Elliott (1971) recommended a minimum aspect ratio of 5:1. Rottner and Vali (1974) used a 1 cm vertical separation of parallel plates and a 5.4.1 aspect ratio. The most detailed computation of aspect ratio was carried out by Tomlinson and Fukuta (1979). They concluded that an aspect ratio of 2.5:1 would produce supersaturations within 10% of that produced by a truly linear pressure profile.

Our wedge-shaped thermal diffusion chamber has three walls where aspect ratio problems must be considered, i.e., the front wall and the two tapering side walls. We designed our chamber so that the minimum aspect ratio referenced from the front wall is 2.85:1. The minimum aspect ratio referenced from the two tapering side walls is 3.35:1.

4.2.2 Final Design and Construction

The experimental apparatus was designed carefully by considering operational conveniences, accuracy, cost, ease, adoption of auxiliary devices, etc., and performing some computations for design parameters.

Repetition of discussion and redesigning has improved the design of all parts of the apparatus. Six major pieces of apparatus were constructed in this manner. They are the new wedge-shaped ice thermal diffusion chamber, the pre-chamber, the ice crystal slide mechanism, the lateral microscope slide mechanism, the sample transfer device, and the outer environmental chamber.

4.2.2.1 Wedge-shaped chamber. Once we decided to use the wedge-shaped thermal diffusion chamber similar to that used by Schaller and Fukuta (1979), certain design and operational problems of their chamber had to be re-examined and solved before we could begin construction of our chamber. In section 4.2.1, heat transfer and aspect ratio problems have already been discussed. Additional operational problems existed in the Schaller-Fukuta wedge-shaped chamber. They found that it was difficult to maintain steady-state temperature profiles through the copper plates without temperature stabilization at the top edge of the chamber by a circulating coolant. The Schaller-Fukuta chamber was also semi-dynamic whereby an entire air sample, specifically made dry, was injected into the chamber in order to avoid the possibilities of transient supersaturations (Fitzgerald, 1970) particularly in the initial stages of the experiment. Concerning the appearance of the non-steady supersaturation field in the chamber, two types of problems exist. One is caused by introduction of air which is not under steady-state balance with the chamber plates, and the other by non-steady temperature profiles in the plates. For the former problem, Saxena et al. (1970) presented a solution and confirmed that experimental chambers may experience short-lived peak supersaturations which are several times

times higher than the maximum steady-state supersaturation under certain sample and chamber conditions. Associated with this problem of transient supersaturation is the relaxation time or time to re-establish a steady-state condition within the sample. The relaxation time is sufficiently short in our wedge-shaped chamber. The relaxation time of the supersaturation and temperature field in the sample due to the change of temperature at the edges of plates turns out to be much longer and in order to avoid this problem, it was decided not to change the plate temperatures during an experimental run. Instead of trying to establish steady-state fields after ice crystal introduction in the chamber, ice crystals on a fine fiber were introduced into pre-established fields of temperature and supersaturation with the help of the ice crystal slide mechanism so that within a fraction of a second, the fields around the crystals were re-established and reduced the error to a minimum.

We designed our wedge-shaped chamber with the specific goal of improving the accuracy of the Schaller-Fukuta chamber. First of all, we decreased the wedge angle to 5° to give an acceptable aspect ratio for the chamber. We also increased the thickness and decreased the width of the copper plates, insulated the plates with expanded polystyrene wherever possible, and placed the entire wedge chamber in a deep freezer. This reduced the nonlinear problem of temperature profiles through the plates. It was decided to operate our chamber in the static manner, and as such, would require no direct injection of a sample of air containing ice crystals, thus alleviating any difficulties with transient supersaturations and relaxation times. Instead of injecting ice crystals directly into the wedge-shaped chamber, ice crystals were impregnated on a fine fiber in the prechamber by injecting

a large number of small ice crystals and as explained above, the ice crystal impregnated fiber was then slid into the chamber.

The final design of our wedge-shaped ice thermal diffusion chamber is shown in Figure 4. The top and bottom plates are made of copper with a 0.635 cm thickness and areas of 25.4 cm × 10.16 cm and 24 × 10.16 cm respectively. A 2.5° angle is cut 1.26 cm from the face of the back end of each plate, so that when secured together, they form the 5.0° angle of the wedge. A 0.635 cm copper plate is vertically soldered to the front end of the bottom plate and a second 0.635 cm copper plate, upon which is soldered a brass channel is attached to the first plate by nylon bolts. Sandwiched between these two copper plates are four Cambion thermoelectric modules which provide the cooling to the bottom plate. Power to the thermoelectric modules comes form an Epsco Inc. Model D-126T filtered D.C. power supply. Cooled anti-freeze continuously circulates through the brass channel and carries away the excess heat generated by the thermoelectric modules. A 0.635 cm copper plate, also with a brass channel soldered to it, is itself soldered horizontally to the upper face of the top plate at the front end. Antifreeze circulating through the brass channel furnishes the level of temperature to be set and the stability to the top plate. The anitfreeze is cooled and circulated by a Forma Scientific Model 2160 Bath and Circulator. The front and both side walls of the chamber are made of 0.635 cm Plexiglass.

Due to aspect ratio and microscope field diameter considerations, the workable interior area of our wedge-shaped chamber is approximately 14.6 cm long, i.e, 2.54 cm from the Plexiglass front wall and 5.72 cm from the point where the top and bottom plates converge. The

height of the workable area of the chamber is 1.78 cm at the wise end and 0.5 cm at the narrow end.

Temperature measurements are made with copper-constantan thermocouples with 30 gauge extension wires. The thermocouples were soldered to obtain a good contact between the copper and constantan wires and were painted with a Plexiglass solution to electically insulate them from the copper plates. They are secured to the outside surfaces of the top and bottom plates by electrical tape. The temperature is measured at six points in the workable chamber: wide end, center, and narrow end of both the top and bottom plates. The voltage output of the thermocouples is measured using a Keithley Model 174 Digital Multimeter. Temperatures from the six locations are recorded and displayed automatically by a TERAK minicomputer where thay are recorded every 25 seconds on a magnetic disk and displayed on a video screen.

To act as a guide for the ice crystal transfer mechanism, two 0.476 cm diameter brass tubes extend into the wedge-shaped chamber from both the front and back ends. They are aligned through the vertical center of the chamber and located 3.00 cm from the left-hand side wall, giving a minimum aspect ratio of 3.35:1 at the wide end of the workable chamber.

A nylon fiber 0.05 mm in diameter suspended between two glass rods can be moved in and out of the vertical center of the wedge-shaped chamber and will be discussed in more detail in later sections.

Figures 7 and 8 illustrate different close-up views of our wedge-shaped ice thermal diffusion chamber while Figure 9 shows the chamber in its operational configuration.

4.2.2.2 Pre-chamber. It was determined that a pre-chamber was

Figure 7. Photograph of the wedge-shaped ice thermal diffusion chamber.

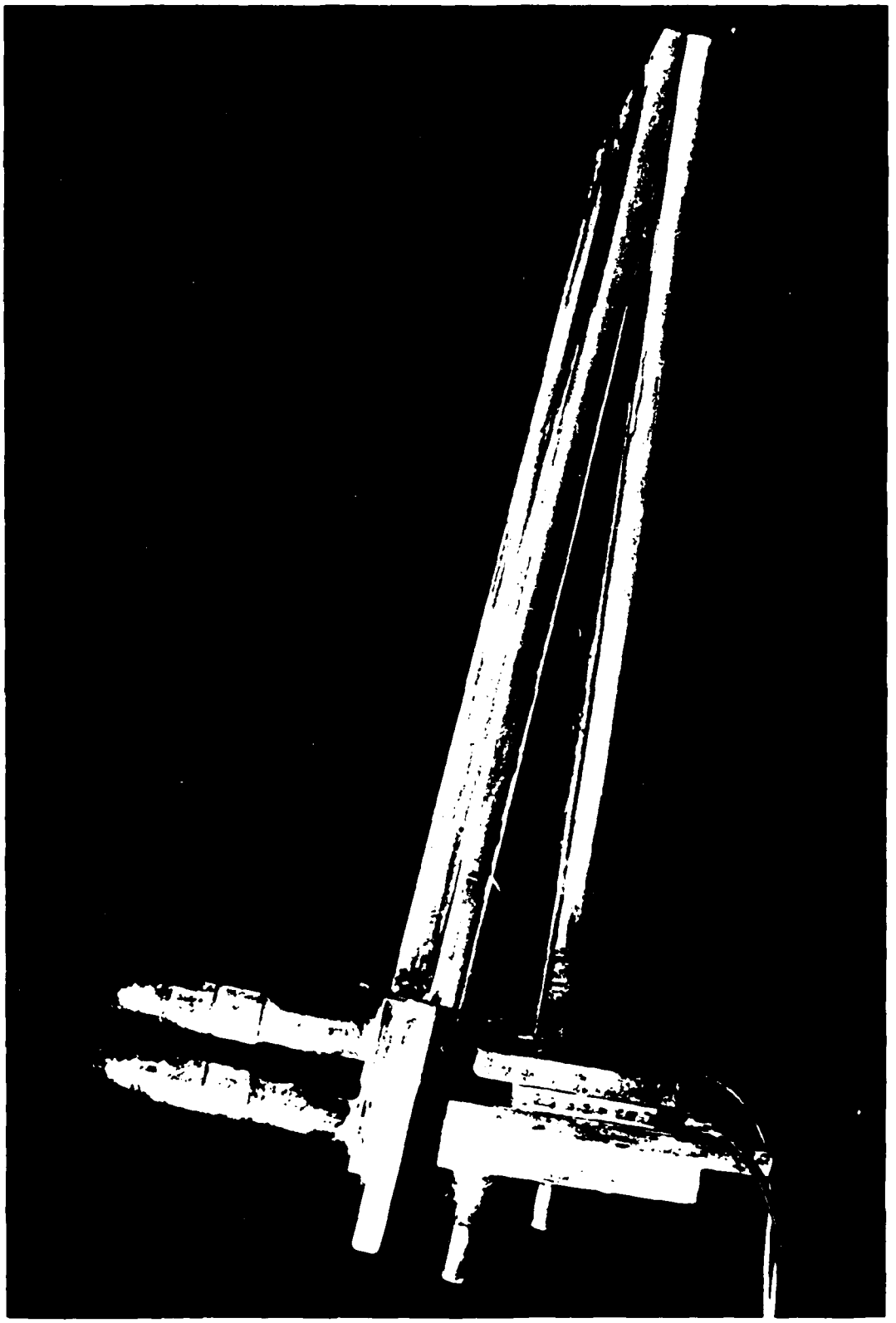

Figure 8. Photograph of the wedge-shaped ice thermal diffusion chamber with top plate removed.

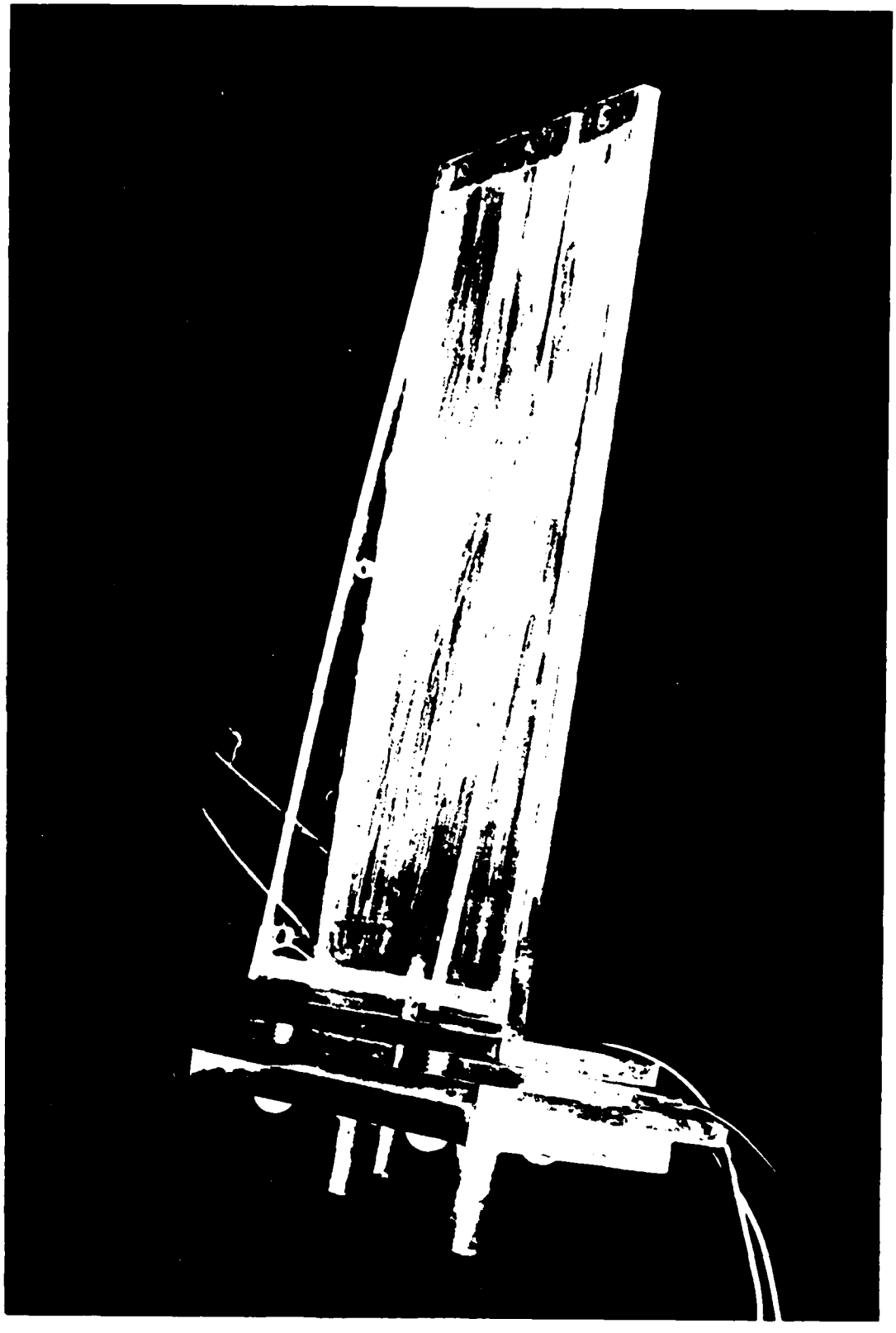

Figure 9. Photograph of the wedge-shaped ice thermal diffusion chamber and primary support equipment in their operational configuration.

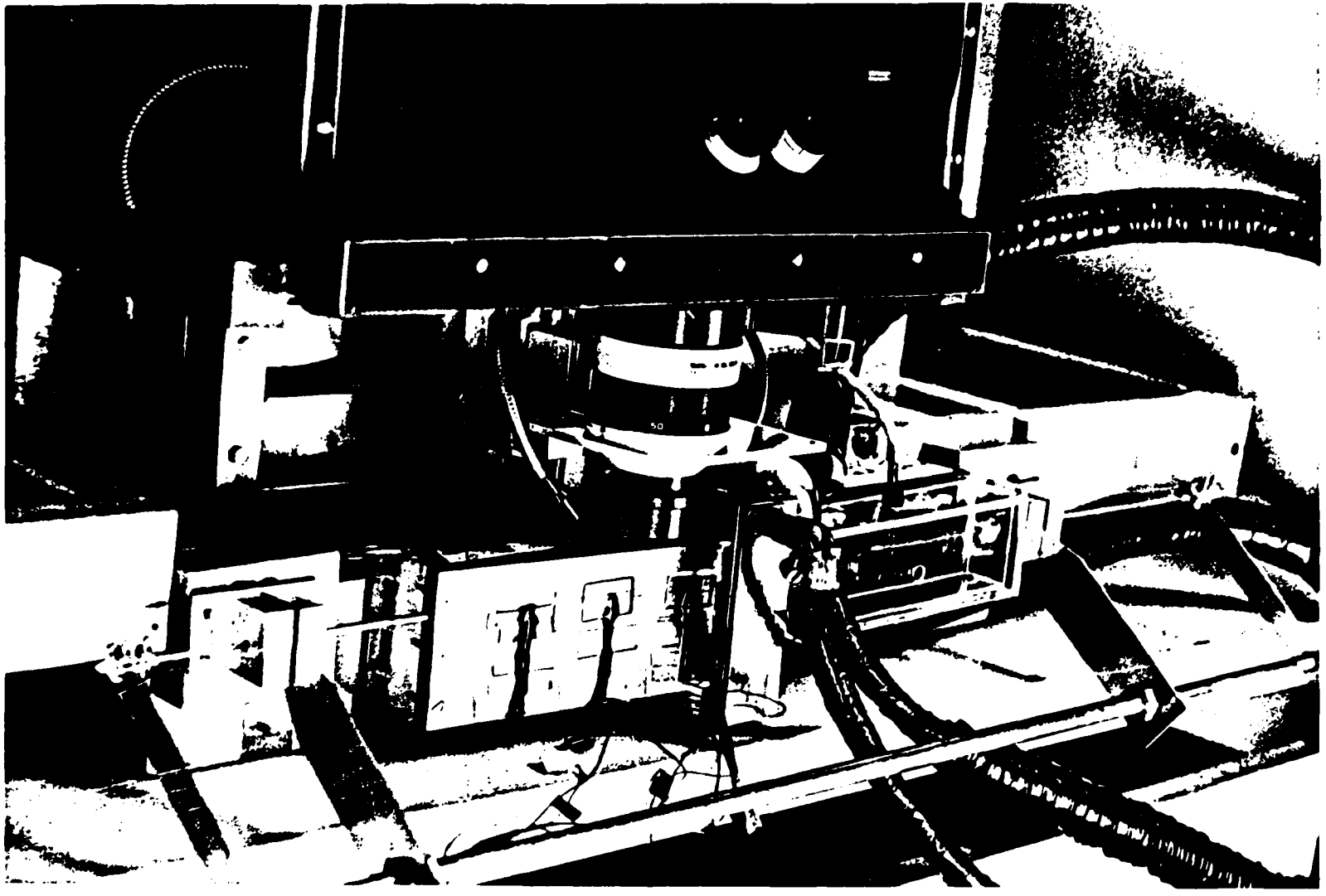

required in addition to the primary wedge-shaped ice thermal diffusion chamber. The purpose of this pre-chamber was to impregnate the nylon fiber with ice crystals previously nucleated. After a sufficient number of crystals were determined to have stuck, the nylon fiber would be traversed horizontally into the wedge-shaped chamber where ice crystal growth would commence immediately in the final environmental condition. The original pre-chamber, a Plexiglass cylinder 24 cm long with a 6.5 cm outside diameter and 0.318 thick, was located horizontally directly to the left of the wedge-shaped chamber. Holes were cut in both ends of the pre-chamber and aligned with holes made in the wedge-shaped chamber to allow horizontal movement of the fiber in and out of the vertical center of the primary chamber. Additional holes were cut in the top of the pre-chamber through which nucleated ice crystals could be injected. The pre-chamber would also serve in another capacity, i.e., that of a post chamber. Once cystals were grown and studied in the wedge-shaped chamber, the fiber would be moved back into the pre-chamber where the crystals would be evaporated by compressed air dried with Baker Chemical Company 6-20 Mesh Silica Gel. When evaporated, additional ice crystals would be injected and another experiment would begin.

Problems with the pre-chamber developed when preliminary testing took place. Upon nucleation of ice crystals by the "popping bubble" technique, the crystals were injected into the pre-chamber. Observation of the pre-chamber air immediately after the ice crystals were injected, showed that none had survived the transportation process. All facets of the nucleation, transportation, and injection process were examined and it was found that the ice crystals sublimed immediately after their

arrival into the pre-chamber because of the temperature difference between the freezer of ice nucleation (-27°C) and the pre-chamber (-12°C). Since the temperature of the pre-chamber could not be changed, a new type of chamber was built and used.

The new pre-chamber (Fig. 10) is a rectangular diffusion chamber with ice coated top and bottom plates. Even though the temperature of the freezer for ice nucleation and that of the new rectangular diffusion chamber were the same as previously used, the vapor diffusional process of the new chamber allowed enough moisture for the ice crystals to survive after transportation from one temperature to another. The new pre-chamber has dimensions 24 cm by 9 cm by 7 cm with the side walls constructed of 0.635 cm Plexiglass and the top and bottom walls constructed of 0.317 cm Plexiglass. The front wall is removable and supports are designed on the inside walls of the chambe so that additional 0.317 cm Plexiglass plates, coated with ice, could be inserted just interior to the top and bottom walls. Holes are cut in the two ends, the top, and front side, similar to that of the previous Plexiglass cylinder. When injection of ice crystals into the pre-chamber is required, the ice plates are inserted and when drying of the nylon fiber is desired, the ice plates are removed and dry air is injected through the center hole.

4.2.2.3 Ice crystal slide mechanism. In order to avoid the problems of initial transient supersaturations and relaxation time, as discussed above, a mechanism was required to transport the ice crystals from the pre-chamber, where ice crystals are injected, into the wedge-shaped chamber. We decided to grow the ice crystals on a very fine

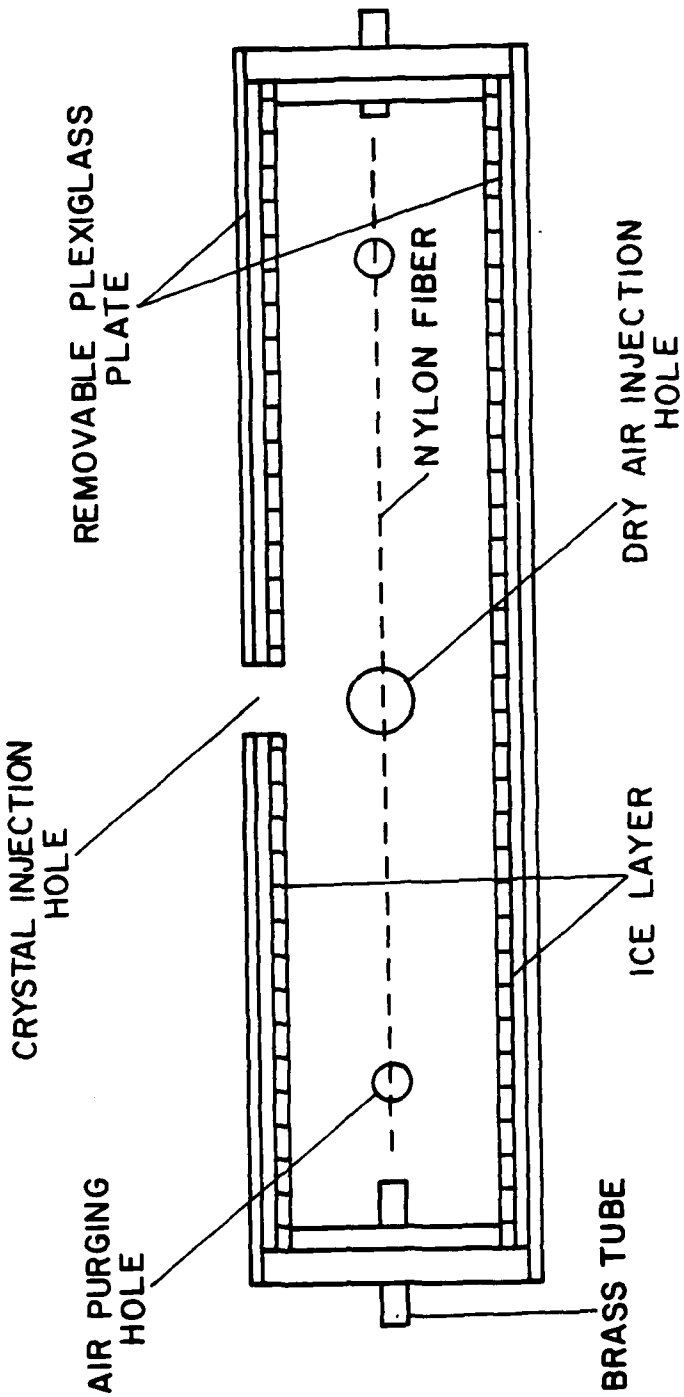

Figure 10. Pre-chamber.

gauge fiber which could be moved back and forth between the pre-chamber and the wedge-shaped chamber. Another requirement for this mechanism was the ability to rotate the fiber inside the wedge chamber in order to be able to turn the crystals so that ice crystals could be observed and photographed at different angles.

The ice crystal slide mechanism shown in Figure 11 is the final version of various designs and test models. It is constructed almost entirely of aluminum. The two inner rotating supports have dimensions of 20.96 cm × 5.08 × 0.318 cm and support the sliding rod guide. The inner rotating supports are secured at the bottom by 3.8 cm × 4.45 cm × 1.905 cm aluminum blocks which are bolted to a stationary aluminum plate. A stationary 0.476 cm diameter brass tube runs through the metal blocks and inner rotating support at each end. It acts as the axis of rotation for the inner supports. Movement of the inner rotating supports is in the y-z plane.

The sliding rod guide is a 70.49 cm long aluminum tube with a 1.587 cm outside diameter. It is sandwiched between and secured to the two rotating inner supports by four locking nuts. Movement of the sliding rod guide is also in the y-z plane.

An aluminum rod 104.1 cm long with a 1.587 cm outside diameter was machined so that it would slide easily through the sliding rod guide. This aluminum sliding rod is connected to the outer rotating supports by locking nuts and can be slid in the x-direction and also rotated in the y-z plane.

The outer rotating supports, constructed of 20.3 cm × 2.2 cm × 0.318 aluminum strips, connect the aluminum sliding rod to two glass rods, between which the fiber is connected. The glass rods are connected

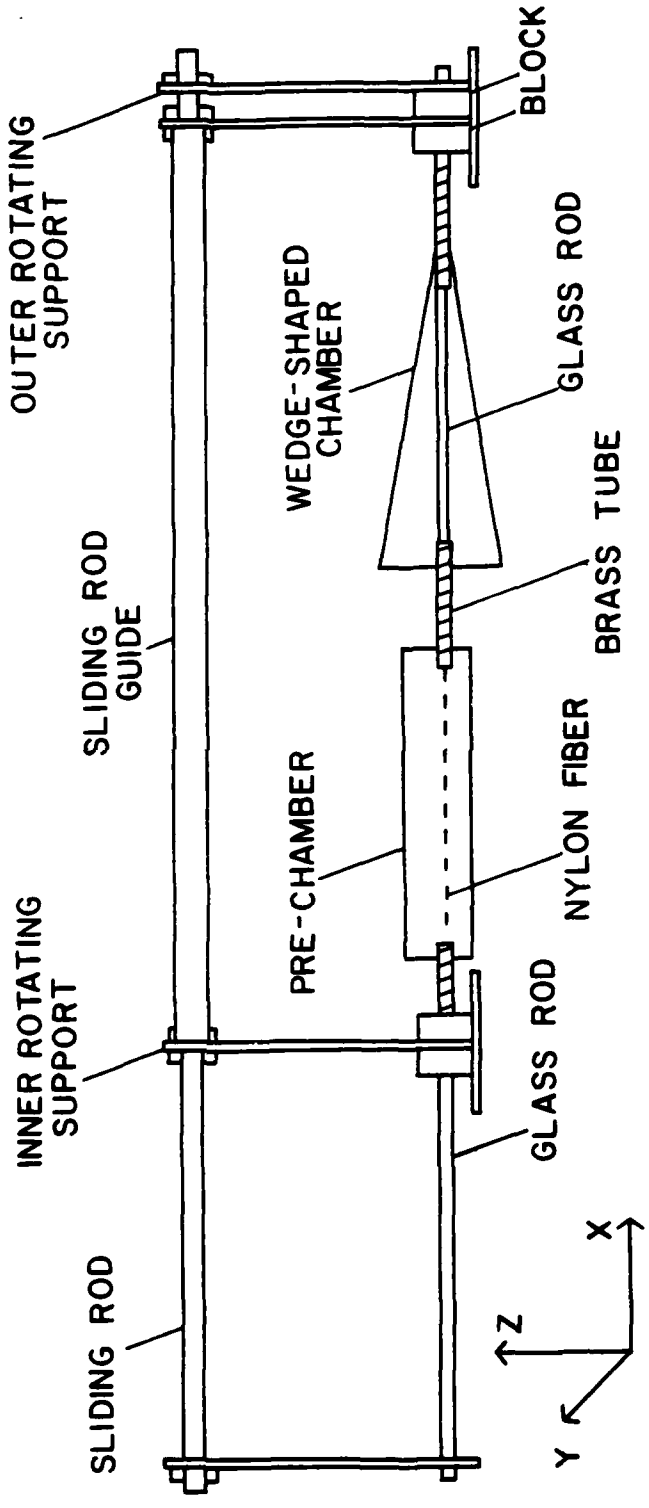

Figure 11. Ice crystal slide mechanism.

to the outer supports by screws and act as the axis of rotation for the outer suppports. Just as the sliding rod can be moved in the x-direction, the glass rods also move simultaneously in the same direction. Rotation of the outer supports, the sliding rod, the sliding rod guide, and the inner supports in the y-z plane causes the glass rods and fiber to turn while still stationary in the x-direction. This, in turn, allows the ice crystals to rotate on the fiber to a proper orientation for measurement.

Three brass tubes are used to guide the glass rods. One tube connects the ice crystal transfer mechanism to the pre-chamber while a second tube links the transfer mechanism to the wedge-shaped chamber. A third tube connects the pre-chamber and the wedge-shaped chamber. All three brass tubes are aligned, in such a manner that the fiber could be transferred into and out of the vertical center of the wedge-shaped chamber.

Black widow spider cobweb was our original choice of the fiber onto which the ice crysals were to be grown. The cobweb was found to be unacceptale for our use because, first, it was hard to get a fresh sample form the spider, second it was sticky and caught multitudes of dust and dirt particles and, third, even though it was fine gauged (50-100 μm), it was generally difficult to attach to the glass rods.

We next tried a synthetic fiber produced by rapidly expanding melted pieces of cloth. This also proved to be unacceptable since it was difficult to get a uniform thickness and the fiber was very brittle and broke in the cold temperatures of the wedge-shaped chamber.

Commericial nylon was tested and offered several advantages. It was easy to obtain, easy to secure to the glass rods, and was strong

and flexible. This nylon thread had one major disqualifying factor. It had a very large diameter (200-250 μm), which obscurred ice crystals growing in the early stages of the experiments.

From our early tests of different fibers, we found that a very fine gauged nylon fiber would be ideal for our use. We found that dental floss string is nylon and consists of many fine interwoven nylon fibers. By unwinding these fibers, we had the ideal strand for ice crystal growth. Individual nylon fiber is easy to obtain, strong and flexible, and more importantly has a diameter of approsimately 50 μm. Subsequent testing of this fiber confirmed that the unwound nylon fibers used in dental floss was satisfactory for our use.

Operation of the ice crystal slide mechanism is in the following manner. Initially the slide mechanism is in the position shown in Figure 11. The inner and outer rotating supports are positioned vertically along the z-axis and combined with the aluminum sliding rod, the sliding rod guide, and glass rods form the x-z plane. The nylon fiber is exposed in the pre-chamber. Ice crystals are then njected into the pre-chamber and the aluminum sliding rod is moved to the right, along the x-axis. The nylon fiber with seed ice crystals is thus oved into the vertical center of the wedge-shaped chamber where ice crystals begin to grow in the prepared environment. Ice crystals are monitored and the sliding rod guide is moved in the y-z plane which in turn rotates the ice crystals on the nylon fiber to a proper orientation for measurement. Maximum rotation of the sliding rod guide is ± 80° from the vertical stating position.

Figure 12 shows a close-up of the ice crystal slide mechanism and Figure 9 shows it in its operational configuration.

Figure 12. Photograph of the ice crystal slide mechanism.

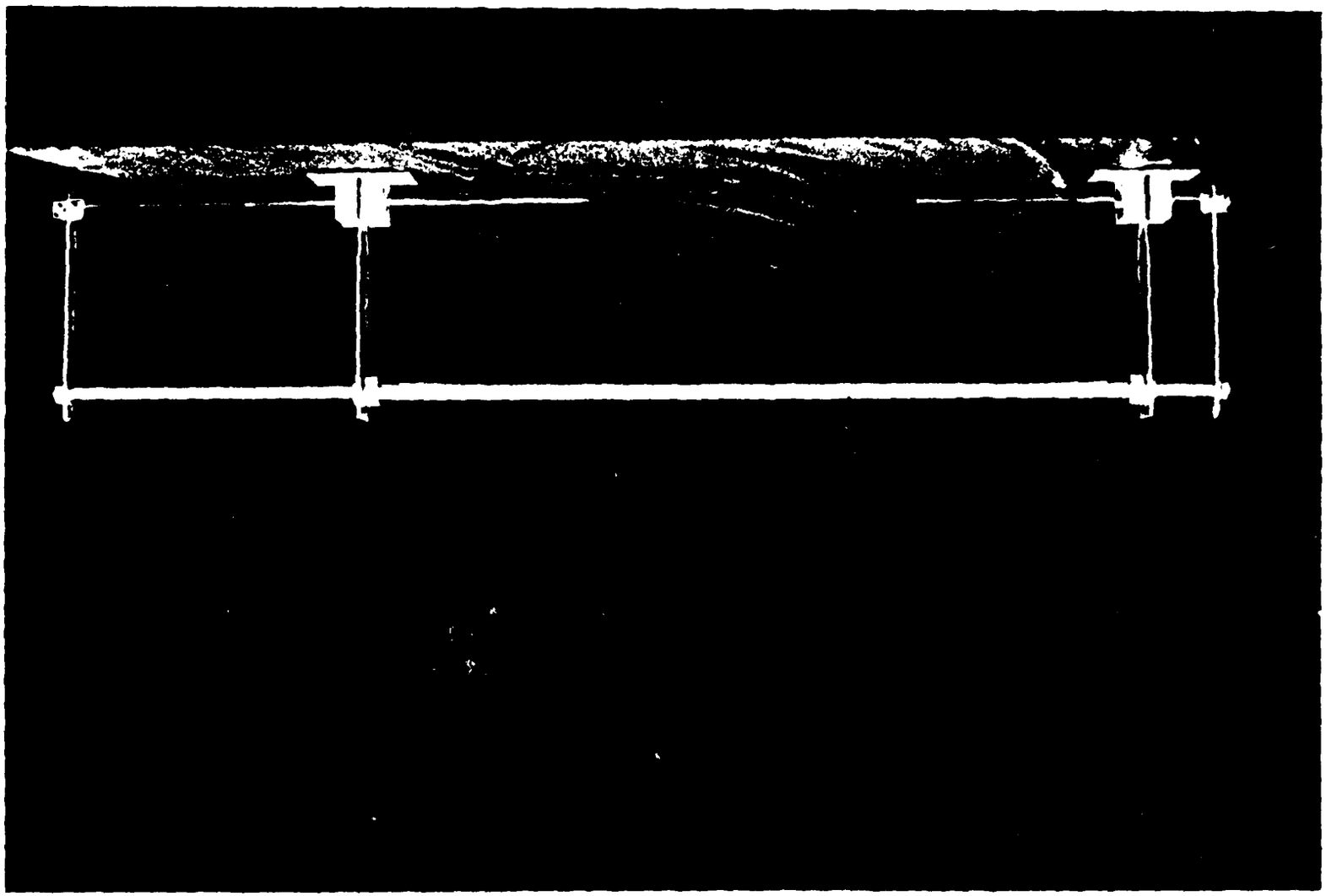

4.2.2.4 Laterial microscope slide mechanism. To observe the habit of ice crystals as they grew in the wedge-shaped chamber, a Wild M5A long working distance microscope was used. This stereomicroscope is unique because it has a maximum working distance from the lens to the object of 270 mm. As in most microscopes, the M5A was designed for vertical observation; but to observe the ice crystals in our wedge-shaped chamber, it was necessary to orient it in a horizontal position. It was also necessary to move the microscope laterally along the working area of the chamber and to align it in such a manner as to be able to focus on the nylon fiber in the vertical center of the chamber. To satisfy these requirements, we designed and constructed the lateral slide mechanism shown in Figure 13. The slide mechanism is constructed almost entirely of aluminum.

An aluminum block with dimensions 8.89 cm × 5.72 cm × 17.5 cm serves as the microscope support and slide. The microscope is secured to this aluminum block, in the horizontal position, on a 17.5 cm long by 2.54 cm outside diameter aluminum tube. The aluminum block also has three holes drilled near its based. A 1.905 cm Tompson Ball Bushing is pressed into each of the two outer holes and the center hole is tapped to accommodate a 1.27 cm 20 all fret steel pipe. A 1.905 cm diameter by 31.8 cm long Tompson Case Steel Shaft runs through each of the outer holes of the aluminum block where a 1.26 diameter by 50.8 cm long 20 all fret steel pipe is fitted. One end of the steel pipe is attached to one of the outside blocks and the other runs through and extends beyond the other outside block where a hand crank is soldered.

To operate the lateral microscope slide mechanism, the microscope is attached in the horizontal position, allowing it to focus on

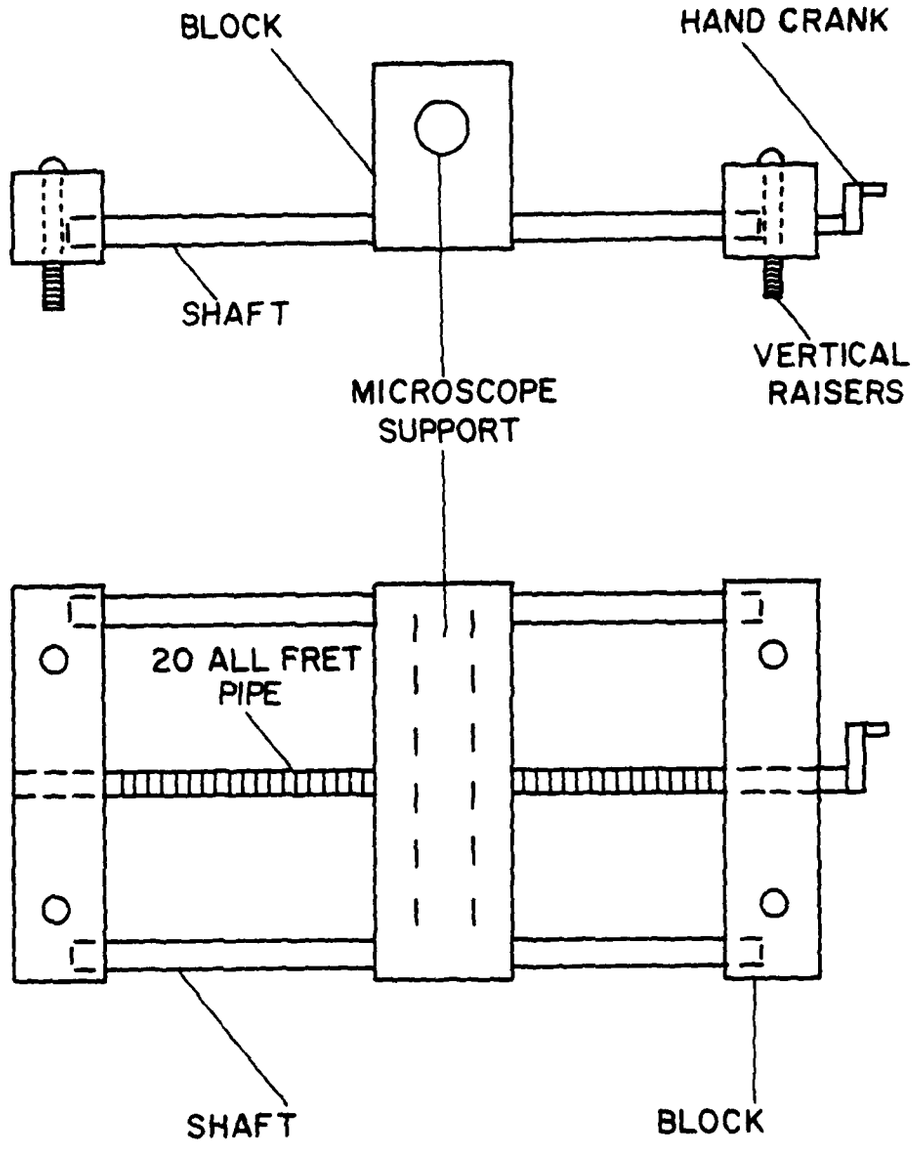

Figure 13. Lateral microscope slide mechanism.

the nylon fiber inside the chamber. As the hand crank is rotated, the microscope traverses along the working area of the chamber. The microscope moves laterally at approximately 1 cm for every eight complete turns of the hand crank. Four screws, two in each outside aluminum block, are used to raise or lower the entire mechanism so that the center of the microscope field can be aligned or adjusted to the nylon fiber in the chamber.

Figure 14 shows a photograph of the lateral microscope slide mechanism and Figure 15 shows the mechanism with the Wild M5A stereomicroscope attached.

4.2.2.5 Sample transfer device. An adequate technique was needed to transfer the ice crystals from the chest freezer, where they were generated by the "popping bubble" method, to the pre-chamber. Factors to be considered in this transfer process included the time ice crystals could survive during the transfer, the total number and concentration of ice crystals transferred, and the device itself. As mentioned in an earlier section, the "popping bubble" technique provided a relatively reproducible number of ice crystals.

Our first series of tests were conducted using a 1500 cc Plexiglass syringe which was coated with ice on its interior walls. Problems became immediately apparent with this method. First, the plunger of the syringe stuck in the cold temperatures of the freezer. Second, the large volume of the syringe, when compressed, caused the ice crystals to impact on the pre-chamber walls rather than suspend in the pre-chamber air. Finally, the survival rate of ice crystals transferred by the syringe was small.

Figure 14. Photograph of the lateral microscope slide mechanism.

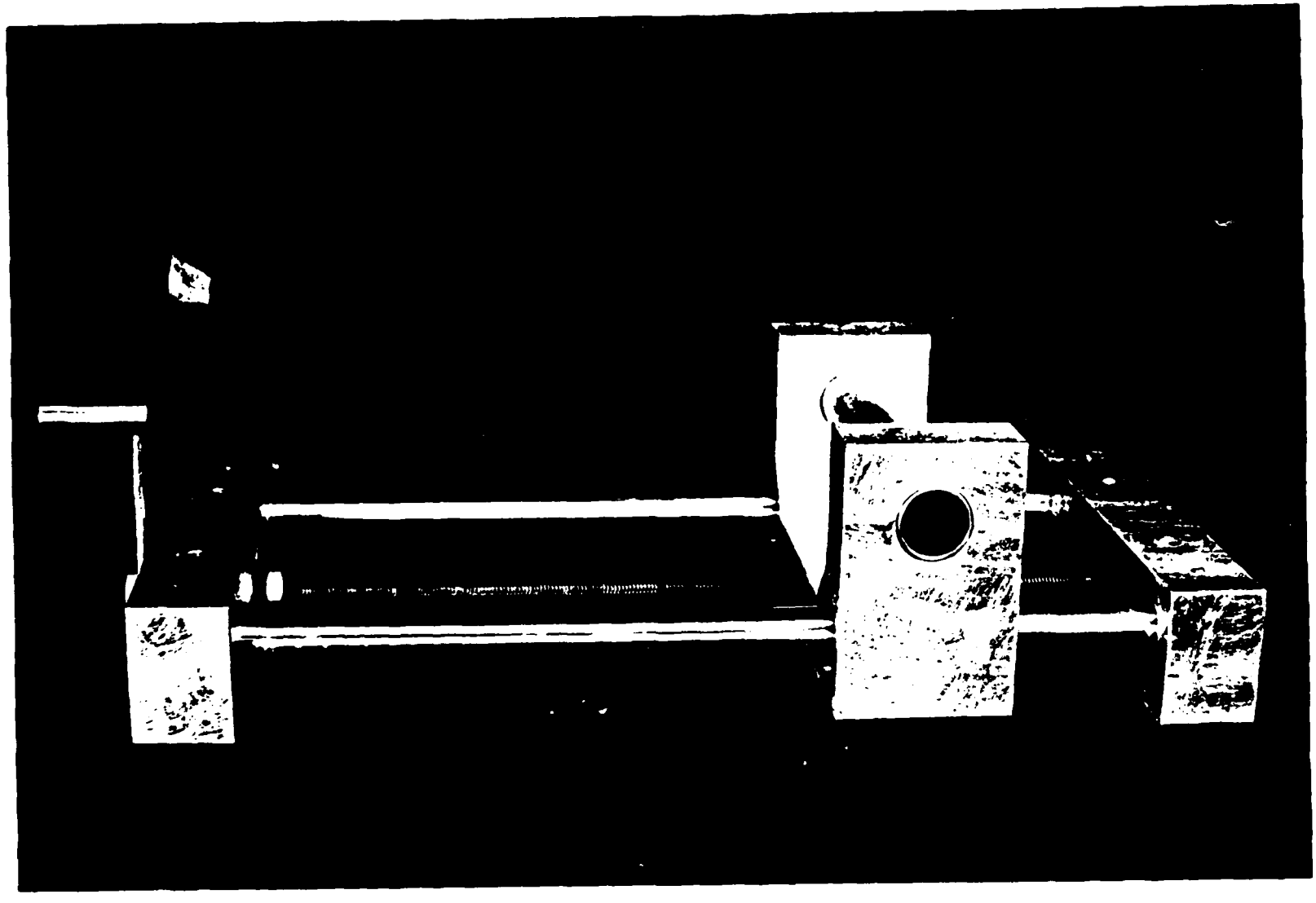

Figure 15. Photograph of the lateral microscope slide mechanism with the Wild M5A stereomicroscope attached.

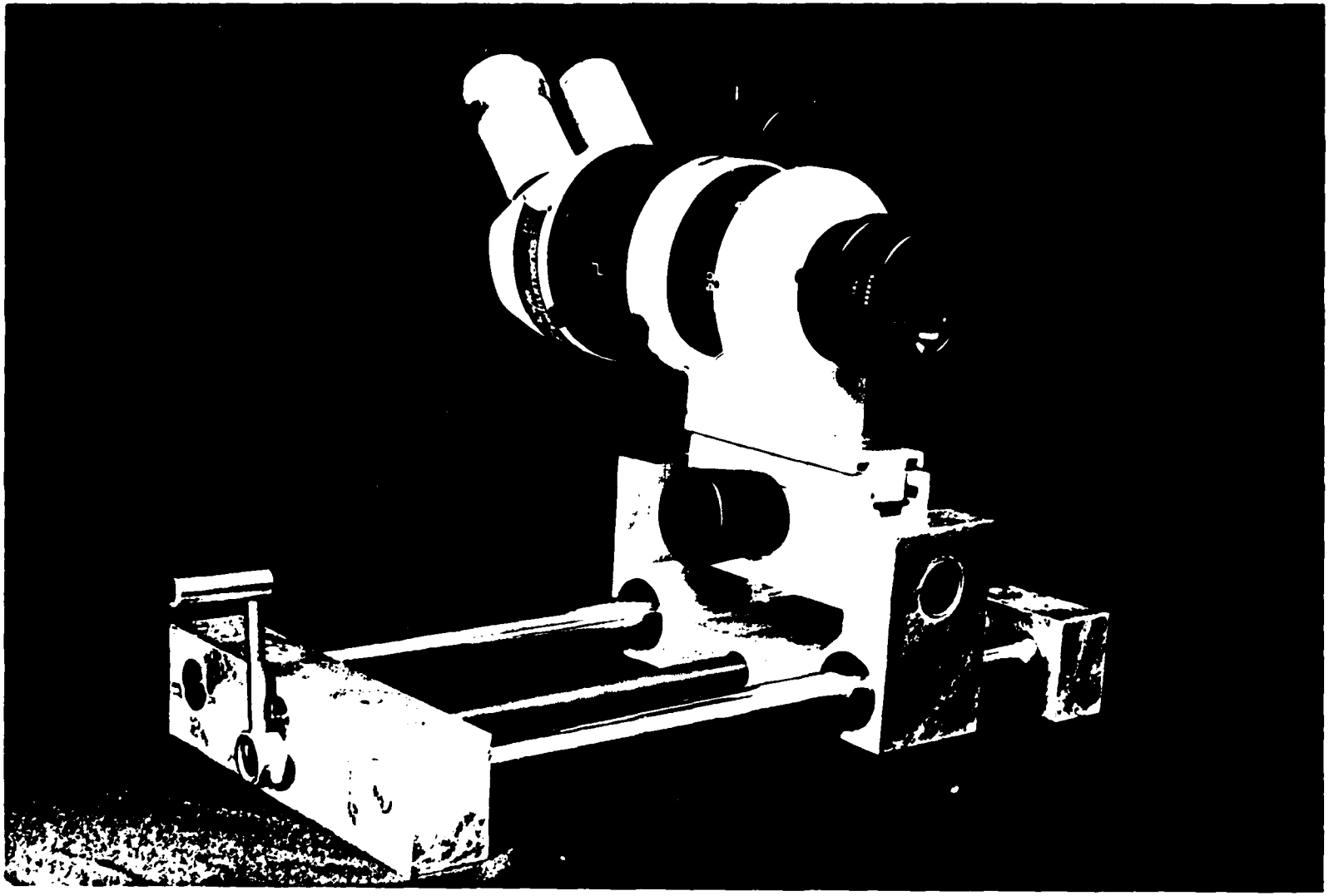

We next tried an ordinary meat baster. The baster was ice coated on its inside walls and cooled to the temperature of the freezer where the ice crystals were generated. This device proved to be highly satisfactory since crystals could survive up to 20 seconds outside the freezer, the flow of the ice crystals out of the baster was slow enough to allow their suspension in the pre-chamber air, and a sufficient number of ice crystals survived the transfer process.

4.2.2.6 Outer environmental chamber. In order to avoid strong nonlinearity in temperature along the copper plates, conditioning of the environment immediately surrounding the wedge-shaped chamber was considered. To do this we mounted the wedge-shaped chamber, the pre-chamber, the lateral microscope slide mechanism, and the ice crystal slide mechanism on a wood supporting frame and set the entire system in a Sears Model 198 chest freezer. The lid of the freezer was removed and replaced with one layer of 1.91 cm thick expanded polystyrene covered with 0.32 cm thick masonite board. Holes were cut in the lid to allow access to the pre-chamber and microscope, and to permit unobstructed movement of the ice crystal slide mechanism. The freezer maintains a temperature of approximately -12°C in the vicinity of the wedge-shaped chamber.

Securing the outer environment of the wedge-shaped chamber enabled us to achieve near linear steady-state temperature profiles along the copper plates and more importantly to maintain this condition once it was achieved.

Figures 9 and 16 show respectively, the outer environmental chamber with lid off exposing the working apparatus, and the chamber

Figure 16. Photograph of the outer environmental chamber with insulated lid attached.

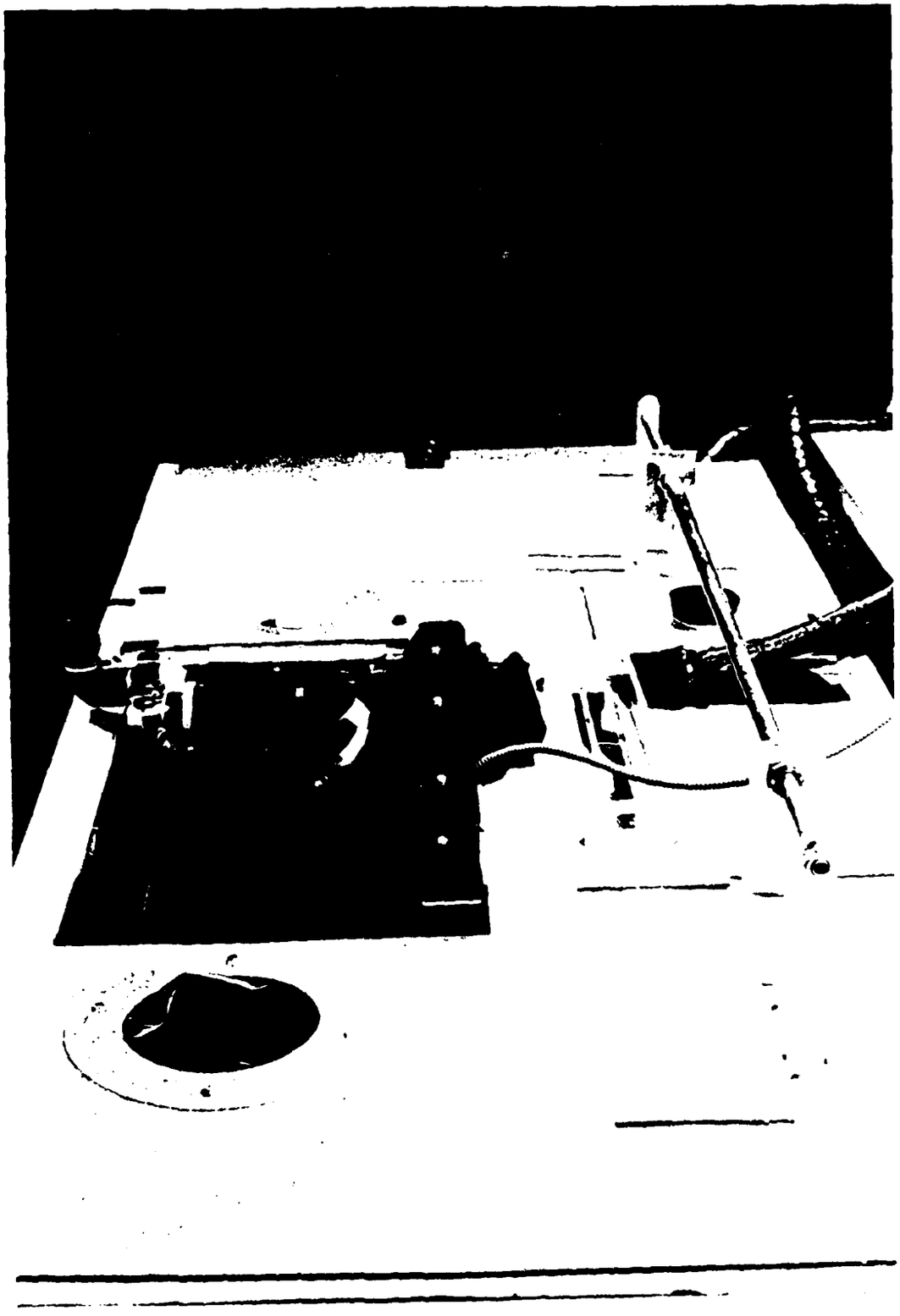

with lid attached.

4.2.3 Supporting Equipment

In addition to the primary apparatus that we designed and constructed, various commercial equipments were used for supplementary purposes.

The Wild M5A Stereomicroscope has a standard working distance from lens to the object of 91 mm. Four auxiliary objective lenses of 0.3x, 0.5x, 1.5x, and 2.0x vary the working distance from 270 mm, 154 mm, 38 mm, and 23 mm, respectively. Also auxiliary to the standard configuration are four interchangeable eyepiece lenses of 8x, 10x, 15x, and 20x. Internally the microscope has four magnification settings of 0.6x, 1.2x, 2.5x, and 5.0x. Depending on the internal magnification setting, the eyepiece, and the additional objective lens, the magnification and field diameter vary from 4.8x:35.0 mm to 200x:1.3mm. A camera can be mounted to the microscope by means of a phototube attachment which replaces the standard binocular tube. The addition of the phototube increases the magnification 1.25x to the camera.

An Olympus OM-2 camera, equippped with an Olympus Winder 2, a motor driven film advancer, an Olympus Varimagni 360° rotating eyepiece attachment, and a Dot Line Corporation electronic cable release, was used for photomicrographic recording of ice crystal growth.

Illumination of ice crystals growing in the wedge-shaped chamber was accomplished with a Volpi I Intralux 150H light source with a fiber-optics attachment.

The main source of cooling for the wedge-shaped chamber was four Cambion Model 801-2001-01-00-00 ceramic modules. These thermoelectric

modules have a maximum temperature difference between the warm and cold faces of 60°C and a maximum allowable temperature of 100°C. The modules have dimensions of 31.8 mm × 31.8 mm × 0.21 mm and weigh 23 grams. Power to the modules was supplied by an Epsco Incorporated Model D-612T Filtered D.C. Power Supply with a D.C. output of 0-16 volts and maximum of 10 amperes.

A secondary source of cooling was provided by a Forma Scientific Model Incorporated 2160 Bath and Circulator. The bath is designed to maintain a constant temperature in the 37 liter capacity tank. The temperature is controlled to ± 0.02°C by an ultrasensitive thermoregulator and the bath has a temperature range of -30 to +100°C. A commercial antifreeze was used as the circulating fluid which cooled and stabilized the top plate temperatures and also carried away the excess heat produced by the four thermoelectric modules.

The thermocouples used to measure the temperatures in the wedge-shaped chamber were Honeywell Incorporated Model 48B1B8 30 Gauge copper-constantan thermocouple wires. The voltage output of the thermocouples was measured using a Keithley Model 174 Digital Multimeter. Temperatures from the thermocouples were recorded and displayed automatically by a TERAK minicomputer (Fig. 17).

Figure 17. Photograph of the TERAK mini-computer.

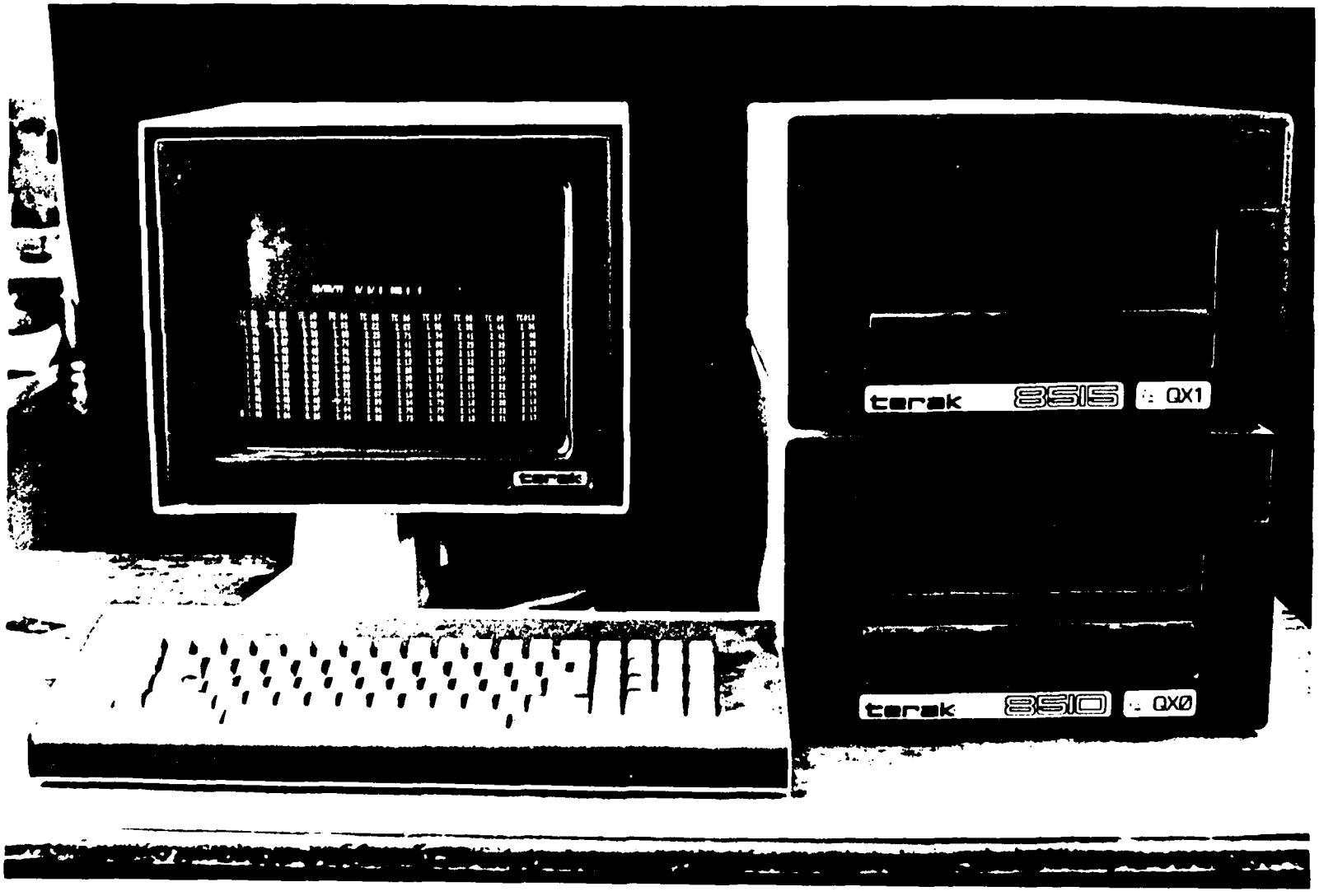
terak
8515
QX1
terak
8510
QX0

Chapter 5

EXPERIMENTAL PROCEDURE

5.1 Nylon Fiber Preparation

A single strand of unwound dental floss was the fiber on which ice crystals were grown and studied in the wedge-shaped chamber. The unwaxed dental floss, in its commerical form, is a combination of many intertwined nylon fibers. The dental floss was cut in an approximately 17 cm piece and carefully unwound so that we could procure one individual strand of fiber. A single loop was made on each end of the fiber and tied to and suspended between the two glass rods of the ice crystal slide mechanism. A dab of Dupont DUCO quick drying cement secured the nylon fiber to the glass rods. Although the nylon fiber was relatively strong for its size, extreme care was taken when moving the nylon fiber back and forth between the pre-chamber and the wedge-shaped chamber since on occasion the fiber would break from a torque produced by the ice crystal slide mechanism. Replacement of the fiber required a total warming of the outer environmental chamber and pre-chamber resulting in at least a day's time loss.

5.2 Chamber Air Pre-conditioning

The possibility of contamination of the pre-chamber and wedge-shaped chamber air by atmospheric aerosols was anticipated prior to the

start of our experiments. As mentioned in previous sections, we used a homogeneous method of ice crystal generation, i.e., the "popping bubble" technique, and the potentiality of heterogeneous nucleation on artificial ice nuclei, in either chamber prior to the beginning of our experiment, would lead to erroneous data acquisition. We, therefore, tested our experimental system under operational conditions, without injecting ice crystals into the pre-chamber, to determine if heterogeneous ice nucleation would occur in either chamber. The result of our tests were negative and we thus concluded that neither the pre-chamber nor the wedge-shaped chamber required that the air be filtered prior to our experiments.

Compressed air dried by passing through a plastic tube filled with silica gel was introduced into the pre-chamber prior to the beginning of the first experiment each day. We found that frost would usually develop on the nylon fiber in the pre-chamber each night. This occurred when all cooling systems, except the storage freezer acting as the outer environmental chamber, were turned off at the end of a day's experiments. A ten minute flow of dry air each morning rapidly evaporated the frost on the nylon fiber. At the conclusion of each experiment, the nylon fiber was returned to the pre-chamber from the wedge-shaped chamber. Ice crystals that had grown on the nylon fiber were similarly evaporated by a steady flow of dry air. Dry air flow through the pre-chamber of approximately 30 minutes duration was sufficient to evaporate ice crystals of 1000 μm size. Evaporating the ice crystals in this manner allowed us to rapidly move from one experiment to another.

Frost problems also occurred on the outside front Plexiglass wall of the wedge-shaped chamber, affecting our ability to view the

crystals with the microscope. The temperature difference of the exposed edge of the copper plates of the wedge-shaped chamber and the air of the outer environmental chamber produced either frost or fog on the outer Plexiglass wall. Air, also dried with silica gel, was continually blown on the Plexiglass wall to inhibit the formation of frost or fog.

5.3 Preparation of the Ice Surfaces

The wedge-shaped chamber is supersaturated with respect to ice throughout the interior except on the top and bottom boundaries where ice saturation is maintained. The ice supersaturation, therefore, varies from zero at the boundaries to a maximum near the center of the chamber. For sufficiently large temperature differences between the top and bottom plates, supersaturation with respect to water can occur at points in the chamber with the maximum again near the center of the chamber.

For these conditions to exist, both the top and bottom plates must be coated with ice. The ice surfaces must be of uniform thickness and smooth. For application of the ice layer on the bottom plate, the plate is first cooled to a temperature between -3°C and -5°C. Next water is applied to the surface using a sponge covered with a plastic mesh like those used in service stations. The thin water layer rapidly freezes and the procedure is repeated until a smooth uniform ice layer approximately 1 mm thick builds up. This procedure was accomplished just prior to the attachment of the nylon fiber and was repeated only when the fiber was replaced. At the conclusion of each day's experiments, the bottom plate ice surface was covered and protected by a 1 mm thick rubber sheet.

Application of the ice layer on the top plate was accomplished in the same manner as for the bottom plate for the temperature range -10°C to -30°C. For temperatures warmer than -10°C, filter paper was taped to the top plate and then covered with ice in a similar manner. The filter paper was used because temperatures warmer than 0°C were required on the top plate for warm centerline temperatures and the filter paper kept the melting ice from dripping in the chamber. Under both situations, the top plate was removed and placed in the ambient room air at the end of each day's experiments and thus had to be recoated with ice each morning.

5.4 Ice Crystal Generation and Transfer

An important phase of each experiment was the generation of ice crystals and their subsequent transfer from the point of generation, i.e., the chest freezer, to the pre-chamber.

The pre-chamber air was pre-conditioned by placing ice plates at the top and bottom of the chamber, creating a thermal diffusion chamber. This provided sufficient moisture to allow the transfer of the ice crystals from the cold air of the chest freezer to the warmer pre-chamber air without sublimation loss. The meat baster, acting as the sample transfer device, was coated with ice on its interior walls by blowing breath into it and then cooled to the temperature of the chest freezer.

A supercooled fog was created in the chest by blowing breath into it. Next, a single polyethylene bubble was compressed and popped in the supercooled fog, producing copious ice crystals. Equilibrium conditions were rapidly reached in the freezer and the baster was filled with crystals, transferred to the pre-chamber, and injected into the

pre-chamber air through a hole in the top of the chamber. Care was taken so that the warm room air was at no time ingested into the baster.

The number of basterfuls used in each experiment was determined by trial and error and the ideal number was found to be a function of the supersaturation with respect to ice in the wedge-shaped chamber. Three basterfuls were used at supersaturations of 1%, two at supersaturations of 5 and 7%, and one at supersaturations of 10%.

5.5 Ice Crystal Insertion into the Wedge-Shaped Chamber

In our experimental sequence, the nylon fiber was initially suspended in the pre-chamber. Once ice crystals had been generated, transferred, and injected into the pre-chamber air, a number of these crystals became attached to the nylon fiber. The number of ice crystals that became attached to the fiber and the spacing of these crystals were dependent upon how long the fiber remained in the pre-chamber after ice crystals were injected. A period of 10-20 seconds was found to give both the best number and spacing of ice crystals. After this period of time, the nylon fiber was rapidly but carefully moved laterally into the pre-conditioned wedge-shaped ice thermal diffusion chamber by the ice crystal slide mechanism.

5.6 Photographic Measurement of Ice Crystals

Accurate measurement of both the basal and prism planes of ice crystals grown in the wedge-shaped ice thermal diffusion chamber was imperative to our study. To accomplish this, a photomicrographic record of a 1 mm (0.01 mm divisions) stage micrometer was taken for all

power setting combinations of the Wild M5A stereomicroscope, using an Olympus OM-2 35 mm camera. The 35 mm black and white film was developed and the negatives served as a measuring device for the subsequent analysis of photographs of ice crystals grown in the chamber. This method of measurement was both easy and accurate, and also allowed us to maintain a permanent record of the ice crystals for use in later comparison and analysis. Ice crystals were photographed after 10 minutes of growth in the wedge-shaped ice thermal diffusion chamber and every 5 minutes thereafter until 60 minutes after insertion in the wedge-shaped chamber.

Chapter 6

EXPERIMENTAL RESULTS AND DISCUSSION

The primary purpose of our experimental study was the observation and accurate measurement of ice crystals growing under steady-state temperature and supersaturation fields in the wedge-shaped ice thermal diffusion chamber. Certain operational limitations occurred as our experiments proceded. The first limitation was design oriented. In the wedge-shaped chamber maximum supersaturations were sustained at the wide end of the chamber and ice-crystals, impregnated on the fine nylon fiber in the pre-chamber, had to be traversed into the chamber through this wide end. When supersaturations were held near or at water saturation at the wide end of the chamber, condensation followed by rapid freezing occurred on the entire fiber producing one continuous string of ice crystals. These crystals were unsuitable for measurement, thus limiting the experimental condition to below water saturation. A second limitation was the range of temperatures reproducible in the wedge-shaped chamber. This and the first lmitation allowed us to observe crystals under the following conditons: $(S_i-1) = 1\%$, T = (-2 to -28°C); $(S_i-1) = 5\%$, T = (-6 to -30°C); $(S_i-1) = 7\%$, T = (-6 to -24°C); $(S_i-1) = 10\%$, T = (-10 to -30°C) where S_i is the saturation ratio with respect to ice and T the temperature. Ice crystal growth was also observed under conditions in between those mentioned above to fill gaps in our data.

6.1 Growth Behavior of the Basal Plane of Ice

Figure 18 shows the diameter of the longest dimension of the ice crystal basal plane 2a plotted as a function of temperature at 10, 30, and 50 minutes under conditions of ice supersaturation (S_i-1) at 1%. In the figure, as temperatures warm from -30 to about -12°C, a gradual increase in 2a occurs for all growth times. A more rapid increase in the 2a values appear at temperatures between -12 and -5°C as conditions surrounding the ice crystal approach water saturation. This rapid increase is more pronounced at growth times of 30 and 50 minutes. Just below water saturation, the 2a values decrease, very rapidly for the 30 and 50 minutes curves.

Similar behavior of 2a values may be seen for (S_i-1) at 5% as shown in Figure 19. A gradual increase in 2a values while warmed from cold temperatures exists followed by a rapid increase at warmer temperatures as conditions approach water saturation. The curves for all growth times show an unexplicable dip between -18 and -14°C which could be the result of experimental error. The decrease in 2a at -8°C for the 30 and 50 minute curves was attributed to measurement error but further experiment and analysis showed this dip was associated with a change in habit as a function of time at that temperature. Additional data were taken for -8°C and it was found that the basic habit of ice crystals grown at this temperature, under (S_i-1) values between 5 and 7%, did in fact vary with time (Fig. 20). During the initial growth time of 10 minutes at this temperature, ice crystals exhibited a plate habit which gradually transformed into columns later. This transformation took place more rapidly as the ice supersaturation increased.

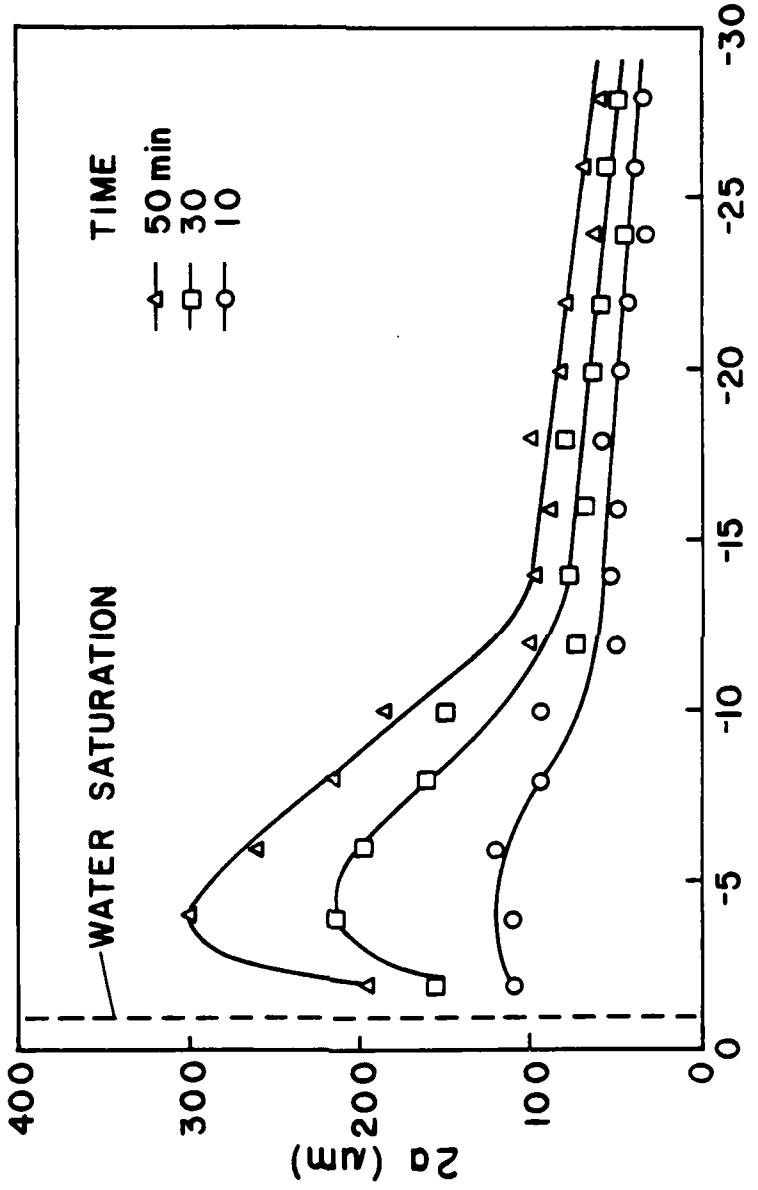

Figure 18. Ice crystal diameter 2a plotted as a function of temperature at different times of growth under ice supersaturation (S_i-1) at 1%.

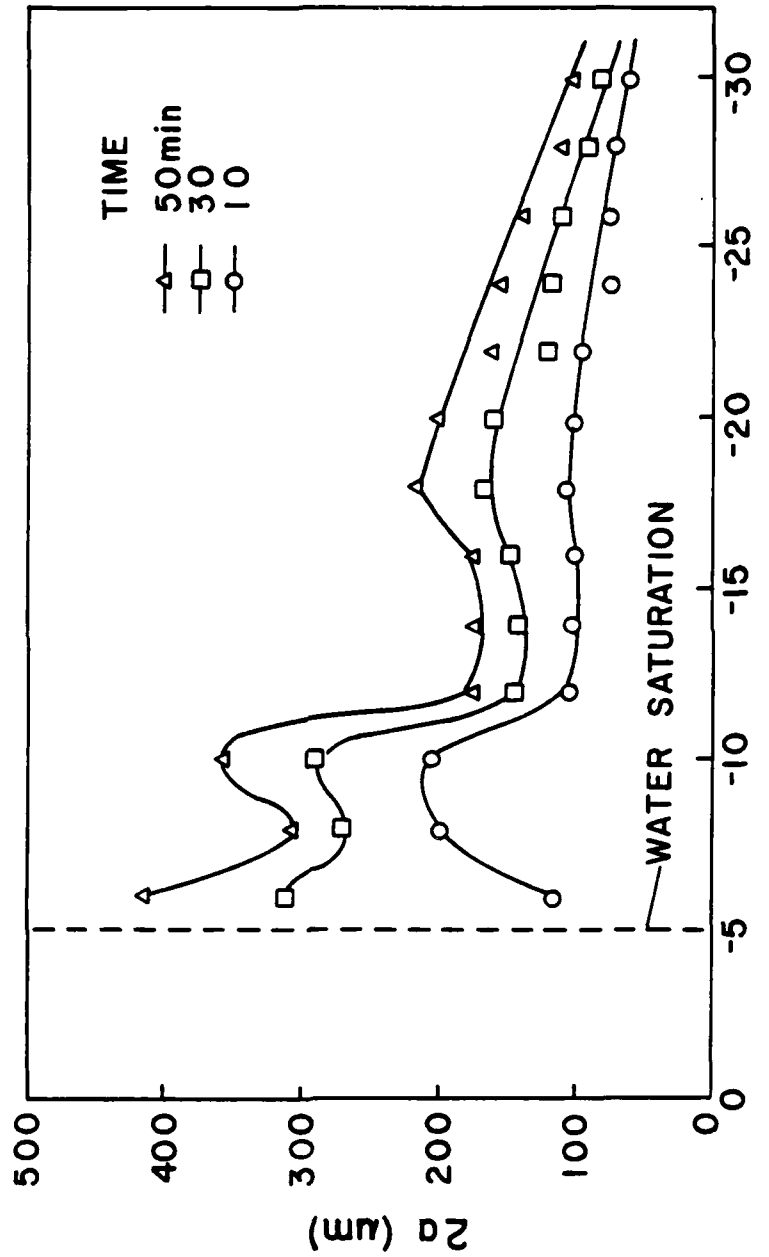

Figure 19. Ice crystal diameter 2a plotted as a function of temperature at different times of growth under ice supersaturation (S_i-1) at 5%.

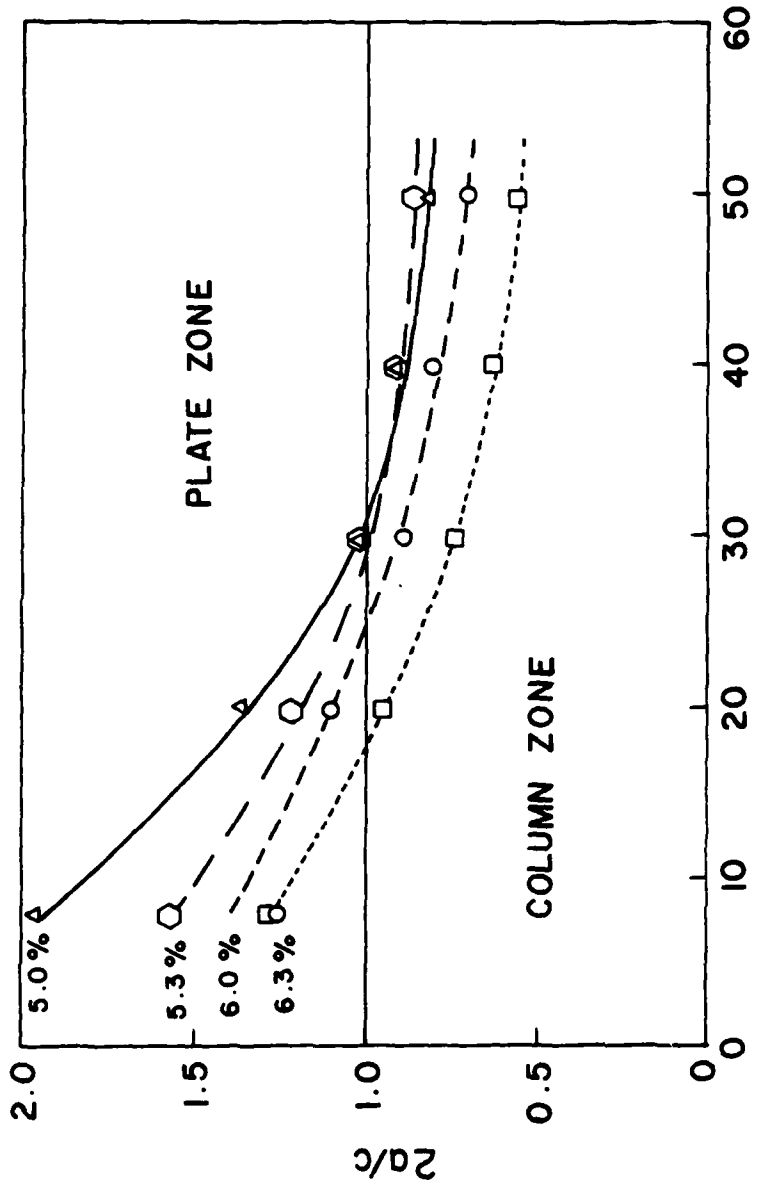

Figure 20. Variation of ice crystal habit plotted as a function of time at a temperature of -8°C and different ice supersaturations (S_i-1).

General trends of the 2a value change with temperature, for different growth times under (S_i-1) at 7% (Fig. 21), were found to be the same as those at 1%. As the temperature warmed from -24°C, an increase in 2a values was observed, more rapidly as conditions surrounding the ice crystal approach water saturation. A rapid decrease in the 2a values occurred at (S_i-1) values just below water saturation. Under (S_i-1) at 7%, ice crystals were observed above water saturation at -6°C. The 2a values continued the same decreasing trend as they did just below water saturation.

Figure 22 shows the 2a variation under (S_i-1) at 10%. A trend practically the same as the others occurs; a gradual increase in 2a as temperatures warm from -30°C, more rapidly as water saturation is approached. No downward trends are detected as conditions approach water saturation.

Several basic trends, in the growth of 2a, are common for all ice supersaturation levels. First, a gradual increas in 2a values is noted as the temperature warms, followed by a rapid increase as conditions approach water saturation. A second trend of a rapid 2a decrease at conditions just below water saturation is observed for all growth times under (S_i-1) of 1 and 7% and for the 10 minute time period of 5%. This trend is not apparent under other supersaturations.

6.2 Growth Behavior of the Prism of Ice

Figure 23 shows the height of the ice crystal prism plane c plotted as a function of temperature at 10, 30, and 50 minutes under conditions of (S_i-1) at 1%. In the figure, as temperatures warm from

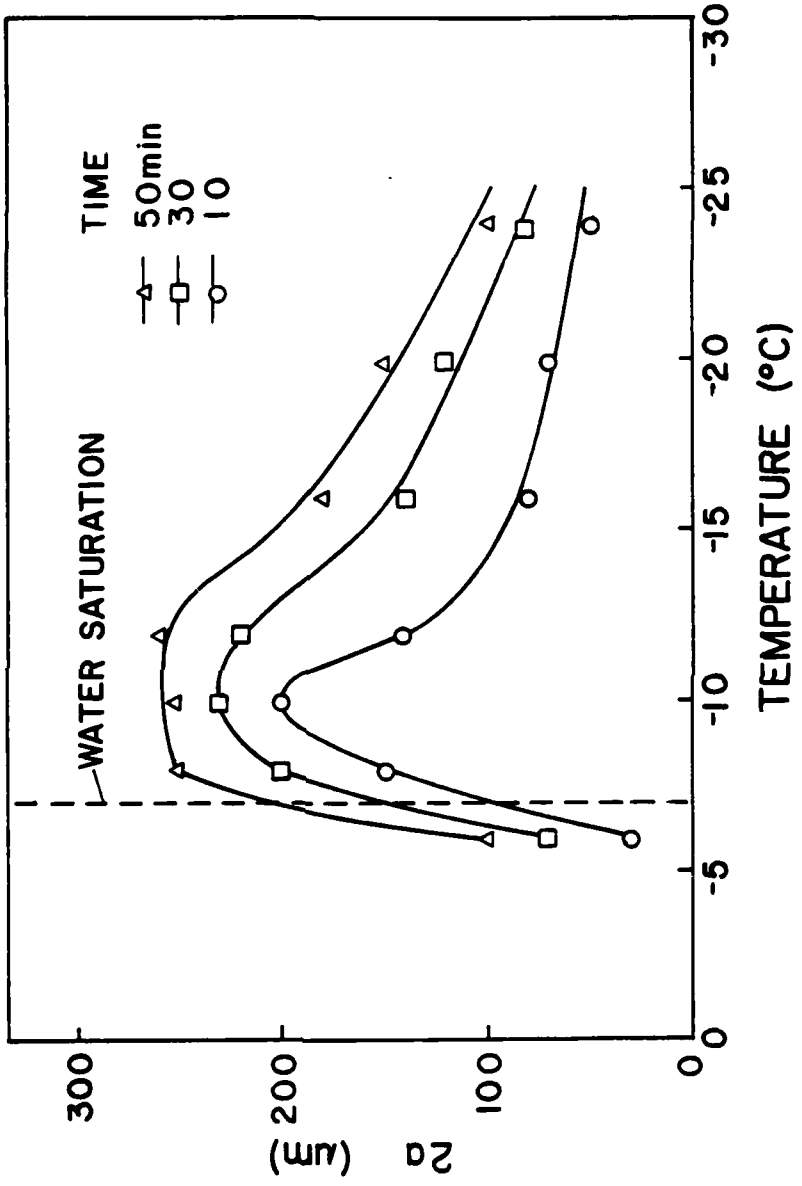

Figure 21. Ice crystal diameter 2a plotted as a function of temperature at different times of growth under ice supersaturation (S_i-1) at 7%.

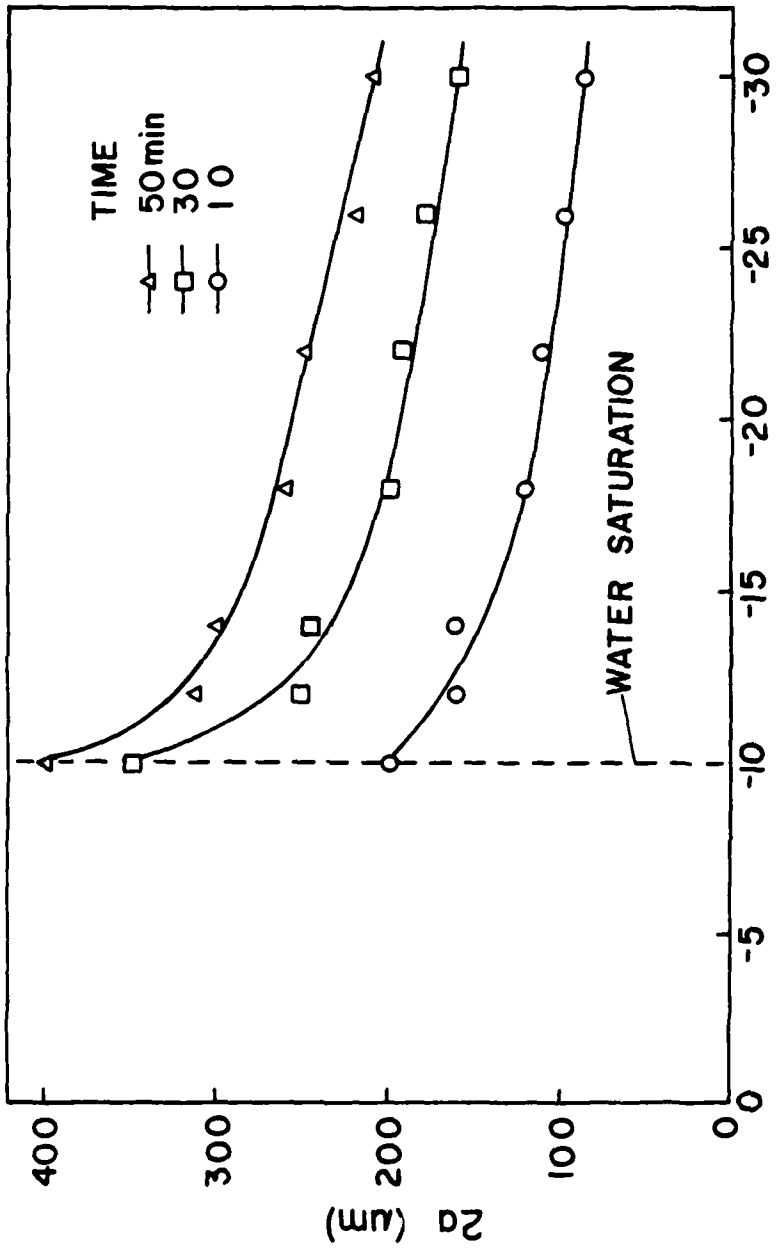

Figure 22. Ice crystal diameter 2a plotted as a function of temperature at different times of growth under ice supersaturation (S_i-1) at 10%.

AD-A105 520 AIR FORCE INST OF TECH WRIGHT-PATTERSON AFB OH F/G 8/12
MECHANISM OF ICE CRYSTAL GROWTH HABIT AND SHAPE INSTABILITY DEV--ETC(U)
AUG 81 G D SWOBODA
UNCLASSIFIED AFIT-CI-81-32T NL

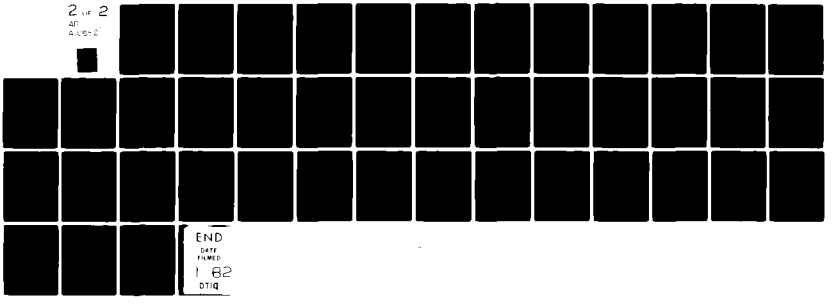

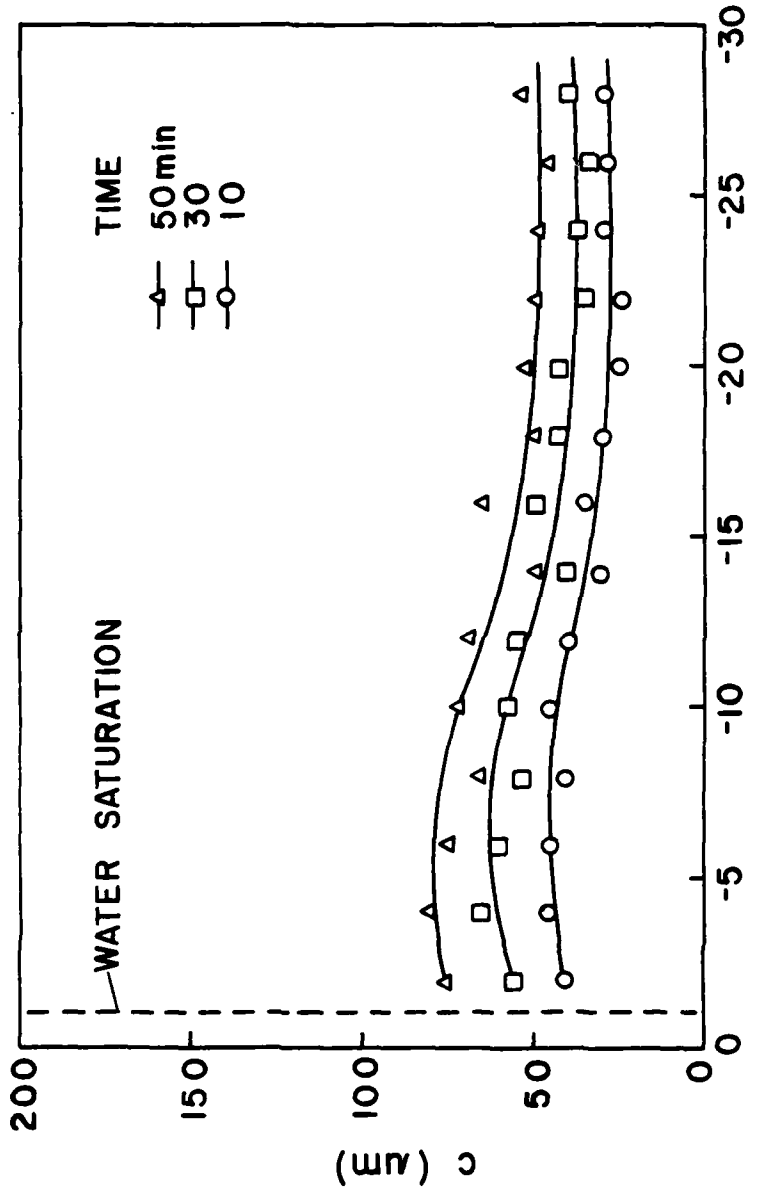

Figure 23. Ice crystal height c plotted as a function of temperature at different times of growth under ice supersaturation (S_i-1) at 1%.

-28 to about -20°C, relatively constant c values occur for all growth times. A gradual increase in c values appear between -20 and about -6°C as the conditions approach water saturation, with a gradual c decrease just below water saturation.

Similar behaviors of c values may be seen for (S_i-1) at 5% as shown in Figure 24. A gradual increase in c values occurs as temperatures warm from -30 to about -12°C followed by a rapid increase from -12 to -8°C. A rapid decrease in c values is seen between -8 and -6°C as the conditions surrounding the crystal approach water saturation. This decrease is much more pronounced for the 30 and 50 minute growth curves.

The c values for conditions of ice supersaturation (S_i-1) at 7% are depicted in Figure 25. Like the 1 and 5% data, a gradual increase in c occurs followed by a rapid increase as the water saturated condition is approached. Just above water saturation at -6°C, a very rapid increase in c values is seen.

The c values for (S_i-1) at 10% (Fig. 26) show the same basic trends as the others, i.e., a gradual increase in c values as temperatures warm followed by a rapid increase as the water saturated condition is approached. At about water saturation, no decrease in c is noted, as in the 1 and 5% data, but a leveling off or constant c is observed between -14 and -10°C.

Trends observed in the data for c are much the same as those observed for 2a. A gradual increase takes place in both 2a and c as temperatures warm from -30°C to a point where a more rapid increase occurs; however, for some values of (S_i-1), a rapid decrease in 2a or c happens as environmental conditions immediately surrounding the ice

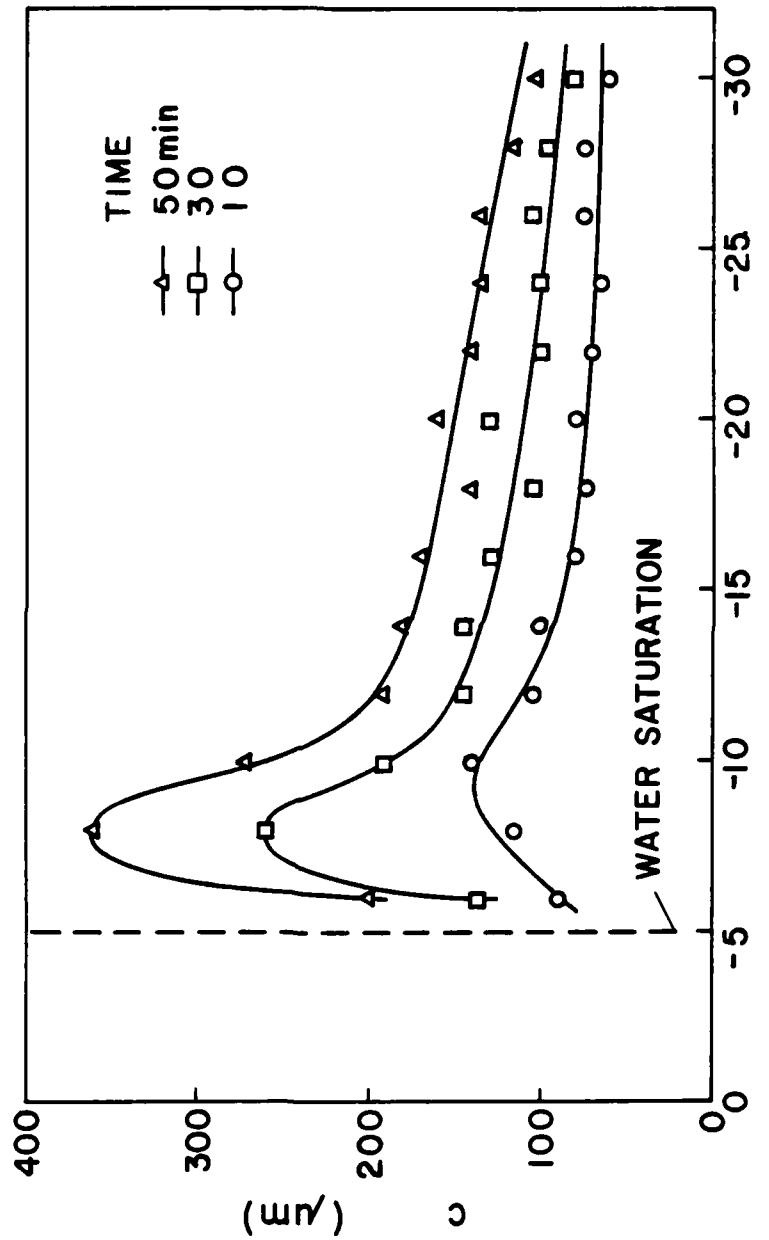

Figure 24. Ice crystal height c plotted as a function of temperature at different times of growth under ice supersaturation (S_i-1) at 5%.

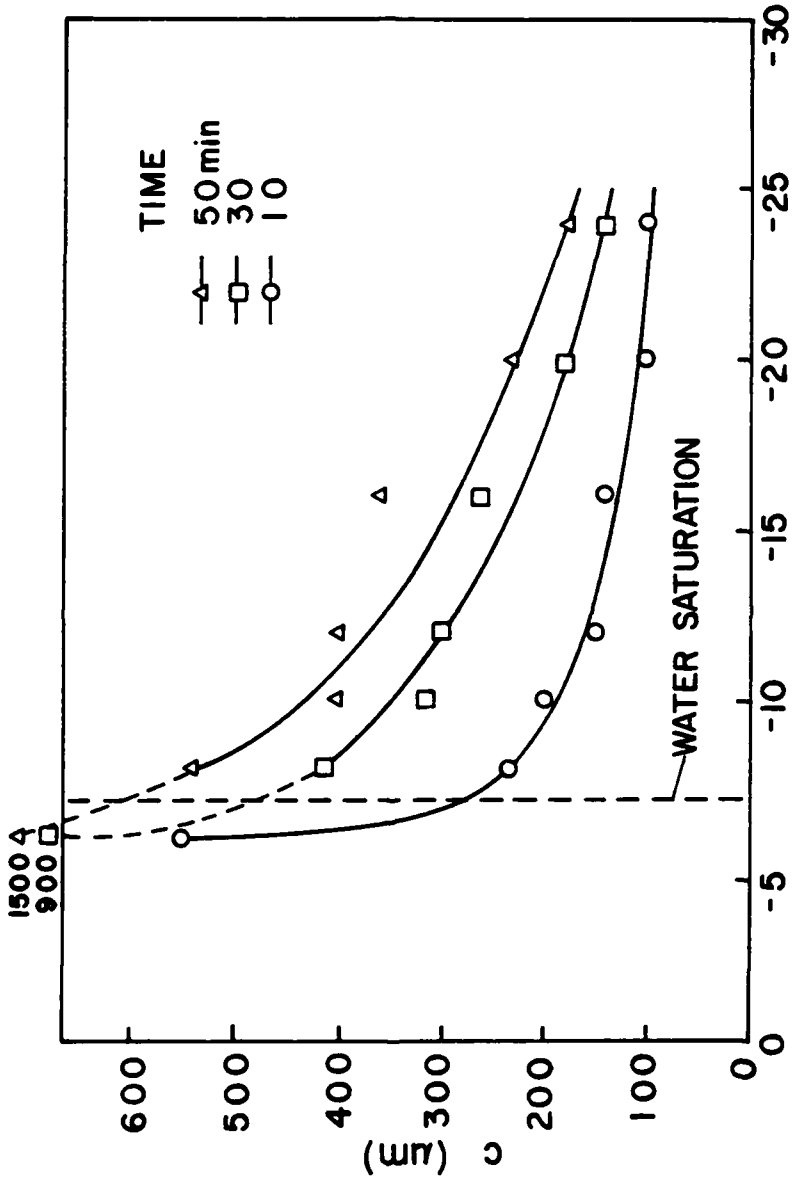

Figure 25. Ice crystal height c plotted as a function of temperature at different times of growth under ice supersaturation (S_i-1) at 7%.

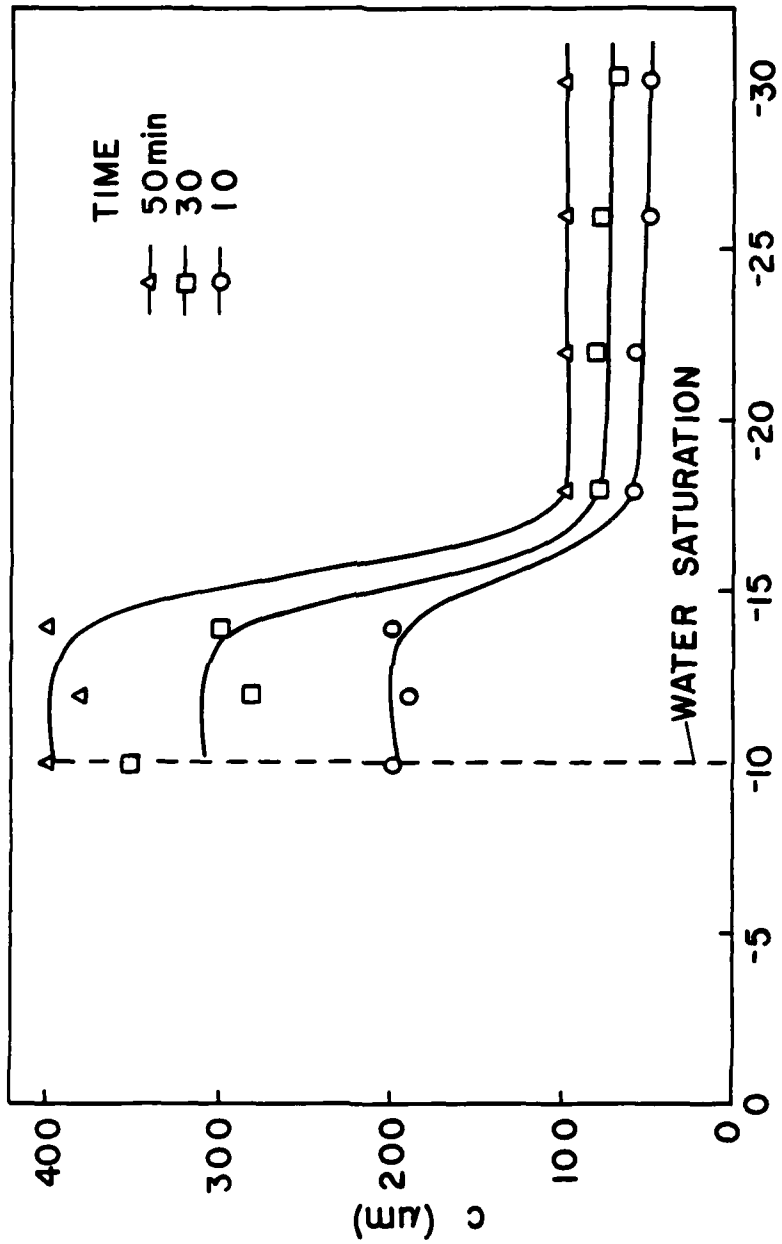

Figure 26. Ice crystal height c plotted as a function of temperature at different times of growth under ice supersaturation (S_i-1) at 10%.

crystal approach water saturation.

6.3 Ratio of the Diameter of the Basal Plane and Height of the Prism Plane or 2a/c

A way to describe ice crystal habit variation is to make the ratio of 2a and c, with values greater than unity indicative of plates, those less than that prisms, and those equal to that isometric crystals. Much experimental evidence has been provided as to the ice crystal habit regimes for conditions at or above water saturation (Nakaya, 1954; aufm Kampe et al., 1951; Mason, 1953; Hallett and Mason, 1958; Kobayashi, 1961; Magono and Lee, 1966; Fukuta, 1969; Ryan et al., 1976). Only sparse information has been reported in the region between ice and water saturation (Hallett and Mason, 1958; Kobayashi, 1961; Magono and Lee, 1966; Rottner and Vali, 1974). Hallett and Mason used a thermal diffusion chamber in their study which was subject to problems previously discussed and, in addition, limitations of their apparatus prevented them from achieving ice crystal growth at low ice supersaturations for temperatures colder than -10°C. Kobayashi's work, although quite extensive, is subject to careful scrutiny since environmental conditions in his apparatus were not clearly defined. Magono and Lee studied natural snow crystals, under estimated atmospheric conditions, and their results in regions of low ice supersaturations were sparse. Using a parallel plate ice thermal diffusion chamber, Rottner and Vali took into consideration aspect ratio problems and therefore their chamber conditions should have been reasonably accurate. Nevertheless, certain theoretical as well as procedural problems accompanied their results. First, they tried to define conditions at the growing ice crystal surface

based on the vapor desnity difference between the environment and the crystal surface. However, once the surface conditions are assumed, say, Maxwellian, the temperature and supersaturation of the environment, in addition to state variables such as pressure can also define the conditions. By using the environmental conditions rather than Rottner and Vali's surface conditions to describe ice crystal growth, we estimated an ice crystal surface temperature deviation (warming) from the environment by only 0.3° at the maximum vapor density excess condition at -11.6°C. Their attempt to describe surface condition was, therefore, not particularly more advantageous than using the environmental temperature and supersaturation values. Also, a theoretical error was discovered in Rottner and Vali's calculation of the excess vapor density at the ice crystal surface. In equation 5 (Rottner and Vali, 1974),the term describing the latent heat of deposition must be removed.

Rottner and Vali's data were of qualitative nature and the data were measured only at five temperatures (-8, -12, -16, -20, and -24°C). Their ice crystal growth was not carried out at a constant ice supersaturation as the temperature was varied. In addition, very large frozen drops used at the start of growth in a rather short chamber induced large errors in terms of temperature and supersaturation around the crystal. In order to compare our data with theirs, their values of excess vapor density (the vapor density difference between the environment and the crystal) were multiplied by 1.57 and converted into values in excess from ice saturation.

Little experimental data of ice crystal growth habit, in the region between water and ice saturation, have been reported and, that which have are subject to question due to the uncertainties in defining

experimental conditions. Using the wedge-shaped ice thermal diffusion chamber, we could observe and measure both the diameter and height of ice crystals growing under accurately controlled environmental conditions.

Figure 27 shows the 2a/c values after 50 minutes of growth under (S_i-1) at 1%. Thick plates ($1 < 2a/c < 2$) form in the temperature region between -30 and -15°C with a gradual increase in the ratio as the temperature warms from -30°C. A rapid increase in the ratio (2.0 to 3.5) occurs at temperatures between -15 and -4°C as conditions approach water saturation, followed by a sharp decrease just below water saturation. Hallett and Mason (1958) showed a distinctive plate zone between 0 and -9°C at a (S_i-1) of 1% similar to our data, but they could obtain no data at temperatures below -9°C. Kobayashi (1961) reported plates between 0 and -5°C, and between -10 and -21°C similar to our data but reported solid prisms in the temperature zone -4 to -10°C and for temperatures colder than -21°C. Since the very thick plates we observed from -20 to -30°C have ratios very close to unity, our data and Kobayashi's are in reasonable agreement; however, there exists a definite difference between our data, which agree with Hallett and Mason's, and Kobayashi's in the temperature region -4 to -10°C. Rottner and Vali reported solid columns in the 1% ice supersaturation region with coexisting thick plates at temperatures below -20°C.

Our 2a/c values after 50 minutes of growth under (S_i-1) at 5% are depicted in Figure 28. Isometric crystals ($2a/c = 1$) with very thick plate shapes exist from -30 to -10°C with a thinner plate peak ($2a/c = 1.5$) at about -18 and -10°C. A short prism ($2a/c = 0.9$) occurs at -8°C due to the habit variation with time as described in Section

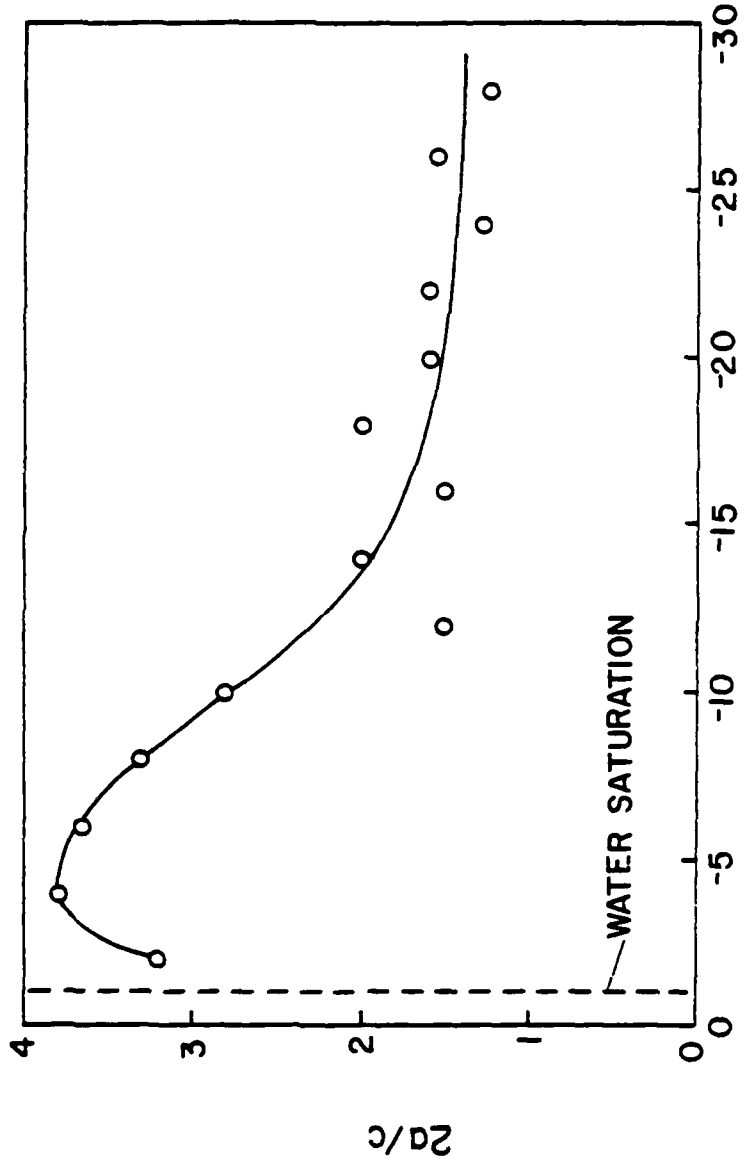

Figure 27. Ratio of ice crystal diameter and height 2a/c plotted as a function of temperature after 50 minutes of growth under ice supersaturation (S_i-1) at 1%.

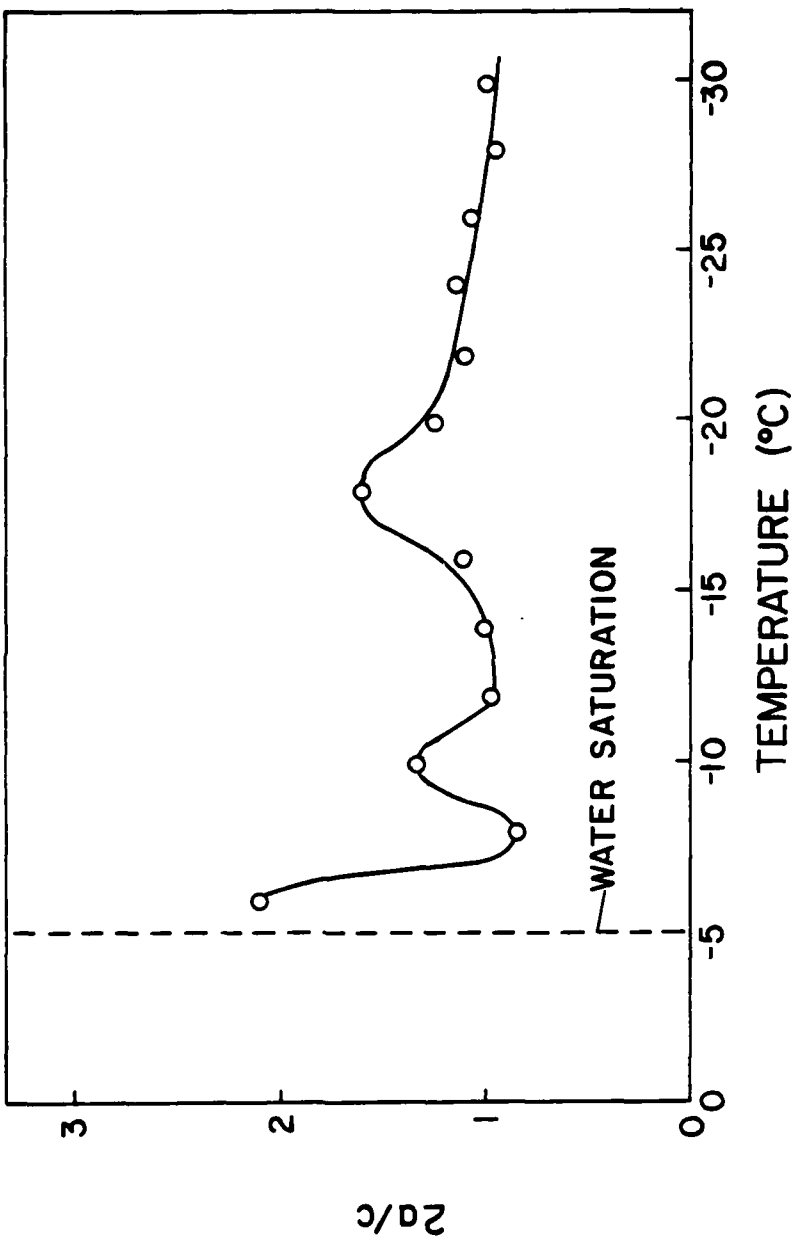

Figure 28. Ratio of ice crystal diameter and height 2a/c plotted as a function of temperature after 50 minutes of growth under ice supersaturation (S_i-1) at 5%.

6.1. Finally, a plate (2a/c = 2) appears at -6°C. Hallett and Mason also observed plates in the temperature zone -6 to -18°C but had no data at colder temperatures. Kobayashi showed prisms between -6 and -10°C, thick plates between -10 and -18°C, and solid prisms at temperatures colder than -18°C. Our crystals being at or slightly above isometric temperatures colder than -20°C are not entirely inconsistent with Kobayashi's observation and are in agreement with Rottner and Vali's observation; both thick plates and flat prisms at -24°C. Rottner and Vali also observed thick plates at -20, -16, and -12°C with prisms occurring at -8°C very similar to our findings.

The 2a/c values measured in the present study after 50 minutes of growth under ice supersaturation at 7% are shown in Figure 29. Prisms can be seen existing between -26 and -10°C followed by a rapid 2a/c decrease as the water saturated condition is approached. As previously mentioned, we observed ice crystals growing above water saturated conditions at a temperature of -6°C. Our observation of needle formation at this temperature is consistent with all previous studies of ice crystal growth at water supersaturated conditions. At 7% ice supersaturations, Hallett and Mason observed thick plates in the temperature zone -7 to -16°C as did Rottner and Vali for all five of their temperatures. These results are slightly contradictory to our findings. Kobayashi obtained plates in the region -10 to -21°C and prisms from -7 to -10°C and colder than -21°C.

Our data for 2a/c plotted as a function of temperature after 50 minutes of growth under ice supersaturation at 10% is shown in Figure 30. Plates with increasing 2a/c ratios grow from -30 to -16°C as the temperature is warmed with a rapid transition to isometric crystals from

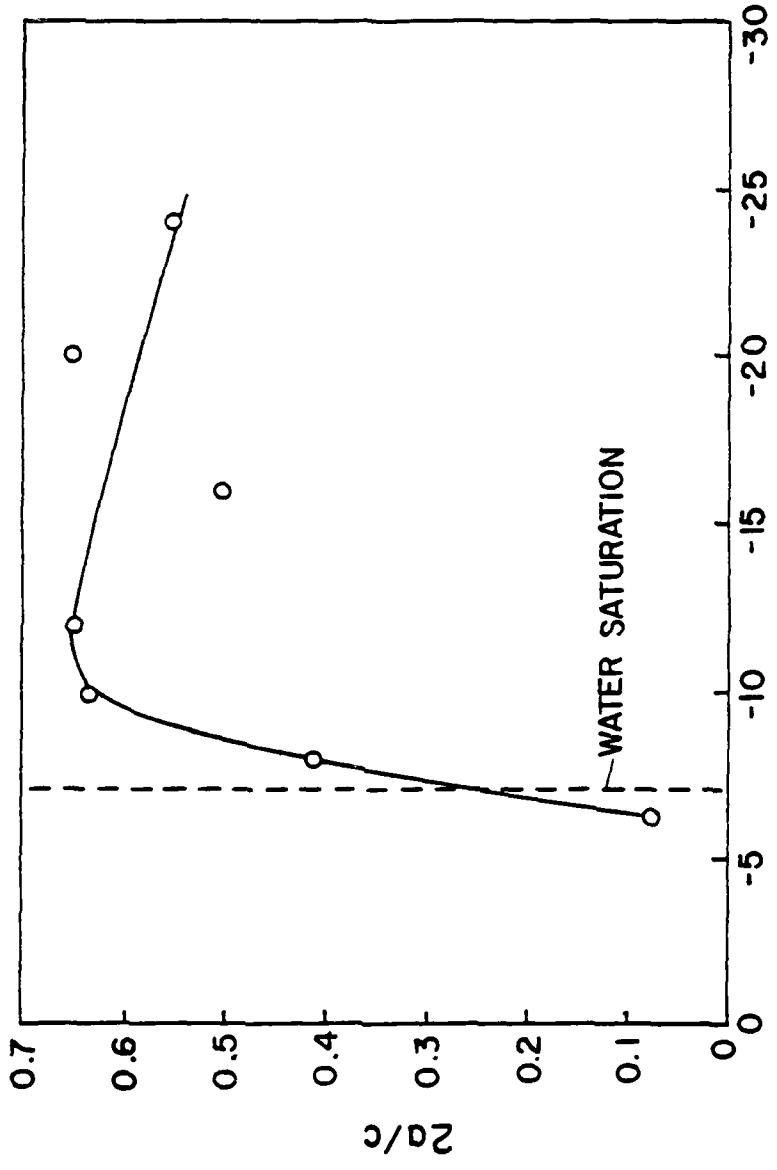

Figure 29. Ratio of ice crystal diameter and height 2a/c plotted as a function of temperature after 50 minutes of growth under ice supersaturation (S_i-1) at 7%.

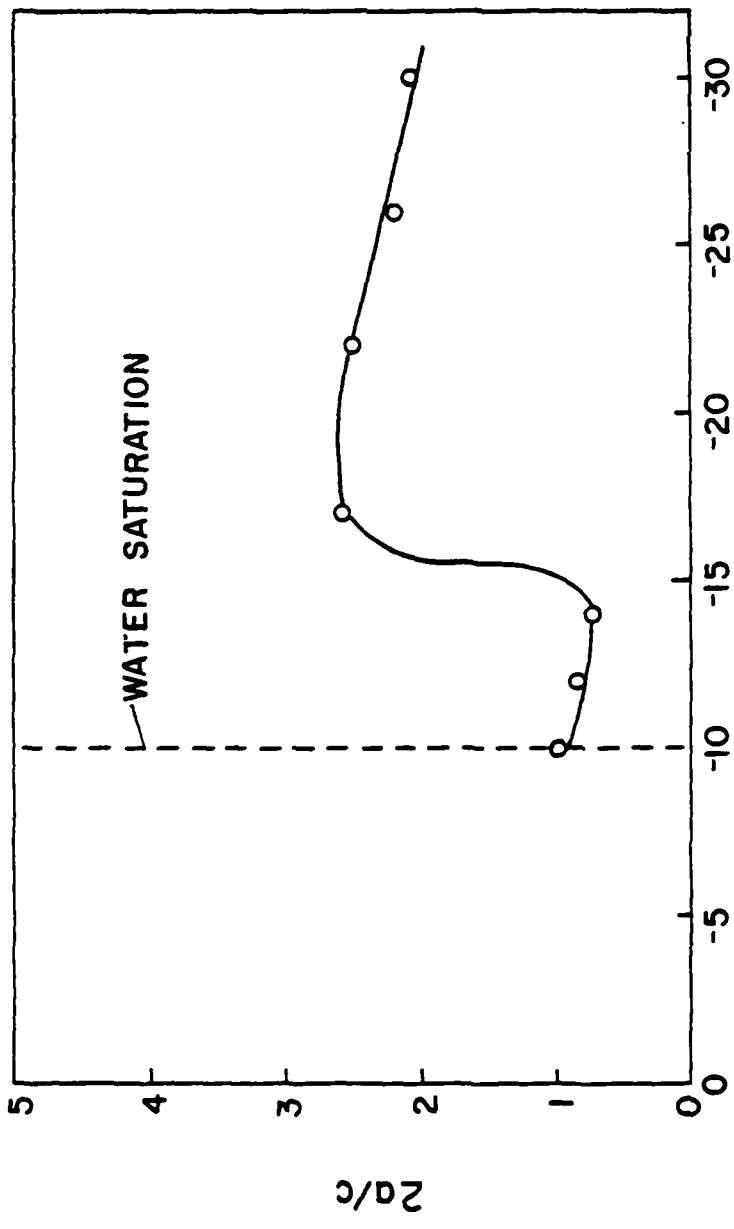

Figure 30. Ratio of ice crystal diameter and height 2a/c plotted as a function of temperature after 50 minutes of growth under ice supersaturation (S_i-1) at 10%.

-16 to -10°C as conditions approach water saturation. Hallett and Mason observed plates at this ice supersaturation from -10 to -26°C and Rottner and Vali observed plates at -12, -16, -20 and -24°C. Kobayashi showed results almost opposite of ours, i.e., plates from -10 to -21°C and prisms at temperatures colder than -21°C.

It appears that the transition zones of plates and prisms are subject to much confusion and the zones just below water saturation are particularly complex.

6.4 Ice Crystal Growth Habit as a Function of Temperature and Ice Supersaturation

Previous studies have provided basic ice crystal growth habit information at supersaturations greater than ice saturation but less than water saturation. However, as mentioned in the previous section, some experimental apparatus and techniques of earlier studies are highly suspect since problems of aspect ratio, convective activity, and transient supersaturations were not known and, therefore, were not properly considered at the time of the studies. In addition, only basic ice crystal growth habit or 2a/c has been described, with very little information available on the growth behavior of the individual basal and prism planes of ice. In our study, both apparatus and technique were designed so that accurate measurement of 2a and c, and the ratio 2a/c could be accomplished for individual ice crystals under properly controlled and reproducible environmental conditions.

Figure 31 shows the variation of the longest dimensions of the ice crystal basal plane 2a, after 50 minutes of growth, plotted as a function of temperature and ice supersaturation. A strong 2a growth

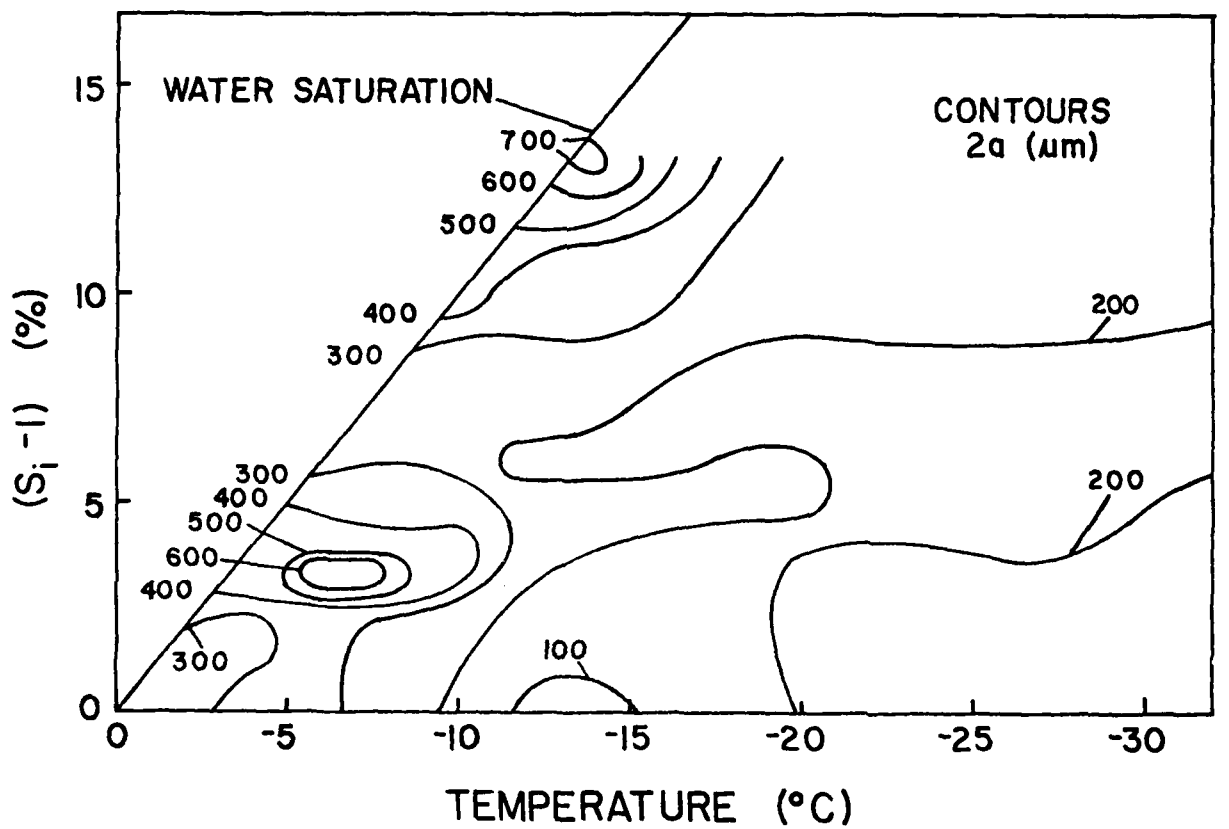

Figure 31. Variation of ice crystal diameter 2a plotted as a function of temperature and ice supersaturation.

peak exists at temeratures between -6 and -7°C under conditions of (S_i-1) at approximately 3%. Another strong growth peak is located at approximately -14°C at (S_i-1) of 14%. Although there are no distinct 2a minima, the trend appears to be one of small 2a values for small ice supersaturations at low temperatures, with a gradual, followed by a rapid increase in 2a values as water saturated conditions are approached. The exception to this is the zone at approximately (S_i-1) at 7% where there is only a slight increase in 2a values as water saturation is approached from a low temperature.

Figure 32 describes the variation of the height of the ice crystal prism place c, grown for 50 minutes, and plotted as a function of temperature and ice supersaturation. A marked c growth peak exists at approximately 7% ice supersaturation at temperatures between -6 and -9°C. As the temperature is warmed form -30°C, under conditions of ice supersaturation (S_i-1) at 7%, a gradual, followed by a rapid c increase occurs as the water saturated condition is approached. At ice supersaturations of 5 and 10%, a fairly gradual increase occurs as the temperature is warmed from -30°C. At 1% ice supersaturated conditions, a steady increase occurs as water saturated conditions are approached from a low temperature.

A very distinctive trend becomes apparent when comparing the 2a (Fig. 31) and c (Fig. 32) values. Both values exhibit a very gradual increase as the temperature is raised from a very low value. As the water saturated condition is approached, the 2a values exhibit a sharp increase at 3 and 14% ice supersaturations where c values show only a slight increase. Correspondingly, a strong c increase is shown at approximately 7% ice supersaturated conditions with only a slight

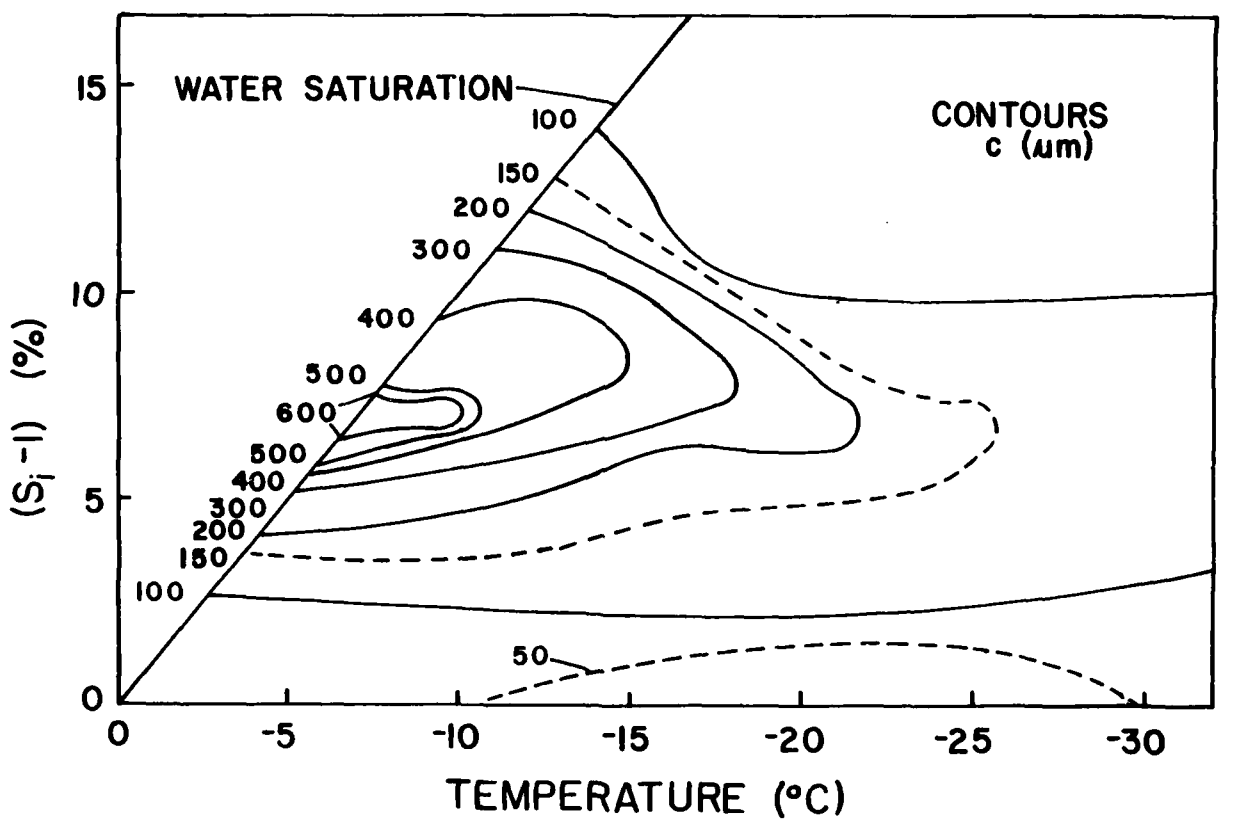

Figure 32. Variation of ice crystal height c plotted as a function of temperature and ice supersaturation after 50 minutes of growth.

increase in 2a values at the same conditions. It should be noted that a slight drop in both 2a and c values occurs for some ice supersaturated conditions but was not observed for others when conditions just below water saturation were reached.

It appears that there are different mechanisms that affect ice crystal growth at conditions between ice and water saturation. Kuroda and Lacman (1980) described 3 growth mechanisms, i.e., Vapor to Quasi-Liquid-Layer to Solid-Mechanism, Adhesive-Mechanism, and Two-Dimensional Nucleation-Mechanism. Their interpretation was that two-dimensional nucleation existed at cold temperatures under conditions of low excess vapor density (conditions much sub-saturated with respect to water) and as excess vapor density values increased at warmer temperatures the adhesive mechanism became the primary mechanism affecting ice crystal growth. As warmer temperatures were achieved and excess vapor density values became large, a liquid-like-layer formed on the surface of ice and it was the vapor to quasi-liquid-like-layer to solid mechanism which controlled ice crystal growth. Previous studies, however, offered very little proof of the existence of this quasi-liquid-like-layer.

Our study does show these three distinct regions of different growth behavior. At very cold temperatures and at conditions much sub-saturated with respect to water, both 2a ans c values show a very gradual increase. This could be interpreted as the region of two-dimensional nucleation where the flux of vapor to both the basal and prism faces is equal and constant. As the temperature is warmed, the flux of water vapor to the crystal increases, i.e., closer to water saturation conditions, where our 2a and c values show a more rapid

increase. The adhesive mechanism could well explain this rapid increase since nucleation is enhanced in this mechanism by the proximity of two-dimensional pre-nucleation clusters expected to exist as the conditions approach water saturation. The very rapid growth of 2a at 3% ice supersaturation and of c at 7% ice supersaturation as water saturation conditions are approached appears to be associated with this mechanism. However, as the environmental condition approaches water saturation, the free energy difference between ice and water decreases. This permits the strained surface of the ice crystal (origin of surface free energy) to transform into a liquid-like structure and suppresses pre-nucleation cluster formation on the ice surface. This leads to a decrease in growth of the ice crystal plane in question. As the temperture is further warmed, the depth of the liquid-like layer is increased and its straining effect to the pre-nucleation clusters reduces. Then, ice crystal growth becomes easier due to two-dimensional nucleation of ice now taking place in unstrained liquid water. The growth peak of 2a at 14% may be due to an adhesive growth mechanism and responsible, at least partially, to the growth of plates at -14°C at conditions above water saturation.

The existence of a liquid-like-layer on ice has long been postulated, but the availability of accurate data in the region between ice and water saturations has been extremely limited. Our observation of rapid growth decrease just below water saturated conditons appears to verify that, at warm temperatures and near water saturation, a liquid-like-layer does exist on the surface of ice.

Figure 33 shows the variation of habit 2a/c of ice crystals grown for 50 minutes plotted as a function of temperature and ice supersaturation. The contours of 2a/c are plotted in logarithmic scale so

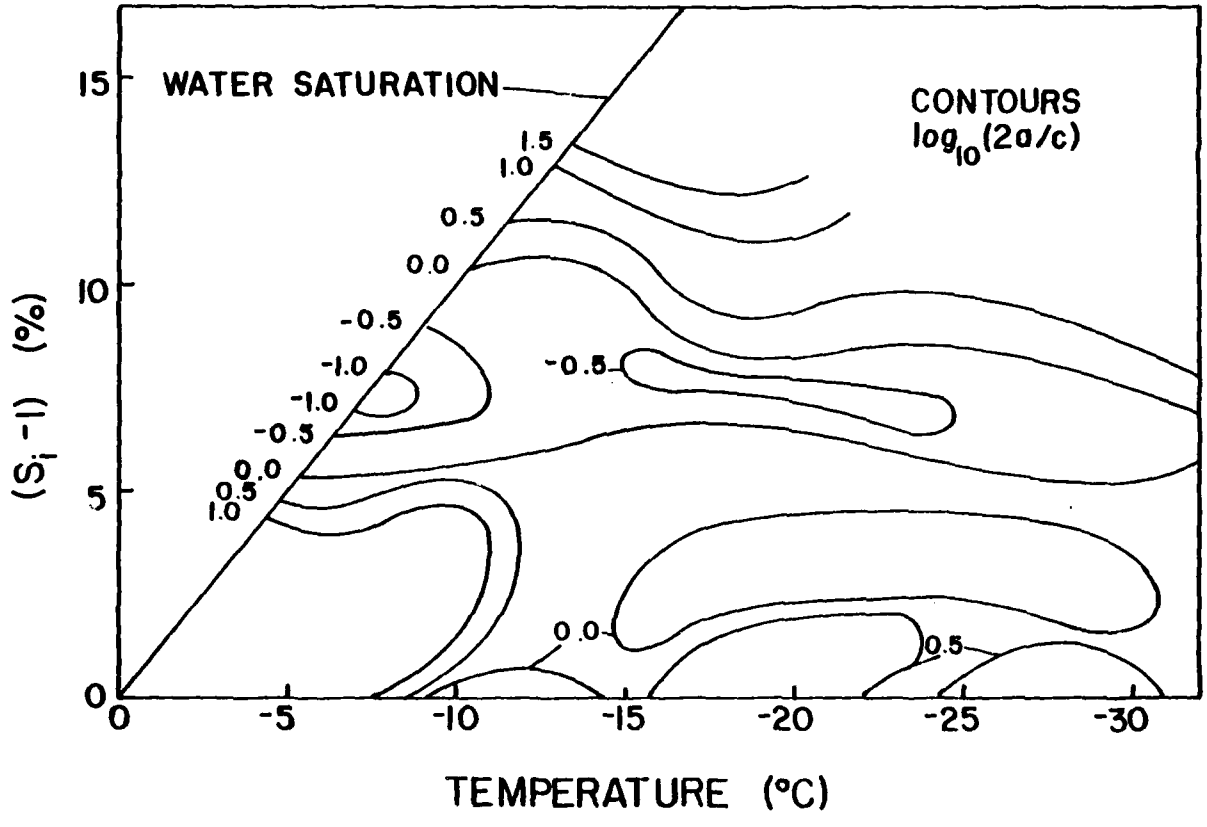

Figure 33. Variation of the ratio of ice crystal diameter and height 2a/c plotted as a function of temperature and ice supersaturation after 50 minutes of growth.

that plates are shown as positive, isometric crystals as zero, and prisms as negative. Our results clearly show that temperature does not appear to be the controlling factor of ice crystal habit in the region between ice and water saturations as it is at conditions above water saturation. Thin plates exist from 0 to approximately -10°C at ice supersaturations between 0 and 4%, and in the vicinity of -14°C and ice supersaturations of 13 to 14%. Thick plates exist at temperatures between -15 and -30°C at ice suersaturations of approximately 1%; at the temperatures between -15 and -30°C at 5% ice supersaturation; and at temperatures colder than -14°C at an ice suersaturation of 10%. Prisms exist in the region between -15 and -30°C between ice supersaturations of about 2 to 4%, and in the region between 5 and 10% ice supersaturations at all temperatures and conditions below water saturation. Isometric crystals exist at approximately 5% ice supersaturation at temperatures below -5°C; at 10% ice supersaturation at temperatures between -10 and -15°C; at approximately 9 to 10% ice supersaturations at temperatures colder than -15°C; and at approximately 2 to 4% ice supersaturations at temperatures colder than -15°C. For temperatures colder than -15°C, ice supersaturation appears to be the controlling factor of ice crystal growth habit with plates at 0 to 2%, prisms from 2 to 4%, plates at approximately 4 to 5%, prisms from 5 to 9%, and plates at ice supersaturated conditions greater than 9%. At temperatures warmer than -15°C, there appears to be 3 distinct zones of ice crystal habit, i.e., thin plates at ice supersaturations of 0 to 4%, elongated prisms between 5 and 9%, and thin plates at ice supersaturations greater than 10%.

Ice crystal growth habit has been shown to be a function of

temperature at conditions above water saturation by previous studies. Our study shows that below water saturation, ice crystal habit is a function of ice supersaturation at temperatures below -15°C with an alternating plate, prism, plate, prism, plate habit as ice supersaturation is increased from 1 to 10%. At temperatures warmer than -15°C and conditions approaching water saturation, there appears to be 3 habit zones, i.e., plates between 0 and 4%, prisms between 5 and 9%, and plates greater than 10%. In this zone, ice crystal growth habit does not appear to be a function of either temperature or ice supersaturation alone. This may be because it is a transition zone between temperature dependent and ice supersaturation dependent ice crystal habit which is further made complex by the mechanisms of ice crystal growth at temperatures and ice supersaturations just below water saturation, especially with the liquid-like-layer-mechanism.

6.5 Ice Crystal Growth Characteristics

Our study focused primarily on the observation of ice crystal growth habit (2a/c) and the measurement of the dimensions of the basal (2a) and prism (c) planes of ice. Certain additional characteristics or features of ice crystal growth were observed as our experiments progressed.

Wulff's theorem describes an ice crystal in equilibrium and states: In equilibrium, the distance of any crystal face from its center is proportional to the surface tension at that face. Thus, for an ice crystal in equilibrium, Wulff's theorem predicts (Pruppacher and Klett, 1978)

$$\frac{c}{2a} \simeq 0.81 \qquad (12)$$

where c is the height of the prism plane and 2a is the longest dimension of the basal plane of ice. Kobayashi (1961), indeed, found that at very low excess vapor pressures, the c/2a value was 0.8 for ice crystals grown between -10 to -22°C. However, at warmer temperatures no trend to limit the habit was observed, while at temperatures colder than -22°C the c/2a values approach 1.4 (prisms). These last two results could be explained if it is assumed that Kobayashi's experimental system could not reproduce equilibrium conditions at temperatures warmer than -10°C and colder than -22°C. It may be interesting to relate our 2a/c values measured under (S_i-1) at 1% (Fig. 27). In the temperature range warmer than -20°C, the reciprocal of our 2a/c values are smaller than 0.81 showing that, as in Kobayashi's observations, near equilibrium conditions or Wulff's crystals do not exist in this region. At temperatures from -22 to -28°C our average c/2a are 0.71 which are a little lower than the equilibrium value but both of two points, which showed the highest value, do match the predicted value of 0.81.

Another new characteristic of ice crystal growth that we found was the formation of double plates. Two identical plates, connected together on the basal plane by a thin, flat mass of ice were observed for almost all temperatures warmer than -10°C under (S_i-1) less than 5% after 10 minutes of growth. At later times of growth, the plates grew identically symmetrical to each other under conditions very much subsaturated with respect to water; however, under conditions approaching water saturation, one plate would begin a rapid growth at the expense of the other plate. Therefore, after initally observing a symmetrical double plate, a single thin plate with a small hexagonal appendage was seen at the end of the growth period. At -8°C under (S_i-1) of

approximately 5%, the growth behavior was especially peculiar. As previously mentioned, under these conditions, ice crystals exhibited a change of habit from plate to prism as a function of time. Double plates of equal proportions existed during the initial 10 minutes, but as growth continued, one plate began a rapid growth in the prism (c) direction while little growth took place in the plate (2a) direction. The other plate experienced no growth at all in either direction. Subsequently, after a period of time, the initial double plate was transformed into a single prism.

In our present studies, ice crystals were observed for varying periods of time from 10 to 60 minutes, at tempratures ranging from -30 to -2°C under different ice supersaturations. We describe, in Sections 6.1 and 6.2, the general trends of a gradual increase in 2a and c values as the temperature warmed from -30°C followed by a more rapid increase of these values as conditions approached water saturation. In Section 6.4, we interpreted these phenomena by growth based on two-dimensional nucleation at the very cold temperatures and by growth based by an adhesive mechanism as conditions in the environment approached water saturation. The ice crystals grown at very cold temperatures, i.e., -15 to -30°C, had very smooth surfaces with distinct edges on both the basal and prism faces. On the other hand, as conditions approach water saturation, the basal and prism surfaces became ragged where surface defects, appendages, and general deformation were commonly seen. This was the area where rapid growth of the ice crystals took place. The adhesive mechanism, speculated to be responsible for the rapid growth, may also have contributed to formation of appendages, etc., through easier nucleation at the surface.

The transformation from pure hexagonal plates to sector plates and the appearance of cavities on the prism faces were also observed. At very cold temperatures, hexagonal plates transformed into sector plates and cavities appeared on the prism faces at times between 30 and 35 minutes. These same transformations took place at our initial observation time of 10 minutes at warmer temperatures as environmental conditions approached water saturation.

Chapter 7

CONCLUSIONS AND RECOMMENDATIONS

Schaller and Fukuta (1979) designed and built the wedge-shaped ice thermal diffusion chamber for their studies in ice nucleation. Their chamber was semi-dynamic since, at the start of each experiment, an entire air sample was injected into the chamber and then allowed to achieve steady-state conditions in the chamber. In an attempt to modify their chamber in an entirely static mode, a number of apparatus and experimental techniques were developed. The subsequent use of the chamber for ice crystal growth habit and shape instability studies resulted in a number of new findings. Our main contributions in development of apparatus and experimental techniques, and in ice crystal growth habit and shape instability studies followed by recommendations for future research and development are listed below.

7.1 Instrument Development

The concept of the wedge-shaped ice thermal diffusion chamber (Schaller and Fukuta, 1979) has been shown, with several new modifications, to applicable for studying ice crystal growth habit and shape instability. Main features of this modified chamber, primary supporting equipment and experimental techniques are as follows:

1. The wedge-shaped ice thermal diffusion chamber was modified in order to minimize errors in aspect ratio, transient

supersaturations, relaxation time, and non-linearity of temperature. Growth of ice crystals in adequately controlled environmental conditons has been demonstrated.

2. A method of transferring nucleated ice crystals from one environment to another using an ordinary pre-conditioned meat baster has been demonstrated. Ice crystals survived up to 30 seconds in the device during the transfer.
3. A pre-chamber (simplified parallel plate ice thermal diffusion chamber) was desinged and constructed to allow the transferred seed ice crystals to be impregnated on a fine fiber.
4. The ice crystal slide mechanism was designed and constructed to quickly transfer small seed ice crystals from the pre-chamber to the wedge-shaped chamber and allow rotation of the ice crystals in the wedge-shaped chamber for observation from different angles.
5. The lateral microscope slide mechanism was designed and built so that ice crystals could be observed and photographed in all points of the vertical center of the working area of the wedge-shaped chamber.

7.2 Ice Crystal Growth Habit and Instability Findings

The accurate temperature and supersaturation control available in the wedge-shaped ice thermal diffusion chamber allowed us to conduct a quantitative study of ice crystal growth habit and shape instability.

New findings are as follows:

1. Under all (S_i-1) tested in the study, i.e., 1, 5, 7, and 10%, as the temperature warms from low values, a gradual increase in 2a and c values occurred followed by a more rapid increase as water saturated conditions were approached. For some (S_i-1), a sharp decrease in 2a and c was noted just below water saturation. This can be explained at this time only if we assume three distinct ice crystal growth mechanisms: two-dimensional nucleation at cold temperatures with environmental conditions much sub-saturated with respect to water, an adhesive mechanism as temperatures warm and conditions approach water saturation, and the liquid-like-layer mechanism at conditions around or just below water saturation.
2. Ice crystal habit varies as a function of time at -8°C and under (S_i-1) between 5 and 7%. At early growth times, plates existed which were transformed to prisms later.
3. The 2a and c data plotted as a function of temperature and supersaturation showed definite zones of growth maxima. Gradual increases in 2a and c values occurred at all (S_i-1) as the temperature warmed from cold temperatures and conditions approached water satuation with 2a maxima centered between -6 and -7°C under (S_i-1) at 3%, and -14°C under (S_i-1) at 14%. Maximum c values were found with (S_i-1) at approximately 7% between the temperatures of -7 and -10°C.
4. Ice crystal habit (2a/c) showed a complex relationship with temperature and supersaturation. Habit varied as a function

of ice supersaturation at temperatures lower than -15°C and (S_i-1) less than 10%, i.e., plates at 0 to 2%, prisms from 2 to 4%, plates at approximately 4 to 5%, prisms at 5 to 9%, and plates greater than 9%. Three distinct zones of 2a/c existed at temperatures warmer than -15°C, i.e, thin plates at (S_i-1) of 0 to 4%, elongated prisms at (S_i-1) between 5 and 9%, and thin plates at (S_i-1) greater than 10%.

5. Wulff's crystals did not exist at lower supersaturations and temperatures warmer than -22°C; however, they were observed at temperatures between -22 and -28°C.
6. Double plates were found at temperatures warmer than -10°C under (S_i-1) between 0 and 5%.
7. Surface characteristics of the basal and prism planes varied as a function of temperature and sub-saturation with respect to water. Between the temeratures of -15 and -30°C under low (S_i-1), the basal and prism surfaces exhibited very smooth surfaces but at warmer temperatures, as conditions approached water saturation, appendages, surface defects and general crystal deformation were detected.
8. The transformation of hexagonal plates to sector plates and the appearance of prism face cavities were observed at cold temperatures at a time of 30 to 35 minutes, and at warmer temperatures, as conditions approach water saturation, within the initial observation time of 10 minutes.

7.3 Recommendations for Future Research

Possible improvements for the present apparatus may be achieved

in the following points:

1. Ice crystals impregnated on the fine nylon fiber should be slid into the wedge-shaped chamber from the narrow end rather than the wide end. This may allow ice crystal growth to be observed at environmentl conditions above water saturation.
2. Motorization of the lateral microscope slide mechanism would help achieve almost simultaneous observation of ice crystals in all points of the workable area of the wedge-shaped chamber.
3. If the temperature of the outer environmental chamber can be varied with the center line temperature of the wedge-shaped chamber, non-linearity of temperature through the copper plates of the wedge-shaped chamber can be eliminated.
4. A continuation and expansion of this study would entail a finer grid of observations between 1 and 10% ice supersaturations and extension of ice supersaturations greater than 10%. Special emphasis should be placed on distinguishing the zones and overlapping zones of the mechanisms affecting ice crystal growth, i.e., mechanisms of two-dimensional nucleation, adhesion, and liquid-like-layer.
5. The complex area, just below water saturation at all temperatures, should be thoroughly examined for more evidence of the liquid-like-layer mechanism of ice crystal growth.

APPENDICES

Appendix A

SOLUTION FOR $\nabla^2 p = 0$

Under the steady state transportation of water vapor, $\nabla^2 p = 0$ holds with sufficient accuracy. Since the chamber has the same shape along one of the horizontal axis,

$$\frac{\partial^2 p}{\partial x^2} + \frac{\partial^2 p}{\partial y^2} = 0 \ , \tag{A1}$$

showing that the curvatures in the x and y directions are oppositive. In addition, if we express the saturation vapor pressure along the top and bottom plates with a quadratic function of temperature, the type of surface satisfying the above conditions is a hyperbolic paraboloid,

$$\frac{x^2}{a^2} - \frac{y^2}{b^2} = \frac{p}{c} \ . \tag{A2}$$

Consequently,

$$\frac{\partial p}{\partial x} = \frac{2cx}{a^2} \ , \tag{A3}$$

$$\frac{\partial^2 p}{\partial x^2} = \frac{2c}{a^2} \ , \tag{A4}$$

$$\frac{\partial^2 p}{\partial y^2} = \frac{2c}{b^2} \ , \tag{A5}$$

However, in order to satisfy the condition (A1), a = b. Therefore, the

surface which satisfies the above conditions is that of a hyperbolic paraboloid having the equation,

$$x^2 - y^2 = \frac{a^2}{cp} \quad . \tag{A6}$$

Appendix B

NON-LINEARITY OF TEMPERATURE

It was found that the temperature profiles through the copper-plates became non-linear under certain temprature conditions. To determine the extent of this non-linearity, temperature through the plates was varied. The results are shown in Figure B1. A constant temperature difference of 20°C was maintained between the top and bottom plates at the wide end; however, the range of centerline temperatures was varied from -30 to -7°C.

The figure shows that when we tried to achieve very low centerline temperatures, the wedge-shaped chamber experienced a heat gain from the outer environment. The main gain of heat is at the coldest point of the workable chamber, i.e., the bottom plate at the wide end. The top plate under these temperature conditions remains linear. Conversely, when we tried to achieve warm centerline temperatures, the chamber experienced a heat loss to the environment. The main heat loss is experienced at the warmest point of the workable chamber, i.e., the top plate at the wide end. The bottom plate under these conditions remains linear. At a centerline temperature of approximately -12°C, which is the temperature of the outer environment in the vicinity of the chamber, almost perfect temperature-linearity is found through both the top and bottom plates.

Non-linearity of temperature through the plates resulted in a

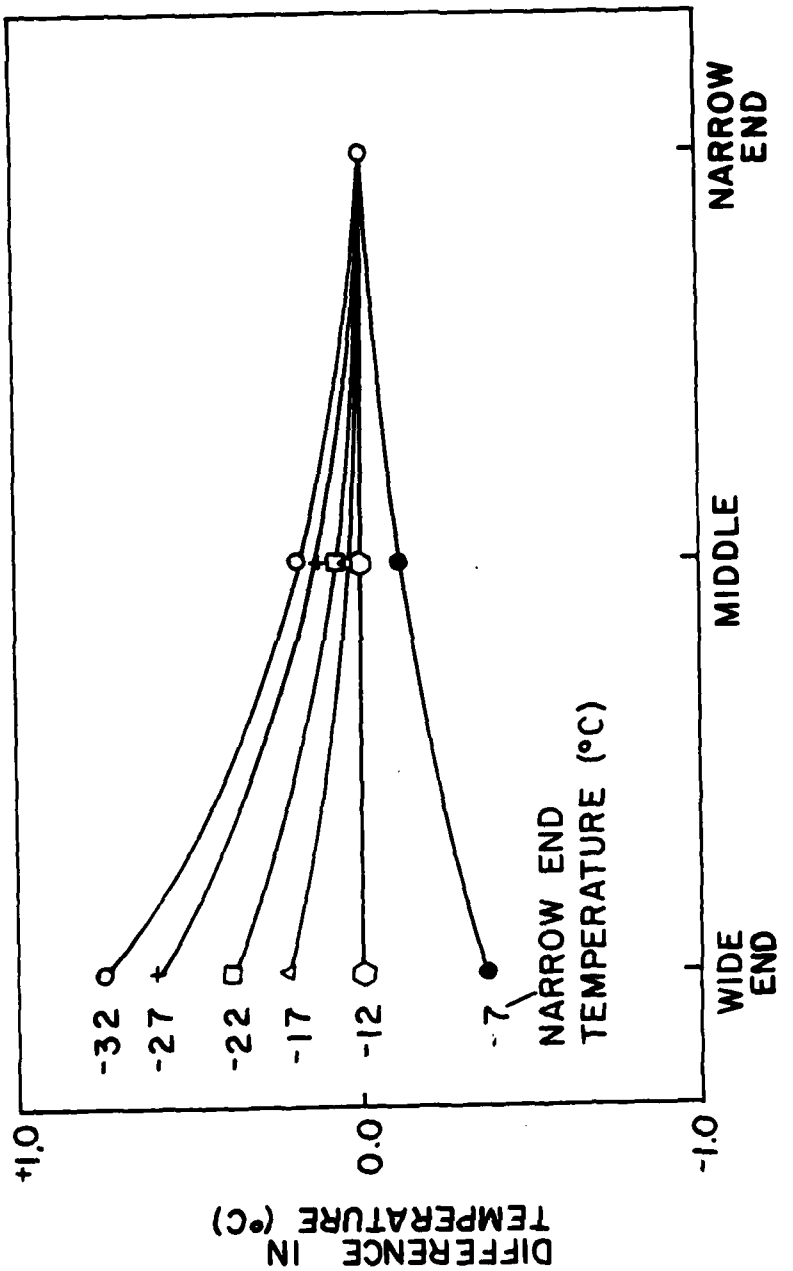

Figure B1. The center-line temperature deviation T plotted under different narrow end temperatures of ice in the wedge-shaped ice thermal diffusion chamber. The temperature difference at the wide end is 20°C and the environmental temperature is -12°C.

temperature field within the chamber that is not horizontally stratified. This could cause convective activity which would lead to undeterminable temperature and supersaturation fields within the chamber. To check this, smoke tests were performed for different temperature conditions and we found that very little convective activity was present in the chamber even under the worst cases; i.e., very cold or very warm. We concluded that with the rapidity of the rate of molecular vapor and heat diffusions, the small non-linearity of temperatures through the copper plates would not cause a problem.

Appendix C

DERIVATION OF THE RADIATIVE HEAT TRANSFER EQUATION

The radiative heat transfer in the wedge-shaped ice thermal diffusion chamber is independent of the distance between the top and bottom plates; therefore, we used the assumption of two parallel plates in our calculations. The radiative heat transfer from the top plate to the bottom plate is given by:

$$Q_{tb} = E_t F_{tb} A_t - E_t F_{bt} A_t , \tag{C1}$$

where E is the total emissive power of a non-black body and $E = \varepsilon E_b$, ε is the emissivity of ice and $\varepsilon = 0.95$, E_B is the total emissive power of a black body and $E_B = \sigma T^4$, σ is the Stephan-Boltzman constant, T is the temperature, F is the integrated factor of Lambert's Cosine Law and $F = 1/4$ for a unit area overlooking an infinite plane, and A is the surface area of the plates. For this case we define the reflectivity of ice R such that $R = 1 - \varepsilon$ and $R = 0.05$ for ice, $A_t = A_b = A$, $F_{tb} = F_{bt} = F$ $R_t = R_b = R$, and $\varepsilon_t = \varepsilon_b = \varepsilon$.

The radiative heat transfer equation from the top to bottom plate becomes

$$Q_{tb} = AF(E_t - E_b) , \tag{C2}$$

where

$$E_t - E_b = \sigma\varepsilon(\varepsilon T_t^4 - T_b^4) \ . \qquad (C3)$$

By substitution for $E_t - E_b$ back into equation (C2), the radiative heat transfer becomes

$$Q_{tb} = AF\sigma\varepsilon(\varepsilon T_t^4 - T_b^4) \ . \qquad (C4)$$

The radiative heat contribution emitted and reflected by the top plate B_t in the direction of the bottom plate is

$$B_t = \sigma\varepsilon T_t^4 + RH_b \ , \qquad (C5)$$

and likewise, the radiative heat contribution emitted and reflected from the bottom plate B_b in the direction of the top plate is

$$B_b = \sigma\varepsilon T_b^4 + RH_t \ . \qquad (C6)$$

Noting that $H_t = B_t$ and $H_b = B_b$, we have

$$B_t = \sigma\varepsilon T_t^4 + RB_b \ , \qquad (C7)$$

and

$$B_b = \sigma\varepsilon T_b^4 + RB_t \ . \qquad (C8)$$

Substituting the equality for B_t in (C7) into (C8)

$$B_b = \frac{\sigma\varepsilon(T_b^4 + RT_t^4)}{1 - R^2} \qquad (C9)$$

and substituting B_b in (C9) into (C7)

$$B_t = \frac{\sigma\varepsilon}{1 - R^2}(T_t^4 + RT_b^4) \ . \qquad (C10)$$

The radiative heat transfer per unit area is

$$\therefore q = H_t - B_b = B_t - H_b ;$$

therefore,

$$q = B_t - B_b , \tag{C11}$$

or

$$q = \frac{\sigma\epsilon}{1 - R^2} \left[(T_t^4 + RT_b^4) - (T_b^4 + RT_t^4) \right] , \tag{C12}$$

and for total radiative heat $q_r = Aq$; therefore,

$$q_r = \frac{A\sigma\epsilon}{1 - R^2} \left[(T_t^4 + RT_b^4) - (T_b^4 + RT_t^4) \right] . \tag{C13}$$

REFERENCES

Armstrong, J., and N. Fukuta, 1977: Deposition coefficient measurements of water vapor onto ice over an extended temperature and vapor flux range. Rarefied Gas Dynamics, Progress in Astronautics and Aeronautics, 51, 1241-1252.

aufm Kampe, H. J., H. K. Weickmann, and J. J. Kelly, 1951: The influence of temperature on the shape of ice crystals growing at water saturation. J. Meteor., 8, 168-174.

Byers, H.R., 1965: Elements of Cloud Physics. The University of Chicago Chicago Press, 191 pp.

Elliott, W.P., 1970: Dimensions of thermal diffusion chambers. J. Atmos. Sci., 28, 810-811.

Faraday, M., 1859: On regelation and on conservation of force. Phil. Mag., 17, 162-169.

Fitzgerald, J. W., 1970: Non-steady-state supersaturation in thermal diffusion chambers. J. Atmos. Sci., 27, 70-72.

Fletcher, N. H., 1962: Surface structure of water and ice. Phil. Mag., 7, 255-269.

_____, 1963: The Physics of Rainclouds. Cambridge University Press, 386 pp.

_____, 1968: Surface structure of water and ice. I. A revised model. Phil. Mag., 18, 1287-1300.

Frank, F. C., 1975: Snow Crystals. Rep. Proc. XVI General Assembly of IUGG, IAMAP, Grenoble, Aug.-Sept., 1975, 93.

Fukuta, N., 1969: Experimental studies on the growth of small ice crystals. J. Atmos. Sci., 26, 522-531.

_____, 1978: Ice crystal growth kinetics and accommodation coefficients. Cloud Physics and Atmospheric Electricity Conference, Seattle, Washington, 31 July - 4 August, 1978.

Gold, L. W., and B. A. Powers, 1954: Dependence of the forms of natural snow crystals on meteorological conditions. J. Meteor., 1, 35-42.

Hallett, J., 1961: The growth of ice crystals on freshly-cleaved covellite surfaces. Phil. Mag., 6, 1073-1087.

_____, 1965: Field and laboratory observations of ice crystal growth from the vapor. J. Atmos. Sci., 22, 64-69.

Hallett, J., and B. J. Mason, 1958: The influence of temperature and supersaturation on the habit of ice crystals grown from the vapor. Proc. Roy. Soc. London, A247, 440-453.

Hobbs, P.V., and W. D. Scott, 1965: A theoretical study of the variation of ice crystral habits with temperature. J. Geophys. Res., 70, 5025-5034.

Katz, J. L., and P. Mirabel, 1974: Calculation of supersaturation profiles in thermal diffusion cloud chambers. J. Atmos. Sci., 32, 646-652.

Kikuchi, K., and H. Uyeda, 1979: Cloud droplets and rain drops collected and frozen on natural snow crystals. J. Meteor. Soc. Japan, 57, 273-281.

Kobayashi, T., 1961: The growth of snow crystals at low supersaturations. Phil. Mag., 6, 1363-1370.

Kuroda, T., and R. Lacmann, 1980: Growth kinetics of ice from vapor phase and its growth forms. Preprints, Intl. Conf. of Cloud Physics, Clermont-Ferrand, France, 15-19 July, 1980, 109-112.

Lacmann, R., and I. N. Stranski, 1972: The growth of snow crystals from the vapor phase. J. Cryst. Growth, 13/14, 235.

Lamb, D., and P. V. Hobbs, 1971: Growth rates and habits of ice crystals grown form the vapor phase. J. Atmos. Sci., 28, 1506-1509.

Lamb, D., and W. D. Scott, 1974: The mechanism of ice crystal growth and habit formation. J. Atmos. Sci., 31, 570-580.

Langsdorf, A., Jr., 1934: A continuously sensitive cloud chamber. Phys. Rev., 49, 422.

Magono, C., and C. W. Lee, 1966: Meteorological classification of natural snow crystals. J. Fac. Sci. Hokkaido Univ., Sec. 7, 2, 321-335.

Mason, B. J., 1953: The growth of ice crystals in a supercooled water cloud. Wuart. J. Roy. Meteor. Soc., 79, 104-111.

_____, 1957: The Physics of Clouds. Oxford University Press, 671 pp.

Mason, B. J., G. W. Bryant, and A. P. van den Heuval, 1963: The growth habits and surface structure of ice crystals. Phil. Mag., 8, 505-526.

Maybank, J., and B. J. Mason, 1959: The production of ice crystals by large adiabatic expansions of water vapor. Proc. Phys. Soc., 74,

11.

Mullins, W. W., and R. F. Sikirka, 1963: Morphological stability of a particle growing by diffusion or heat flow. J. Appl. Phys., 34, 323-329.

Nakaya, N., 1954: Snow Crystals: Natural and Artificial. Harvard University Press, 510 pp.

Ono, A., 1969: The shape and riming properties of ice crystals in natural clouds. J. Atmos. Sci., 26, 138-147.

_____, 1970: Growth mode of ice crystals in natural clouds. J. Atmos. Sci., 27, 649-658.

Pruppacher, H. R., and J. D. Klett, 1978: Microphysics of Clouds and Precipitation. D. Reidel Publishing Company, Boston, 714 pp.

Rogers, R. R., and G. Vali, 1978: Recent developments in meteorological physics. Physics Reports, 48, 65-117.

Rottner, D., and G. Vali, 1974: Snow crystal habit at small excesses of vapor density over ice saturation. J. Atmos. Sci., 31, 560-570.

Ryan, B. F., E. R. Wishart, and E. W. Holroyd, III, 1974: The densities and growth rates of ice crystals between -5°C and -9°C. J. Atmos. Sci., 31, 2136-2141.

Ryan, F. V., E. R. Wishart, and D. E. Shaw, 1976: The growth rates and densities of ice crystals between -3°C and -21°C. J. Atmos. Sci., 33, 842-850.

Saxena, V. K., J. N. Burford, and J. L. Kassner Jr., 1970: Operation of a thermal diffusion chamber for measurements of cloud condensation nuclei. J. Atmos. Sci., 30, 73-80.

Schaefer, V. J., 1948: The production of clouds containing supercooled water droplets or ice crystals under laboratory conditions. Bull. Amer. Met. Soc., 29, 175.

_____, 1958b: A method of making snowflake replicas. Science, 93, 239-240.

_____, 1952: Continuous cloud chamber for studying small particles in the atmosphere. Ind. Eng. Chem., 44, 1381-1383.

Schaller, R. C., and N. Fukuta, 1979: Ice nucleation by aerosol particles. Experimental studies using a wedge-shaped ice thermal diffusion chamber. J. Atmos. Sci., 36, 1788-1802.

Shaw, D., and B. J. Mason, 1955: The growth of ice crystals from the vapor. Phil. Mag., 46, 249.

Tomlinson, E. M., and N. Fukuta, 1979: Aspect ratio of thermal diffusion chambers. J. Atmos. Sci., 36, 1362-1365.

_____, 1980: A new horizontal gradient, continuous flow, ice thermal diffusion chamber and detailed observation of condensation-freezing and depositon nucleations. Ph.D. Dissertation, Department of Meteorology, University of Utah, 1980.

Twomey, S., 1963: Measurement of natural cloud nuclei. J. Tech. Atmos., 1, 101-105.

Weyl, W. A., 1951: Surface structure of water and some of the physical and chemical manifestations. J. Colloid. Sci., 4, 389-405.


DAT
FILM